Chemical Probes to Study Fucosylated Glycans

Thesis by

Chithra Krishnamurthy

In Partial Fulfillment of the Requirements for the degree

of

Doctor of Philosophy

CALIFORNIA INSTITUTE OF TECHNOLOGY

Pasadena, California

2013

(Defended 15 April 2013)

© 2013
Chithra Krishnamurthy
All Rights Reserved

ACKNOWLEDGEMENTS

I would first and foremost like to thank my advisor, Professor Linda Hsieh-Wilson, for her advice and guidance throughout my years at Caltech, without which this work could not have been possible. I would also like to thank the members of my committee, Professors Dennis Dougherty, Shu-ou Shan, and David Tirrell, for their excellent feedback and endless support.

I'd also like to acknowledge my collaborators in the Hsieh-Wilson lab, Dr. Heather Murrey and Jean-Luc Chaubard, who have been critical to the work described. Drs. Sarah Hanson and Sherry Hsu of Dr. Chi-Huey Wong's laboratory at The Scripps Research Institute provided synthetic compounds and helpful guidance necessary for work in described Chapter 1 and 2. Drs. Eric Peters and John Venable at the Genomics Institute of the Novartis Research Institution were instrumental to the work described in Chapter 2, and Rochelle Diamond of the Caltech Flow Cytometry and Cell Sorting Facility was a key collaborator in the work described in Chapter 4. I'd also like to thank all the members of the Hsieh-Wilson lab for help, guidance, and friendship throughout the past several years.

I am indebted to the staff at the Caltech animal facility, especially Jennifer Constanza, Scott Wang, Reyna Sauza, Jeremy Willenborg, Ana Colon, Dr. Karen Lencioni, and Dr. Janet Baer, all of whom have maintained and cared for my mouse colonies as well guided me through new experimental techniques.

Lastly, I'd like to acknowledge my family and friends for their support. I would not be here without the support of my parents and dear friends, and especially that of my fiancé, Benjamin Keith Keitz.

ABSTRACT

Fucosylated glycans have many critical biological roles, from leukocyte adhesion to host-microbe interactions. However, a molecular level understanding of these sugars has been lacking, in part due to the chemical and structural diversity of glycans that make them challenging to study. In order to gain a deeper understanding of fucosylated glycans, we have explored the use of chemical probes to study these structures. In Chapters 1 and 2, we apply a metabolic labeling technique for the investigation of fucosylated glycans in neurons, where they have been implicated in learning and memory processes. However, the molecular mechanisms by which these sugars influence neuronal processes are not well understood, and only a handful of fucosylated glycoproteins have been identified. In order to facilitate our understanding of these processes, we exploit non-natural fucose analogs to identify the fucose proteome in rat cortical neurons, identifying proteins involved in cell adhesion, neuronal signaling, and synaptic transmission. Moreover, we track fucosylated glycoproteins in hippocampal neurons, and show that fucosylated glycoproteins localize to the Golgi, axons, and dendrites, and are enriched in synapses. In Chapter 4, we report a new chemoenzymatic strategy for the sensitive detection of the Fucα(1-2)Gal epitope, which has been implicated in tumorigenesis as a potential biomarker of cancer progression. We demonstrate that the approach is highly selective for the Fucα(1-2)Gal motif, detects a variety of complex glycans and glycoproteins, and can be used to profile the relative abundance of the motif on live cells, discriminating malignant from normal cells. These approaches represent new potential applications and strategies for the investigation of fucosylated glycans, and expand the technologies available for understanding the roles of this important class of carbohydrates in physiology and disease.

TABLE OF CONTENTS

LIST OF FIGURES AND TABLES

Chapter 1

Chapter 2

Chapter 3

Chapter 4

LIST OF ABBREVIATIONS

2-dgal	2-deoxy-D-galactose
2-fucosyllactose	L-fucoseα(1-2)galactoseβ(1-4)glucose
3-dgal	3-deoxy-D-galactose
4-dgal	4-deoxy-D-galactose
6-dgal	6-deoxy-D-galactose
2-dGlc	2-deozy-D-glucose
AAA	*Anguilla anguilla* agglutinin
Ab	antibody
Ac	acetyl, acetate
$AgNO_3$	silver nitrate
AlkFuc	Alkynyl-fucose
Aq	aqueous
ATP	adenosine triphosphate
AzFuc	Azido-fucose
Baf. A1	bicinchoninic acid
β-Gal	β-galactosidase
Bre A	Brefeldin A
BSA	bovine serum albumin
°C	degree Celsius
$CaCl_2$	calcium chloride
Cacna2d1	alpha2/delta subunit of the dihydropyridine-sensitive channel
cAMP	cyclic adenosine monophosphate
CAMs	cell adhesion molecules
CDG	congenital disorder of glycosylation
CH_3CH	acetonitrile
$CHCl_3$	chloroform
CHO	Chinese hamster ovary
CMF-HBSS	calcium and magnesium free Hank’s Balanced Salt Solution
CNS	central nervous system
CO_2	carbon dioxide

CRMP-2	collapsin response mediator protein
CV	column volume
ddH2O	double distilled water
D-Gal	D-galactose
DIV	days *in vitro*
DMEM	Dulbecco's Minimal Eagle's medium
DMSO	dimethylsulfoxide
DNA	deoxyribonucleic acid
DTT	dithiothreitol
E18	embryo day 18
EBI-IPI	European Bioinformatics Institute-International Protein Index
EDTA	ethylenediaminetetraaetic acid
EGTA	ethylene glycol tetraacetic acid
Endo H	endoglycosidase H
ER	endoplasmic reticulum
FCS	fetal calf serum
Fuc	L-Fucose
Fucα(1-2)Gal	fucose-α(1,2)-galactose
Fucα(1-3)Gal	fucose-α(1,3)-galactose
Fucα(1-4)Gal	fucose-α(1,4)-galactose
Fucα(1-6)GlcNAc	fucose-α(1,6)-*N*-acetylglucosamine
FUT1	α(1-2) fucosyltransferase 1
FUT2	α(1-2) fucosyltransferase 2
FUT3	α(1-3,4) fucosyltransferase 3
FUT4	α(1-3,4) fucosyltransferase 4
FUT5	α(1-3) fucosyltransferase 5
FUT6	α(1-3) fucosyltransferase 6
FUT7	α(1-3) fucosyltransferase 7
FUT8	α(1-6) fucosyltransferase 8
FUT9	α(1-6) fucosyltransferase 9
FUT10	putative α(1-3) fucosyltransferase 10
FUT11	putative α(1-3) fucosyltransferase 11
g	gram

Gal	galactose
GalNAc	*N*-acetylgalactosamine
GDP-fucose	guanosine diphosphatyl-fucose
Glc	glucose
GlcA	D-glucuronic acid
GlcN	D-glucosamine
GlcNAc	*N*-acetylgalactosamine
GluR1	glutamate receptor 1
GTP	guanosine triphosphate
h	hour
HIO_4	periodate
hnRNP	heterogeneous ribonucloprotein
H_2O	water
HOAc	acetic acid
Hsc/Hsp70	heat shock chaperonin/heat shock protein 70
IACUC	institute of animal care and use committee
IgSF	immunoglobulin superfamily
IgG	immunoglobulin
IP	immunoprecipitated
K^+	potassium ion
K_m	Michaelis cosntant
KCl	potassium chloride
kDa	kilodalton
$K_3Fe(CN)_6$	potassium ferrocyanide
KO	knockout
L	liter
LAC	lectin affinity chromatography
LAD II	leukocyte adhesion deficiency type II
LC/MS^n	liquid-chromatography mass spectrometry
LTL	*Lotus tetragonolobus* lectin
LTP	long-term potentiation
M	molar
MALDI-TOF	matrix-assisted laser desorption/ionization time-of-flight

Man	mannose
MAP2	microtubule associated protein
MEM	Minimal Eagle's Medium
MeOH	methanol
µg	microgram
MG132	proteasome inhibitor
$MgCl_2$	magnesium chloride
min	minutes
m	milli
µ	micro
mol	mole
MS	mass spectrometry
Munc18	syntaxin-binding protein
MWCO	molecular weight cut-off
n	nano
N	normal
Na^+	sodium ion
NaCl	sodium chloride
NaOH	hydroxide
Na_2CO_3	sodium biocarbonate
NaN_3	sodium azide
$Na_2S_2O_3$	sodium thiosulfate
NCAM	neural cell adhesion molecule
NCBI	National Center for Biotechnology Information
NETFD	SDS-neutralization lysis buffer
Neu5Ac	sialic acid
NH_4HCO_3	ammonium biocarbonate
NIH	National Institute of Health
NP-40	nonidet P-40 detergent
NPI	neuronal pentraxin I
NSF	*N*-ethylmaleimide sensitive factor
NTCB	2-nitro-5-thiocyanobenzoic acid
OCAM	olfactory cell adhesion molecule

OEt	*O*-ethyl
P0	post-natal day 0 mouse or rat pup
PAGE	polyacrylamide gel electrophoresis
PBS	phosphate buffered saline
PEPcase	phosphoenolpyruvate carboxylase
PNGase F	*N*-glycosidase F
POFUT1	*O*-fucosyltransferase 1
POFUT2	*O*-fucosyltransferase 2
PSA	polysialic acid, prostate-specific antigen
PSD-95	post synaptic density protein 95
PTM	post-translational modification
PVDF	polyvinylidene difluoride
RNA	ribonucleic acid
rpm	revolutions per minute
rt	room temperature
SDS	sodium dodecyl sulfate
Sec1	noncatalytic α(1-2)fucosyltransferase
SEM	standard error of the mean
SPAAC	strain-promoted azide-alkyne cycloaddition
SynI	synapsin I
Syn KO	synapsin knockout
TBST	tris-buffered saline with Tween-20
TCEP	tris(2-carboxyethyl)phosphine
TEAA	triethylammonium acetate
Tris-Cl	tris chloride
TTX	tetrodotoxin
UEA I	Ulex europeaus agglutinin I
UDP	uridyl-diphosphate
UV	ultraviolet
VDAC1	voltage-dependent anion channel 1
vol	volume
w/v	weight per volume
WGA	wheat germ agglutinin

WT	wild type
Xyl	xylose

CHAPTER 1

Introduction

Chemical and Structural Diversity of Glycans

Glycans are carbohydrate biopolymers with important biological roles found in all organisms. These biopolymers, synthesized from eight possible monosaccharide building blocks, can range from single monosaccharide units to polysaccharides containing hundreds of sugars in branched or linear arrays (1). The structural and chemical complexity of glycans give rise to a diverse set of functions within the cell. The cellular "glycome," or the collective set of glycans within the cell, has roles from increasing the complexity of cellular signaling to expanding the ability of a cell to modulate protein function (2-6). Glycosylation is one of the most ubiquitous post translational modifications, with more than 50 percent of the human proteome estimated to be glycosylated (7). Glycolipids are another important class of glycans that serve critical structural roles in cellular membranes and can regulate signal transduction and cellular function (8). As the glycome is influenced by the genome, the transciptome, and the proteome, as well as environmental and nutrient cues, it can report on the physiological state of the cell (9). Specific changes in glycan profiles correlate with certain disease states such as cancer and inflammation (10), suggesting that glycans could be used in clinical diagnostics and perhaps as targets for developing therapeutics**.**

In vertebrates, glycans may be intracellular, membrane associated, or secreted (11, 12). Within the cell, glycans can direct protein folding and trafficking, and are critical for protein quality control (13-16). Membrane associated glycans can mediate molecular recognition events, serving as points of attachment for viruses, bacteria, and other cells and participating in many facets of the vertebrate immune system (17). Additionally, cell-surface glycans participate in cell-cell interactions involved in embryonic development (18), leukocyte homing (19), and cancer cell metastasis (20, 21).

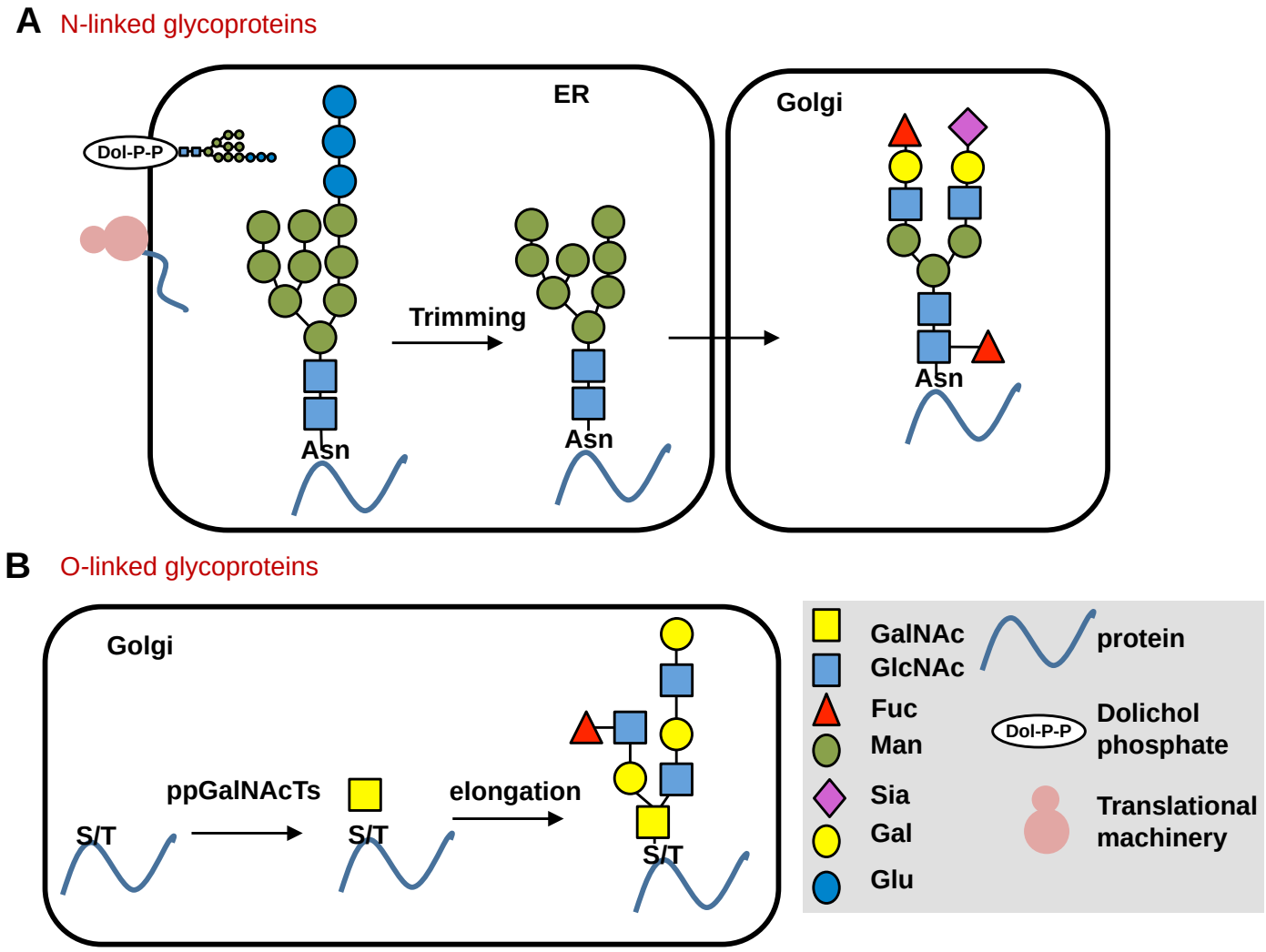

Figure 1.1 Glycoprotein Biosynthesis. (A) N-linked glycoproteins are synthesized in the ER and Golgi and modify Asn residues on the protein backbone. (B) O-linked glycoproteins are synthesized in the Golgi, modifying Ser or Thr residues on the protein backbone.

Biosynthesis of glycans occurs in the endoplasmic reticulum (ER) and the Golgi, to which various glycosyltransferases are localized. Glycosyltranferases accept specific monosaccaharides and transfer them to growing glycan chains via specific linkages. N-linked glycoproteins are formed by the addition of a core structure synthesized on the lipid dolichol in the ER (Figure 1.1A) (1). This core oligosaccharide is formed by the sequential addition of three glucosamine (Glc), nine mannose (Man),

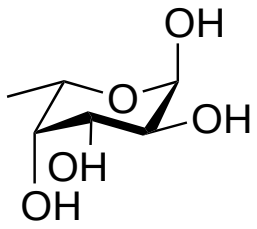

Figure 1.2 The structure of L-Fucose.

and two *N*-acetylglucosamine (GlcNAc) residues, which is transferred to the asparagine (Asn) residue on the nascent protein chain. The modified Asn is generally within a peptide consensus sequence of Asn-X-Ser/Thr, where X can be any amino acid residue except proline, which determines a likely site of N-glycosylation. The glycoprotein is trimmed of the Glc residues and one Man, and is then trafficked to the Golgi apparatus for terminal processing. The carbohydrate structure is subsequently trimmed and elongated by various glycosyltransferases, leading to substantial diversity in composition and chain length of N-linked glycans. N-linked glycans are generally of three types based on how they are processed; these include high-mannose (characterized by unsubstituted Man residues), complex (substituted Man residues), or hybrid glycans (with both substituted and unsubstituted Man residues). The majority of the *N*-glycans within vertebrate cells are of the complex type (22).

In contrast to N-linked glycosylation, O-linked glycosylation occurs in the Golgi apparatus with the attachment of either *N*-acetylgalactosamine (GalNAc) or Man to serine (Ser) or threonine (Thr) residues on nascent proteins (Figure 1.1B) (1). Unlike with N-glycosylation, there is no peptide consensus sequence determining O-glycosylation. The core monosaccharides are then elongated with GlcNAc, Gal, Fuc, or sialic acid (Neu5Ac) in different variations to create heterogeneity in glycan composition. O-linked oligosaccharides tend to be smaller than N-linked glycans. However, the structural diversity in both N- and O-linked glycans is enormous, due to the hundreds of possible combinations of chain length, composition, and monosaccharide linkages present in each glycan structure.

Biological Roles of Fucosylation

Among the monosaccharide building blocks that compose structurally diverse glycans is L-fucose (Figure 1.2). L-Fucose is a monosaccharide that is a common component of many N- and O- linked glycoproteins and glycolipids. It is structurally unique compared to other monosaccaharides in that it lacks a hydroxyl group on the carbon at the 6-position and it exists in the L- configuration. Fucose commonly exists as a terminal modification, and can therefore serve as a molecular recognition element (17). Important roles for fucosylated glycans have been demonstrated in a variety of biological systems (23, 24). Fucosylated glycans include the ABO blood group antigens and are crucial to the recruitment and adhesion of leukocyte antigens. Fucosylated antigens also play a key role in host-microbe interactions (25). Deficiencies in fucosylation are associated with human disease, such as the leukocyte adhesion disorder type II (LAD II). The disease causes an impairment of leukocyte-endothelium interactions and are characterized by immunodeficiency, developmental abnormalities, and deficiencies in cognitive development (26). Fucose is synthesized via one of two cellular biosynthetic pathways: the *de novo* pathway or the salvage pathway (Figure 1.3). In the *de novo* pathway, GDP-fucose is synthetized from GDP-mannose through a series of enzymatic reactions, carried out by two proteins: GDP-mannose 4,6-dehydratase (GMD) and GDP-keto-6-doeoxymanose 3,5-epimerase, 4-reducatase (FX protein) (27). GDP-fucose can also be synthetized via the salvage pathway from free fucose present in the cytosol from lysosomal or extracellular sources. In either case, the GDP-fucose is transported into the Golgi apparatus and made available to the cellular glycosylation machinery. Studies of fucose metabolism in HeLa cells report that more than 90% of GDP-fucose is synthesized from the *de novo* pathway, even in cells supplemented with radiolabeled fucose (28, 29). However, the salvage pathway still provides a mechanism to correct deficiencies in fucose metabolism, such as in LAD II, for which exogenous fucose can be administered for therapeutic purporses (30).

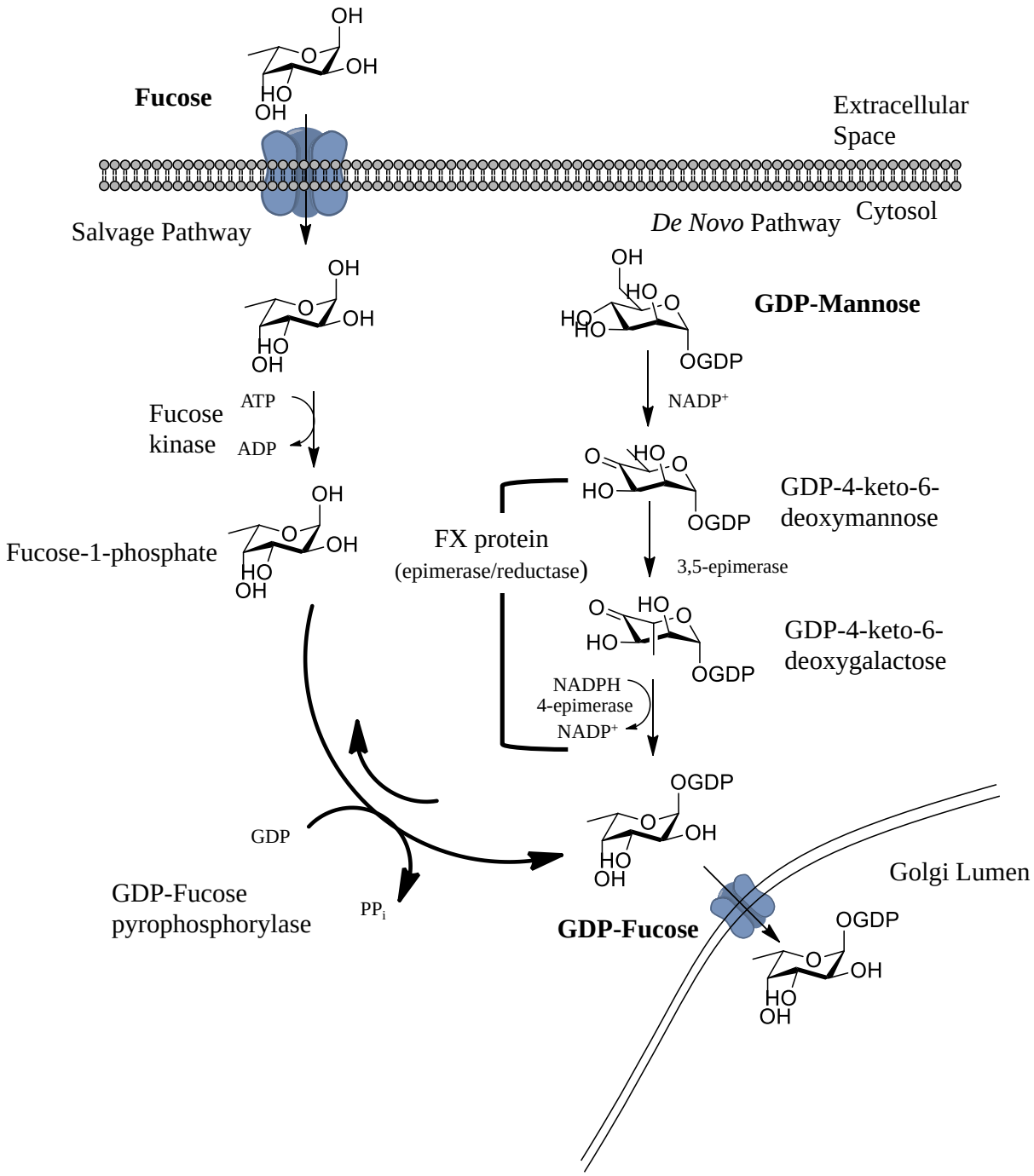

Figure 1.3 Biosynthesis of fucose. In eukaryotes, the biosynthesis of GDP-fucose occurs through two distinct pathways: the *de novo* pathway and the salvage pathway. The *de novo* pathway synthesizes GDP-fucose from GDP-mannose via enzymatic reactions carried out by two proteins, GMD and FX. The salvage pathway "salvages" free fucose found in the cytosol to synthesize GDP-fucose using the enzymes fucose kinase and GDP-fucose pyrophosphorylase. GDP-fucose is then transported into the Golgi lumen for glycosyltransferase reactions.

Enzyme	Representative Structure
FUT1	
FUT2	
FUT3	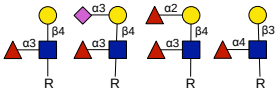
FUT4	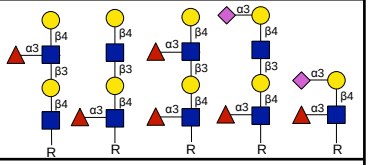
FUT5	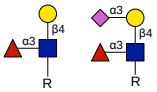
FUT6	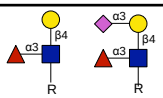
FUT7	
FUT8	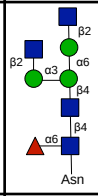
FUT9	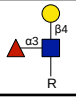
FUT10	unknown
FUT11	unknown
POFUT1	O-fucosylation in EGF repeats
POFUT2	unknown

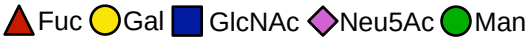

Figure 1.4 Human fucosyltransferases. List of human fucosyltransferases and representative structures synthesized by each fucosyltrasferase.

Fucosylated glycans are synthesized by fucosyltransferases (FUTs) that reside in the Golgi apparatus and ER. Thirteen FUT genes have so far been identified in the human genome, two of which transfer fucose directly to a polypeptide chain (O-fucose) (23). Fucose can be linked to C-2 or C-4 positions of the penultimate galactose in oligosaccharides, or to the C-3 or C-6 position of GlcNAc residue of N-linked glycans (Figure 1.4). O-Fucosylation is the direct modification of Ser or Thr residues by α-L-fucose, and is observed on epidermal growth factor (EFG) repeats of glycoproteins such as Notch (23). While fucose is not elongated in N-linked and O-linked glycans, O-linked fucose can be elongated by other sugars.

FUT1 and FUT2 are dedicated to the synthesis of Fucα(1-2)Gal glycans, the epitope found on the ABO blood group antigens, which determine blood and tissue type (Figure 1.5) (31, 32). FUT3 catalyzes the synthesis of both α(1-3) and α(1-4) fucosylated glycans and can transfer fucose to both a Gal and a GlcNAc, to synthesize structures such as the Lewis y and Lewis b antigens, thought to be critical for host-microbe interactions (Figure 1.5). FUT4-7 form only α(1-3) fucosylated glycans, such as within the sialylated Lewis^x structures, important to leukocyte adhesion

(32, 33). FUT8 and FUT9 generate Fucα(1-6)GlcNAc structures, with FUT8 generally catalyzing attachment of this structure to the core Asn residue of N-linked glycans, and FUT9 catalyzing its attachment to a distal GlcNAc of polylactosamine chains. Core fucosylation, a product of FUT8, may play a role in cancer progression as increased incidences of core fucosylation have been reported in many cancers (34). FUT9 is responsible for the synthesis of Lewis^x structures during embryogenesis, promoting cell-adhesion in early embryos. FUT10 and FUT11 are putative fucosyltransferases that are reported to synthesize α(1-3) structures based on sequence homology. POFUT 1 and 2 are *O*-fucosyltransferases 1 and 2 and catalyze the direct fucosylation of Ser and Thr residues (23).

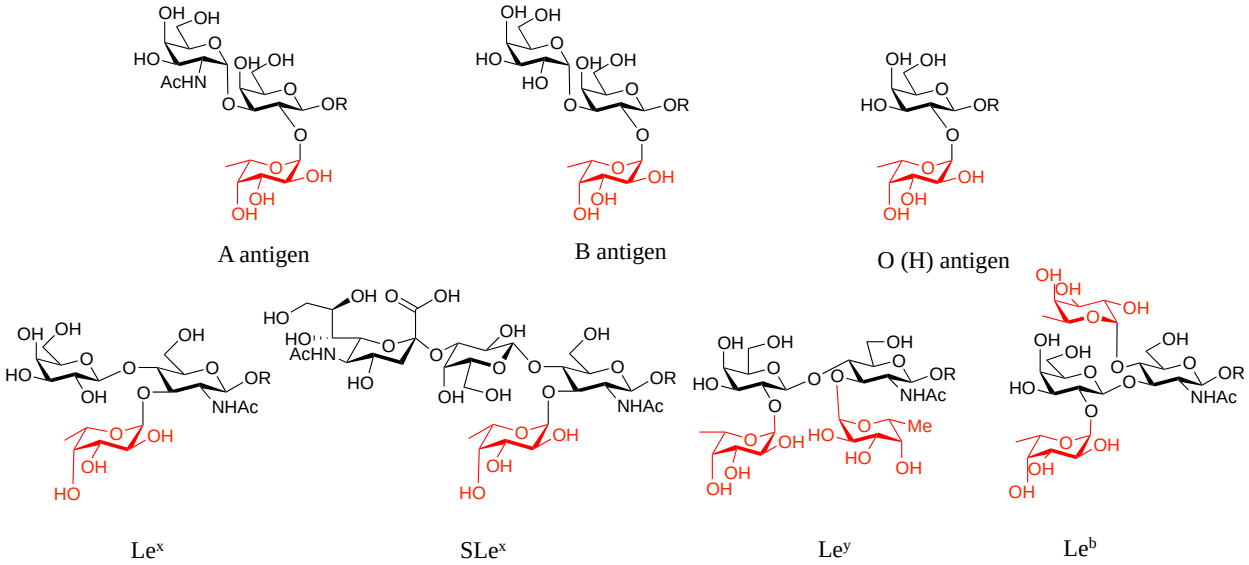

Figure 1.5 Biologically Relevant Fucosylated Structures. Fucosylated glycans include the blood group antigens A, B, and O (H), which determine blood and tissue type. Other biologically relevant fucosylated glycans include the Le^x, SLe^x, and Le^y antigens, which are important molecular determinants in processes such as embryogenesis and leukocyte adhesion.

The Role of Fucosylated Glycans in Neurons

Increasing evidence suggests a critical role for fucosylated glycans in the nervous system (35). For example, fucose has been shown to play an important role in neural development. O-Fucosylation is essential for the activity of Notch, a receptor that controls many aspects of cell fate during development including neuronal progenitor maintenance and regulation of cell-fate decisions in neuronal and glial

lineages (36, 37). Previous studies have suggested that fucosylation modulates Notch signaling by either interacting directly with ligands, or inducing some sort of conformational change (38). In addition to neural development, Notch signaling may have a role in neuronal migration (39). Genetic deletion of POFUT1, the enzyme responsible for *O*-fucosylation, is embryonic lethal and causes developmental defects similar to that of a Notch deletion (40, 41). The Lewis x (Le^x) epitope, an α(1-3) fucosylated glycan, is also implicated in neurogenesis, as it is dynamically expressed at different embryonic stages (42). Recent work has also implicated the Le^x epitope in neurite outgrowth (43-45).

Fucosylated glycans are known to be important in learning and memory processes. Incorporation of fucose into neuronal glycoconjugates was significantly enhanced by task-dependent learning in both chicks and rats (46-49). When trained in a brightness discrimination task, rodents demonstrated an increase in [^{3}H]-fucose into forebrain glycoproteins (48). Moreover, the addition of fucose or 2'-fucosyllactose (a Fucα**(**1-2)Gal containing trisaccharide) enhanced long-term potentiation (LTP), an electrophysiological model of learning and memory, both in hippocampal slices and *in vivo* (50, 51). Fucosylated glycans have also been reported to be enriched in synapses (52-54), where the majority of fucosylated glycans exist as complex N-linked structures (55). Studies have indicated that the activity of fucosyltransferases increases both during synaptogenesis (56), and in response to passive-avoidance training (57). Moreover, the presence of dendritic Golgi (58, 59) raises the intriguing possibility of local protein synthesis and glycosylation in response to neuronal stimulation.

The Fucα(1-2)Gal structure in particular has been implicated in neuronal processes. The probe 2-deoxy-D-galactose (2dGal) has been utilized to inhibit Fucα(1-2)Gal formation by competitively inhibiting fucose incorporation (60). The lack of a C2 hydroxyl group prevents the incorporation of the terminal fucose structure (Figure 1.6). Treatment with 2dGal, but not other sugars, caused reversible amnesia in both chicks and rats, indicating the importance of the Fucα(1-2)Gal linkage (60-62). 2dGal has also been reported to interfere with the maintenance of LTP *in vitro* and *in vivo* (51, 63). Additionally, a monoclonal antibody specific for the Fucα(1-2)Gal epitope (64) inhibited memory

formation in animals, presumably by blocking the interaction of the Fucα(1-2)Gal epitope with its relevant binding partners (65). Hsieh-Wilson and coworkers investigated the effects of 2dGal treatment in cultured hippocampal neurons, observing that 2dGal treatment caused hippocampal neurons to retract their neurites (66). Other sugars had no effect, and treatment with natural galactose moderately rescued the neurite retraction, suggesting that *de novo* synthesis of Fucα(1-2)Gal glycans was necessary for regaining normal morphology.

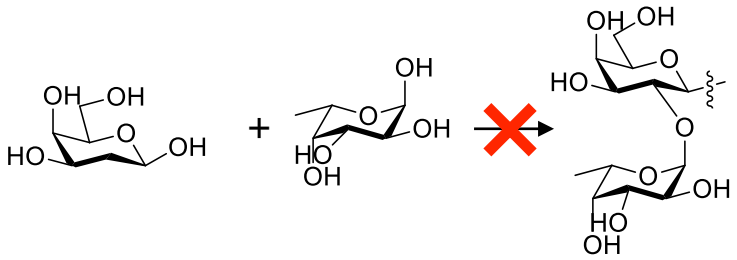

2-dGal Fuc Fucα(1-2)Gal

Figure 1.6 Incorporation of 2-deoxy-D-galactose (2-dGal) inhibits formation of Fucα(1-2)Gal linkages.

Another relevant structure in the brain is the Le^x structure. Downregulation of FUT9 in human NT2N neurons led to significant decrease of Le^x, as well as GAP-43, a marker of neurite outgrowth. In parallel, there was a decrease in neurite outgrowth that was reversed with the overexpression of FUT9 (45). Moreover, Le^x glycans on glial CD24 glycoforms were shown to mediate CD24-induced effects on neurite outgrowth (44).

Despite their importance, only a handful of fucosylated proteins have been identified from the brain. Moreover, the functional relevance of the fucose epitope has only been characterized on one neuronal glycoprotein, synapsin I (52). Synapsin I, a synaptic-vesicle associated protein with critical roles in neurotransmitter release and synaptogenesis (67), was identified as a Fucα(1-2)Gal glycoprotein using a gel-based mass spectrometry approach. Importantly, fucosylation was found to protect synapsin I from proteolytic degradation, suggesting that fucosylation regulates the expression of synapsin I (52).

Additionally, studies using 2dGal and synapsin I deficient mice demonstrated that synapsin I fucosylation contributed to the effects of 2dgal on neurite outgrowth.

To further investigate whether Fucα(1-2)Gal binding receptors, or lectins, exist in neurons, Hsieh-Wilson and coworkers designed a biotinylated Fucα(1-2)Gal probe and assessed binding of the probe to lectins present on hippocampal neurons (66). The Fucα(1-2)Gal probe showed binding to the soma and neurites, suggesting the presence of fucose-specific lectins. Moreover, treating hippocampal neurons with multivalent Fucα(1-2)Gal probes promoted neurite outgrowth, while other sugars had no effect, suggesting the presence of a carbohydrate-regulated pathway mediating neuronal outgrowth.

The Fucα(1-2)Gal Biomarker

In addition to playing a role in neurochemical processes, fucosylation may also play an important role in several pathological processes, such as tumorigenesis (68). Changes in glycosylation are often a hallmark of disease states; cancer cells frequently display glycans at different levels or with fundamentally different structures than those observed on non-diseased cells (10, 21, 69-72). These structural changes may be due to changes in the expression levels of glycosyltransferases in the Golgi compartment of cancerous cells, which can lead to modifications in the core structure of N-linked and O-linked glycans. In addition to changes in the core structures of glycans, altered terminal structures are also associated with malignancy. Glycosyltransferases involved in linking terminating residues on glycans, such as sialyltransferases and fucosyltransferases, tend to be overexpressed in tumour tissue, leading to the overexpression of certain terminal glycans. Examples of terminal glycan epitopes commonly found on transformed cells include sialyl Lewis x (sLe^x), sialyl-Tn (sTn), Globo H, Lewis y (Le^y) and polysialic acid (PSA) (73, 74). Many of these epitopes are observed in malignant tissues throughout the body, including the brain, breast, colon and prostate. Although gross changes in glycosylation of tumor tissues are apparent, no single change seems to distinctly differentiate normal and malignant cells. Instead, each type of malignant tissue is characterized by a distinct set of changes in glycan expression, suggesting that glycans may serve as excellent biomarkers for cancer diagnosis.

One intriguing glycan biomarker is the Globo H antigen, a hexasaccharide with a terminal Fuca(1-2)Gal epitope (Figure 1.6), which is over expressed on a variety of epithelial cell tumors (75-77). Small cell lung carcinoma patients with Globo H positive tumors were shown to experience shorter survival compared to patients with Globo H negative tumors (68). In breast cancer, altered Globo H expression was observed on the majority of ductal lobular and tubular breast carcinomas and was found to be expressed in breast cancer stem cells (78-80). The serum of breast cancer patients contains high levels of antibodies against the Globo H epitope. Fucα(1-2)Gal glycan expression is also elevated in prostate cancer tissue and on the tumorigenic prostate-specific antigen (PSA) protein, when compared to normal epithelial tissue or PSA (77, 81). As such, the Fuca(1-2)Gal epitope is an attractive biomarker and potential therapeutic target for cancer (82-84). However, the extent to which this sugar epitope serves as a marker of disease progress and its precise contributions to cancer pathogenesis are not well understood.

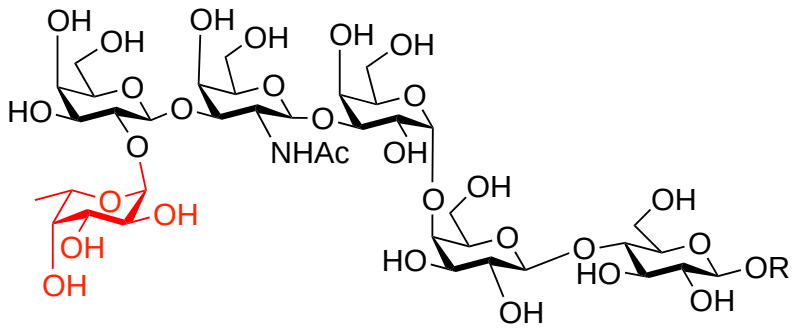

Figure 1.7 The Globo H hexasacharide. The Globo H hexasaccharide is overexpressed on a variety of epithelial cell tumors.

Motivation for Studies

Although glycans have long been known to have critical biological roles, the detection and manipulation of glycans has been challenging. One fundamental obstacle is that glycans have complex, branched structures and are intrinsically heterogeneous, making them inaccessible to common molecular

biological techniques. Traditional tools to study glycans include antibodies and lectins, which are carbohydrate binding proteins. However, lectins and antibodies are known to have weak affinity for their targets and poor specificity to small glycan structures (85). Cross-reactivity with other glycan epitopes may also be a problem (86, 87). For these reasons, the development of methods to chemically perturb and detect glycans would accelerate an understanding of their roles in vital biological processes and disease.

In this thesis, we describe two methods for the detection of fucosylated glycans. In Chapter 2 and 3, we exploit a metabolic labeling approach to identify and image fucosylated proteins in neuronal systems in order to gain insight into the roles of fucosylation in the brain. In Chapter 4, we describe the development of a new chemoenzymatic detection strategy for Fucα(1-2)Gal glycans, which we utilize to probe the surface Fucα(1-2)Gal expression on cancer cell lines. Both of these methods expand the technologies and applications available for the study of fucosylated glycans.

References

1. Kleene R & Schachner M (2004) Glycans and neural cell interactions. *Nat. Rev. Neurosci.* 5(3):195-208.

2. Rexach JE, Clark PM, & Hsieh-Wilson LC (2008) Chemical approaches to understanding O-GlcNAc glycosylation in the brain. *Nat. Chem. Biol.* 4(2):97-106.

3. Rudd PM, Merry AH, Wormald MR, & Dwek RA (2002) Glycosylation and prion protein. *Curr. Op. Struct. Biol.* 12:578-586.

4. Wujek P, Kida E, Walus M, Wisniewski KE, & Golabek AA (2004) N-glycosylation is crucial for folding, trafficking, and stability of human tripeptidyl-peptidase I. *J. Biol. Chem.* 279(13):12827-12839.

5. Yamaguchi H (2002) Chaperone-like functions of N-Glycans in the formation and stabilization of protein conformation. *Trends Glycosci. Glyc.* 14:139-151.

6. Wells L, Vosseller K, & Hart GW (2001) Mapping sites of O-GlcNAc modification using affinity tags for serine and threonine post-translational modifications. *Science* 291:2376-2378.

7. Apweiler R, Hermjakob H, & Sharon N (1999) On the frequency of protein glycosylation, as deduced from analysis of the SWISS-PROT database. *Biochim. Biophyis. Acta* 1473:4-8.

8. Schnaar RL, Suzuki A, & Stanley P (2009) Glycosphingolipids. *Essentials of Glycobiology*, eds Varki A, Cummings RD, & Esko JD (Cold Spring Harbor Laboratory Press, Cold Spring Harbor).

9. Freeze HH (2006) Genetic defects in the human glycome. *Nat. Rev. Genet.* 7(7):537-551.

10. Dube DH & Bertozzi CR (2005) Glycans in cancer and inflammation--potential for therapeutics and diagnostics. *Nat. Rev. Drug Discovery* 4(6):477-488.

11. Ohtsubo K & Marth JD (2006) Glycosylation in cellular mechanisms of health and disease. *Cell* 126(5):855-867.

12. Bishop JR, Schuksz M, & Esko JD (2007) Heparan sulphate proteoglycans fine-tune mammalian physiology. *Nature* 446(7139):1030-1037.

13. Helenius A & Aebi M (2004) Roles of *N*-linked glycans int eh endoplasmic reticulum. *Ann. Rev. Biochem.* 73:1019-1049.

14. Aebi M*ea* (2010) N-Glycan structures: recognition and processign in the ER. *Trends Biochem. Sci.* 35:74-82.

15. Lederkremer GZ (2009) Glycoprotein folding, quality control, and ER-associated degradation. *Curr Op. Struct. Biol.* 19:515-553.

16. Smith MH *et al*. (2011) Road to ruin: targeting proteisn for degradation in the endoplasmic reticulum. *Science* 334:1086-1090.

17. Varki A (1993) Biological roles of oligosaccharides: all of the theories are correct. *Glycobiology* 3(2):97-130.

18. Haltiwanger RS & Lowe JB (2004) Role of glycosylation in development. *Annu. Rev. Biochem.* 73:491-537.

19. Rosen SD (2004) Ligands for L-selectin: homing, inflammation, and beyond. *Ann. Rev. Immun.* 22:129-156.

20. Fuster MM & Esko JD (2005) The sweet and sour of cancer: glycans as novel therapeutic targets. *Nat. Rev. Cancer* 5(7):526-542.

21. Dennis JW, Granovsky M, & Warren CE (1999) Glycoprotein glycosylation and cancer progression. *Biochim. Biophys. Acta* 1473(1):21-34.

22. Varki A, Cummings R, Esko JD, *et al.* (1999) N-Glycans. *Essentials of Glycobiology*, (Cold Spring Harbor Laboratory Press, Cold Spring Harbor).

23. Becker DJ & Lowe JB (2003) Fucose: biosynthesis and biological function in mammals. *Glycobiology* 13(7):41R-53R.

24. Staudacher E, Altmann F, Wilson IB, & Marz L (1999) Fucose in N-glycans: from plant to man. *Biochim. Biophys. Acta* 1473:216-236.

25. Pacheco AR, *et al.* (2012) Fucose sensing regulates bacterial intestinal colonization. *Nature* 492(7427):113-117.

26. Yakubenia S & Wild MK (2006) Leukocyte adhesion deficiency II-Advances and open questions. *FEBS J.* 273(19):4390-4398.

27. Tonetti M, *et al.* (1998) The metabolism of 6-deoxyhexoses in bacterial and animal cells. *Biochmie* 80(11):923-931.

28. Yurchenco PD & Atkinson PH (1975) Fucosyl-glycoprotein and precursor pools in HeLa cells. *Biochemistry* 14:944-953.

29. Yurchenco PD & Atkinson PH (1977) Equilibration of fucosyl glycoprotein pools in HeLa cells. *Biochemistry* 16:944-953.

30. Marquardt T, *et al.* (1999) Correction of luekocyte adhesion deficiency type II with oral fucose. *Blood* 94:3976-3985.

31. Kelly RJ, Rouquier S, Giorgi D, Lennon GG, & Lowe JB (1995) Molecular basis for H blood group deficiency in Bombay (Oh) and para-Bombay individuals. *J. Biol. Chem.* 270:4640-4649.

32. Larsen RD, Ernst LK, Nair RP, & Lowe JB (1990) Molecular cloning, sequence, and expression of a human GDP-L-fucose:8-D-galactoside 2-α-L-fucosyltransferase cDNA that can form the H blood group antigen. *Proc. Natl. Acad. Sci. U. S. A.* 87:6674-6678.

33. Kaneko M, *et al.* (1999) Alpha1,3-fucosyltransferase IX (Fuc-TIX) is very highly conserved between human and mouse; molecular cloning, characterization and tissue distribution of human Fuc-TIX. *FEBS Lett.*

34. Saldova R, Fan Y, Fitzpatrick JM, Watson RW, & Rudd PM (2011) Core fucosylation and alpha2-3 sialylation in serum N-glycome is significantly increased in prostate cancer comparing to benign prostate hyperplasia. *Glycobiology* 21(2):195-205.

35. Murrey HE & Hsieh-Wilson LC (2008) The Chemical Neurobiology of Carbohydrates. *Chem. Rev.* 108:1708-1731.

36. Artavanis-Tsakonas S (1999) Notch Signaling: Cell Fate Control and Signal Integration in Development. *Science* 284(5415):770-776.

37. Rampal R, Arboleda-Velasquez JF, Nita-Lazar A, Kosik KS, & Haltiwanger RS (2005) Highly Conserved O-Fucose Sites Have Distinct Effects on Notch1 Function. *J. Biol. Chem.* 280(37):32133-32140.

38. Haines N & Irvine KD (2003) Glycosylation regulates Notch signalling. *Nat. Rev. Mol. Cell. Biol.* 4(10):786-797.

39. Louvi A & Artavanis-Tsakonas S (2006) Notch signalling in vertebrate neural development. *Nat. Rev. Neurosci.* 7(2):93-102.

40. Lu LC & Stanley P (2006) Functional Glycomics. *Meth. Enzymol.* ed. Fukuda M (Elsevier, Amsterdam), Vol 17.

41. Shi S & Stanley P (2003) Protein O-fucosyltransferase 1 is an essential component of Notch signaling pathways. *Proc. Natl. Acad. Sci. U. S. A.* 100(9):5234-5239.

42. Kudo T, *et al.* (1998) Expression Cloning and Characterization of a Novel Murine Fucosyltransferase, mFuc-TIX, That Synthesizes the Lewis x (CD15) Epitope in Brain and Kidney. *J. Biol. Chem.* 273(41):26729-26738.

43. Wang S (2009) Synapsin I released via exosomes is an oligomannose bearing glycoprotein and an oligomannose binding lectin that promotes neurite outgrowth in Mus musculus (Linnaeus, 1758). (Universitat Hamburg).

44. Lieberoth A, *et al.* (2009) Lewis(x) and alpha2,3-sialyl glycans and their receptors TAG-1, Contactin, and L1 mediate CD24-dependent neurite outgrowth. *J. Neurosci.* 29(20):6677-6690.

45. Gouveia R, *et al.* (2012) Expression of glycogenes in differentiating human NT2N neurons. Downregulation of fucosyltransferase 9 leads to decreased Lewis(x) levels and impaired neurite outgrowth. *Biochim. Biophys. Acta.* 1820(12):2007-2019.

46. McCabe NR & Rose SPR (1985) Passive avoidance training increases fucose incorporation into glycoproteins in chick forebrain slices in vitro. *Neurochem. Res.* 10(8):1083-1095.

47. Sukumar R, Rose SPR, & Burgoyne RD (1980) Increased Incorporation of [H3] Fucose in Rat Hippocampal Structures after Conditioning by Perforant Path Stimulation and after LTP-Producing Tetanization. *J. Neurochem.* 34(4):1000-1006.

48. Pohle W, Acosta L, Ru¨thrich H, Krug M, & Matthies Hr (1987) Incorporation of [3H]fucose in rat hippocampal structures after conditioning by perforanth path stimulation and after LTP-producing tetanization. *Brain Res.* 410(2):245-256.

49. Bullock S, Rose SPR, & Zamani R (1992) Characterization and Regional Localization of Pre- and Postsynaptic Glycoproteins of the Chick Forebrain Showing Changed Fucose Incorporation Following Passive Avoidance Training. *J. Neurochem.* 58(6):2145-2154.

50. Krug MW, M.; Staak, S.; Smalla, K. H. (1994) Fucose and fucose-containing sugar epitopes enhance hippocampal long-term potentiation in the freely moving rat. *Brain Res.* 643:130-135.

51. Matthies H, Staak S, & Krug M (1996) Fucose and fucosyllactose enhance in-vitro hippocampal long-term potentiation. *Brain Res.* 725(2):276-280.

52. Murrey HE, *et al.* (2006) Protein fucosylation regulates synapsin Ia/Ib expression and neuronal morphology in primary hippocampal neurons. *Proc. Natl. Acad. Sci. U. S. A.* 103(1):21-26.

53. Zanetta JP, Reeber A, Vincendon G, & Gombos G (1977) Synaptosomal Plasma Membrane Glycoproteins. II. Isolation of Fucosyl-Glycoproteins by Affinity Chromatography on the Ulex Europeus Lectin Specific for L-Fucose. *Brain Res.* 138:317-328.

54. Krusius T & Finne J (1977) Structural Features of Tissue Glycoproteins: Fractionation and Methylation Analysis of Glycopeptides Derived from Rat Brain, Kidney, and Liver. *FEBS J.* 78:369-379.

55. Taniguchi T, Adler AJ, Mizuochi T, Kochibe N, & Kobata A (1986) The Structures of the Aparagine-Linked Sugar Chains of Bovine Interphotoreceptor Retinol-Binding Protein—Occurence of Fucosylated Hybrid-Type Oligosaccharides. *J. Biol. Chem.* 261(4):1730-1736.

56. Matsui Y, Lombard D, Massareli R, P. M, & H. D (1986) Surface glycosyltransferases activities during development of neuronal cell cultures. *J. Neurochem.* 46(1):144-150.

57. Popov N, *et al.* (1983) Changes in Activities of Fucokinase and Fucosyltransferase in Rat Hippocampus after Acquisition of a Brightness Discrimination Reaction. *Pharmacol. Biochem. Be.* 19:43-47.

58. Gardiol A, Racca C, & Triller A (1999) Dendritic and postsynaptic protein synthestic machinery. *J. Neurosci.*19(1):168-179.

59. Torre ER & Steward O (1996) Protein Synthesis in Dendrites: Glycosylation of Newly Synthesized Protein in Dendrites of Hippocampal Neurons in Culture. *J. Neurosci.* 16(19):5967-5978.

60. Bullock S, Potter J, & Rose SPR (1990) Effects of the Amnesic Agen 2-Deoxygalactose on Incorporation of Fucose into Chick Brain Glycoproteins. *J. Neurochem.* 54(1):135-142.

61. Rose SPRJ, R. (1987) Long-term-memory formation in chicks is blockd by 2-deoxygalactose, a fucose analog. *Behav. Neural Biol.* 48:246-258.

62. Lorenzini CGA, Baldi E, Bucherelli C, Sacchetti B, & Tassoni G (1997) 2-Deoxy-d-Galactose Effects on Passive Avoidance Memorization in the Rat. *Neurobiol. Learn. Mem.* 68(3):317-324.

63. Krug M, Jork R, Reymann K, Wagner M, & Matthies H (1991) The amnesic substance 2-deoxy-d-galactose suppresses the maintenance of hippocampal LTP. *Brain Res.* 540(1-2):237-242.

64. Karsten U, *et al.* (1988) A New Monoclonal-antibody (A46-B/B10) Highly Specific for the Blood Group-H Type-2 Epitope - Generation, Epitope Analysis, Serological and Histological-Evaluation. *Br. J. Cancer* 58(2):176-181.

65. Jork R, *et al.* (1991) Monoclonal-Antibody Specific for Histo-Blood Group Antigens -H (Type-2, and Type-4) Interferes with Long-Term Memory Formation in Rats. *Neurosci. Res. Commun.* 8(1):21-27.

66. Kalovidouris SA, Gama CI, Lee LW, & Hsieh-Wilson LC (2005) A role for fucose alpha(1-2) galactose carbohydrates in neuronal growth. *J. Am. Chem. Soc.* 127(5):1340-1341.

67. Ferriera A, Li L, Chin L-S, Greengard P, & Kosik KS (1996) Postsynaptic Element Contributes to the Delay in Synaptogenesis in Synapsin I-Deficient Neurons. *Mol. Cell. Neurosci.* 8:286-299.

68. Miyake M, Taki T, Hitomi S, & Hakomori S-i (1992) Correlation of Expression of H/LeY/LeB Antigens with Survival in Patients with Carcinoma of the Lung. *New Engl. J. Med.* 327(1):14-18.

69. Dennis JW & Laferte S (1987) Tumor cell surface carbohydrate and the metastatic phenotype. *Cancer Metast. Rev.* 5(3):185-204.

70. Kannagi R, *et al.* (1983) New globoseries glycosphingolipids in human teratocarcinoma reactive with the monoclonal antibody directed to a developmentally regulated antigen, stage-specific embryonic antigen 3. *J. Biol. Chem.* 258(8934-8942).

71. Meezan E, Wu HC, Black PH, & Robbins PW (1969) Comparative studies on the carbohydrate-containing membrane components of normal and virus-transformed mouse fibroblasts. II. Separation of glycoproteins and glycopeptides by sephadex chromatography. *Biochemistry* 8(6):2518.

72. Turner GA (1992) N-Glycosylation of serum-proteins in disease and its investigation using lectins. *Clin. Chim. Acta* 208:149-171.

73. Sell S (1990) Cancer-associated carbohydrates identified by monoclonal antibodies. *Hum. Pathol.* 21:1003-1019.

74. Gabius HJ (1988) Tumor lectinology-at the intersection carbohydrate chemistry, biochemistry, cell biology, and oncology. *Angew. Chem. Int. Ed. Engl.* 27:1267-1276.

75. Mènard S, Tagliabue E, Canevari S, Fossati G, & Colnaghi MI (1983) Generation of Monoclonal Antibodies Reacting with Normal and Cancer Cells of Human Breast. *Cancer Res.* 43(3):1295-1300.

76. Lee JS, *et al.* (1991) Expression of Blood-Group Antigen A — A Favorable Prognostic Factor in Non-Small-Cell Lung Cancer. *New Engl. J. Med.* 324:1084-1090.

77. Zhang S, Zhang HS, Cordon-Cardo C, Ragupathi G, & Livingston PO (1998) Selection of tumor antigens as targets for immune attack using immunohistochemistry: protein antigens. *Clin. Cancer Res.* 4(11):2669-2676.

78. Mariani-Constatini R, Barbanti P, Colnaghi MI, Menard, S, Clemente, C, Rilke, R (1984) Reactivity of a monoclonal antibody with tissues and tumors from the human breast. Immunohistochemical localization of a new antigen and clinicopathologic correlations. *Am. J. Path.* 115(1):47-56.

79. Perrone F, Menard S, Canevari S, Calabrese M, Boracchi P, Bufalino R, Testori S, Baldini M, and Colnaghi MR (1993) Prognostic Significance of the CaMBr1 Antigen on Breast Carcinoma: Relevance of the Type of Recognised Glycoconjugate. *Eur. J. Cancer* 29A(15):2113-2117.

80. Chang WW, *et al.* (2008) Expression of Globo H and SSEA3 in breast cancer stem cells and the involvement of fucosyl transferases 1 and 2 in Globo H synthesis. *Proc. Natl Acad. Sci. U. S. A.* 105(33):11667-11672.

81. Peracaula R, *et al.* (2003) Altered glycosylation pattern allows the distinction between prostate-specific antigen (PSA) from normal and tumor origins. *Glycobiology* 13(6):457-470.

82. Gilewski T, *et al.* (2001) Immunization of metastatic breast cancer patients with a fully synthetic globo H conjugate: a phase I trial. *Proc. Natl Acad. Sci. U. S. A.* 98(6):3270-3275.

83. Ragupathi G, *et al.* (1999) A Fully Synthetic Globo H Carbohydrate Vaccine Induces a Focused Humoral Response in Prostate Cancer Patients: A Proof of Principle. *Angew. Chem. Int. Ed. Engl.* 38(4):563-566.

84. Slovin SF, *et al.* (1999) Carbohydrate vaccines in cancer: Immunogenicity of a fully synthetic globo H hexasaccharide conjugate in man. *Proc. Natl Acad. Sci. U. S. A.* 96(10):5710-5715.

85. Chang CF, *et al.* (2011) Rapid characterization of sugar-binding specificity by in-solution proximity binding with photosensitizers. *Glycobiology* 21(7):895-902.

86. Manimala JC, Roach TA, Li Z, & Gildersleeve JC (2006) High-Throughput Carbohydrate Microarray Analysis of 24 Lectins. *Angew. Chem. Int. Ed. Engl.* 45(22):3607-3610.

87. Manimala JC, Roach TA, Li Z, & Gildersleeve JC (2007) High-throughput carbohydrate microarray profiling of 27 antibodies demonstrates widespread specificity problems. *Glycobiology* 17(8):17C-23C.

CHAPTER 2

Identifying the Fucose Proteome from Rat Cortical Neurons

Introduction

Detailed studies of glycans and their functional roles have been hindered by a lack of tools. However, the recent development of methods such as metabolic labeling with non-natural sugar analogs has made it possible to more readily perturb and profile glycans. The strategy of metabolic labeling with non-natural sugar analogs, originally pioneered by Bertozzi and co-workers (1), relies on the uptake of non-natural monosaccharide analogs into endogenous biosynthetic pathways and their subsequent incorporation into glycoconjugates. As the non-natural analog contains a reactive bioorthogonal group (e.g., azide, alkyne, ketone), glycoconjugates containing the monosaccharide can be covalently tagged with a variety of chemical reporters, including enzymatic, fluorescent, and affinity labels (2-4).

In order to specifically tag a metabolically labeled glycan, we can take advantage of a bioorthogonal ligation strategy, in which a detection tag is chemoselectively reacted with the metabolically labeled glycan. Bioorthogonal ligation strategies include oxime chemistry, in which ketone/aldehyde is reacted with an amine nucleophiles (5, 6); the Staudinger ligation, in which a triarylphosphine reacts with an azide to form an amine (7, 8); the Cu(I)-catalyzed [3+2] azide-alkyne cycloaddition (CuAAC), in which an azide reacts with an alkyne to form a triazole (9); or strain-promoted azide-alkyne cycloaddition (SPAAC), in which an azide reacts with a strained alkyne (Figure 2.1) (10). In each of these reactions, two bioorthogonal reactive groups, which are not natively found within the cellular environment, are reacted rapidly at physiological conditions to form a covalent bond between the structure of interest and a tag that is conducive to the desired mode of detection.

Metabolic labeling can be a powerful approach to enrich glycoproteins for proteomic analysis (2-4). Once a non-natural sugar analog is incorporated within cellular glycans, the glycan of interest

can be tagged using a bioorthogonal ligation strategy with an affinity probe. Subsequent enrichment and purification of the target glycans allows for proteomic identification. Non-natural sugar analogs that have been utilized for proteomic analyses include azido-*N*-acetylgalactosamine (GalNAz) to label O-linked mucin type glycoproteins (11), alkynyl- or azido-*N*-acetylmannosamine (alkynyl ManNAc or ManNAz) to label sialylated glycoproteins (3), and alkynyl- or azido-*N*-acetylglucosamine (GlcNAz

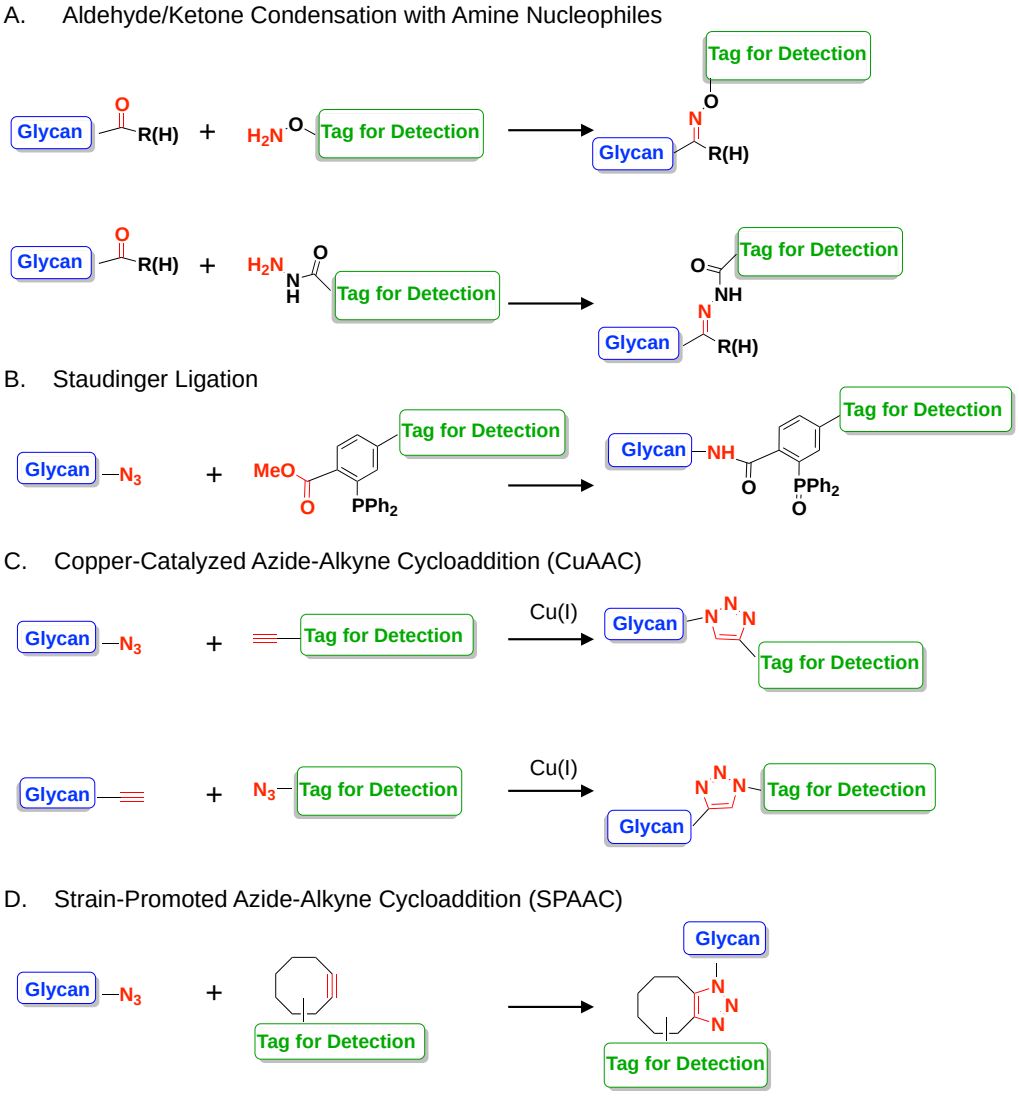

Figure 2.1 Bioorthogonal ligation strategies. (A) Aldehyde/ketone condensation with amine nucleophiles (B) the Staudinger ligation (C) CuAAC chemistry (B) SPAAC chemistry

or GlcNAlk) to label *O*-glcnacylated proteins (12). For example, Chi-Huey Wong and coworkers have used the alkynyl ManNAc analog for the enrichment and proteomic identification of sialylated glycoprotein in a strategy termed GIDmap (glycoprotein identification and glycan mapping) (3). In this strategy, sialylated N-linked glycoproteins in PC3 cells were metabolically labeled with alkynyl ManNAc, bioorthogonally tagged with an affinity probe, and isolated before analysis by multidimensional nano-LC-MS^2. Similarly, O-linked mucin type glycoproteins have been metabolically labeled with GalNAz and enriched for proteomic identification in PC3 cells (11). While metabolic labeling with non-natural fucose analogs has been used to detect fucosylated glycans in multiple biological systems (2, 13), the technique has not yet to date been applied to proteomic analyses in the mammalian neuronal system.

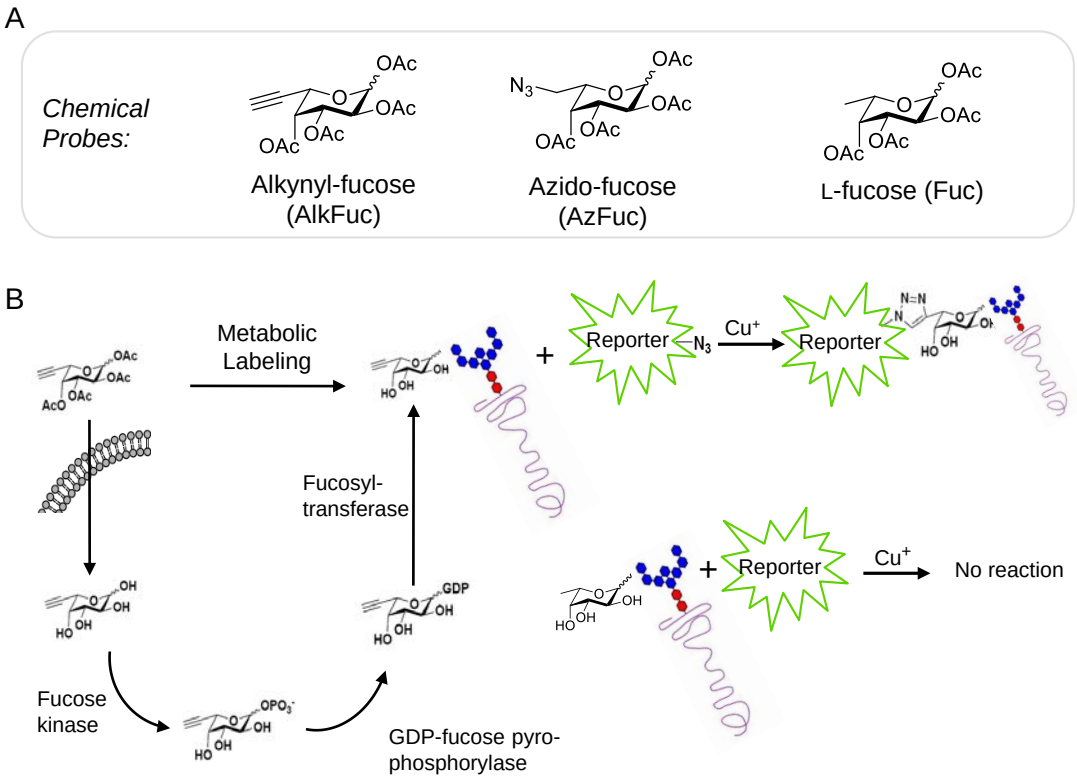

Figure 2.2 Metabolic labeling with non-natural fucose analogs. (A) Non-natural fucose analogs AlkFuc, AzFuc and the natural control analog, Fuc (B) AlkFuc, AzFuc, or Fuc diffuse through the cell membrane and are incorporated into cellular glycans via the salvage pathway. Once incorporated, the fucose analogs can be detected using bioorthogonal ligation strategies with the appropriate reporters.

In the following chapter, we explore the potential of metabolic labeling using non-natural fucose analogs to identify fucosylated glycoproteins in primary neurons. We use the non-natural fucose analogs alkynyl fucose (AlkFuc), azido fucose (AzFuc), and as a control, natural fucose (Fuc; Figure 2.2A). In all cases, the sugar analogs are peracetylated to allow diffusion across the cellular membrane. These molecules are incubated in the cellular growth media where they diffuse into the cells and are available for incorporation into cellular glycans via the fucose salvage pathway, one of the two cellular pathways by which fucose is incorporated into glycans (Figure 2.2B). Once the non-natural analogs are incorporated, the azide or alkyne chemical handle facilitates the chemical detection of fucosylated glycans. Cellular lysates that have been metabolically labeled with AlkFuc or AzFuc can be tagged with the corresponding reactive probe to allow enrichment and identification. Cellular lysates that have been metabolically labeled with the control analog Fuc will not undergo any reaction. We demonstrate that an AlkFuc analog can be successfully incorporated into neuronal proteins, both in culture and *in vivo.* Additionally, we identify the first fucose proteome from cortical neurons, identifying proteins involved in cell adhesion, neuronal signaling, and synaptic transmission.

Results and Discussion

Non-natural Fucose Analogs are Incorporated into Neuronal Glycoproteins

We first examined if the non-natural fucose analogs AlkFuc and AzFuc could be incorporated into neuronal glycoproteins. We expected that labeling of neuronal glycoproteins might be challenging due to the facts that neuronal cells are post-mitotic and that fucose is expressed in fairly low abundance (14). Indeed, when labeling with AzFuc was compared to parallel labeling experiments with azido-*N*-acetylmannosamine (ManNAz) and azido-*N*-acetylgalactosamine (GalNAz), two sugar analogs commonly used to probe N- and O- glycoproteins and glycolipids, the extent of AzFuc labeling was significantly lower than that of ManNAz or GalNAz (Figure 2.2). Cortical neurons at 4 DIV were treated with either 50 μM AzFuc, ManNAz, GalNAz, or an equivalent volume of the vehicle DMSO. Subsequent to 3 d of treatment, cell were lysed and the lysates were reacted with the

corresponding alkyne-biotin tag via the [3+2] copper catalyzed azide-alkyne cycloaddition (CuAAC). Analysis by SDS-PAGE followed by Western blot and detection with streptavidin conjugated to Alexa Fluor 680 revealed AzFuc, ManNAz, and GalNAz labeled proteins. Though each sampled contained an equivalent amount of protein as determined by tubulin blot, the extent of labeling by ManNAz and GalNAz was significantly higher. Besides the low abundance of fucosylated glycans in general, it is also possible that the relevant biosynthetic enzymes are less tolerant of the non-natural fucose analogs than other sugar analogs, contributing to the low-level of metabolic incorporation (15).

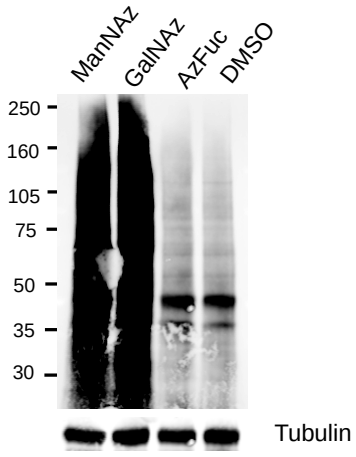

Figure 2.3 Incorporation of ManNAz, GalNAz, and AzFuc into neuronal glycoproteins. Cortical neurons at 4 DIV were incubated with 50 μM ManNAz, GalNAz, AzFuc, or an equivalent volume of vehicle, for 3 d. Cells were lysed, "click" labeled, and probed for labeling after Western blot.

However, both the AlkFuc and AzFuc analogs could be incorporated into neuronal proteins. Cortical neurons at 4 DIV were similarly treated with 50 - 200 μM AzFuc, AlkFuc, or Fuc in neuronal growth media for 3 d. Subsequent to treatment, cells were lysed and the lysates were reacted with the alkyne-biotin tag via CuAAC chemistry. The lysates were resolved by SDS-PAGE followed by Western blot and detection with streptavidin conjugated to Alexa Fluor 680, revealing metabolically labeled proteins in cells treated with AzFuc and AlkFuc, but not Fuc (Figure 2.3). However, treatment with AzFuc followed by CuAAC labeling with alkyne-biotin gave significantly higher background than

treatment with AlkFuc followed by CuAAC with azido-biotin (Figure 2.3). Treatment of neurons with any concentration of AzFuc also resulted in significant cytotoxicity, consistent with previous reports (2). Though previous studies have utilized concentrations of 200 μM AlkFuc or AzFuc (2), concentrations above 100 μM were toxic to cultured neurons even in the case of AlkFuc, and thus

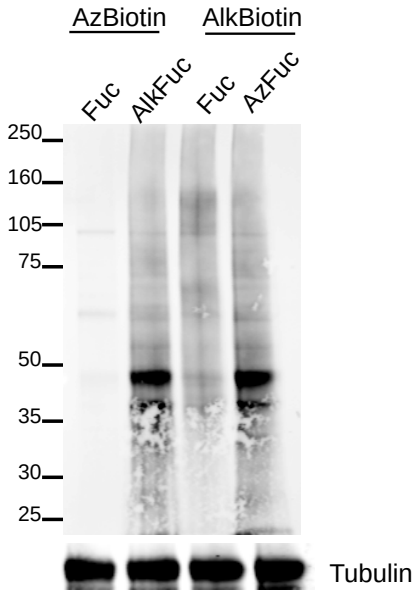

limited the concentrations of metabolic labeling. Due to the cytotoxicity and increased background resulting from AzFuc treatment and alkyne-biotin labeling, we proceeded with our studies utilizing only AlkFuc. To determine the specificity of the AlkFuc treatment, cells were co-treated with tunicamycin, an N-glycosylation inhibitor. As previous reports suggest that the majority of neuronal fucosylation exists in complex N-linked glycans (16), we expected treatment with tunicamycin to largely abolish AlkFuc labeling.

Figure 2.4 AlkFuc labeling results in higher signal. Cortical neurons at 4 DIV were incubated with either 100 μM AlkFuc, AzFuc, or Fuc. Lysates were labeled with either azido-biotin or alkyne-biotin and probed with streptavidin conjugated IR Dye 800. Labeling with alkyne-biotin resulted in increased background when compared with labeling with azido-biotin.

Cortical neurons at 4 DIV were treated with 100 μM AlkFuc or Fuc for 3 d, and co-treated during the last day of metabolic labeling with either 25 μM tunicamycin in ethanol or vehicle (0.01% final concentration), followed by lysis and CuAAC labeling with azido-biotin. Analysis by Western blot indicated that AlkFuc labeling had been abolished in cells treated with tunicamycin (Figure 2.4), suggesting that AlkFuc was specifically incorporated into N-linked glycoproteins. Thus, the AlkFuc analog is incorporated into neuronal glycoproteins, and specifically into N-linked glycoproteins.

Given our goal of undertaking proteomic studies with the AlkFuc analog, it was necessary to maximize the labeling of fucosylated glycoproteins in neurons. In order to optimize labeling, we more closely investigated CuAAC reaction conditions. Previously reported conditions included a labeling solution of 50 mM $CuSO_4$ as the source of the copper catalyst, 2 mM sodium ascorbate as the Cu(II) reducing agent, 0.1 mM tristriazoleamine ligand (triazole), and 0.1 mM azido-biotin; the suggested reaction time was a period of 1 h at rt (17).

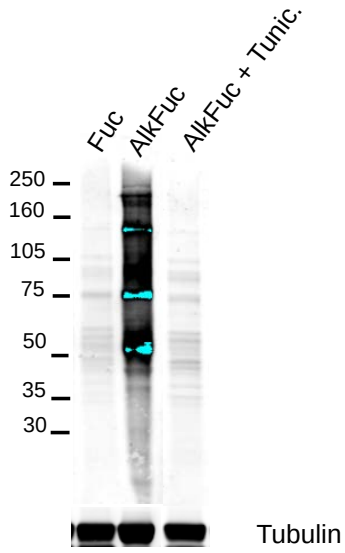

Figure 2.5 AlkFuc is incorporated into N-linked neuronal glycoproteins. Cortical neurons at 4 DIV were metabolically labeled with 100 μM Fuc or AlkFuc for 3 d before the cells were lysed and the lysates labeled with azido-biotin. SDS-PAGE and Western blotting with a streptavidin conjugated IR Dye 800 reveals specifically labeled glycoproteins in cultures metabolically labeled with AlkFuc, but not Fuc. Co-treatment with 25 μM tunicamycin abolished the signal, indicating that AlkFuc is incorporated into N-linked glycoproteins.

These reaction conditions often resulted in indistinct labeling and caused significant protein degradation of AlkFuc treated neuronal glycoproteins. Upon investigation of the specific parameters, we noted that $CuSO_4$ seemed to cause protein degradation, as opposed to CuBr (Figure 2.5). Freshly prepared 50 mM CuBr was subsequently used as the source of the copper catalyst for lysate labeling conditions, and the concentration of the sodium ascorbate was maintained. The addition of sodium ascorbate ensured that the copper catalyst remained as the active Cu (I) species. Additionally, decreased protein degradation was observed when the reaction was allowed to proceed for 3 h at 4 °C, rather than 1 h at rt.

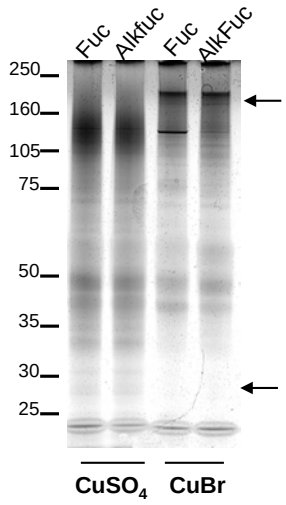

Figure 2.6 $CuSO_4$ causes protein degradation during CuAAC chemistry. Cell lysates, labeled with Fuc and AlkFuc, were labeled via CuAAc using two different sources of copper and visualized by silver stain. Arrows indicate high molecular weight proteins that appear with CuBr, but not with $CuSO_4$, and low molecular proteins that appear with $CuSO_4$, but not with CuBr.

Capture of Fucosylated Glycoproteins by Streptavidin-Affinity Chromatography

Subsequent to optimizing the CuAAC parameters, we sought to develop a protocol for the affinity purification and proteomic analysis of neuronal fucosylated glycoproteins (Figure 2.7). Briefly, our strategy would entail metabolically labeling fucosylated glycoproteins in primary cortical neurons, tagging labeled proteins with an affinity probe via CuAAC chemistry, and affinity purification of tagged proteins. Isolated proteins would then be resolved by SDS-PAGE and

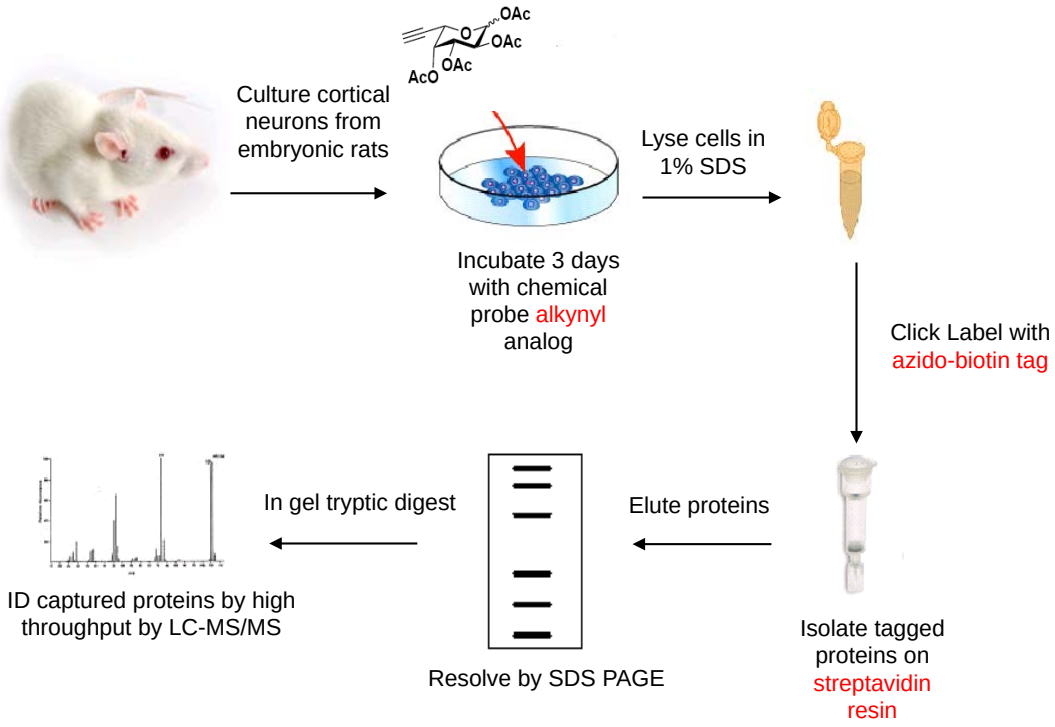

Figure 2.7 Strategy for the identification of the fucose proteome in rat cortical neurons via metabolic labeling, CuAAC chemistry, and affinity chromatography.

identified by LC-MS^2 after in-gel digestion. As we were metabolically labeling relatively low amounts of protein due to the apparent low abundance of fucosylated glycoproteins and the sub-quantitative incorporation of the metabolic labeling analogs, it was critical to minimize any non-specific interactions of highly abundant proteins, such as tubulin or actin, with the enrichment resin**.** Because of these limitations, we decided to utilize streptavidin affinity chromatography to capture biotin-labeled fucosylated glycoproteins due to the strong streptavidin-biotin interaction. Due to the strength of the streptavidin-biotin interaction, it was possible to take advantage of very stringent wash conditions to minimize any non-specific interactions. However, due to the strength of the streptavidin-biotin interaction, we also expected that it would be difficult to elute the captured proteins. As such, we spent a significant amount of time optimizing capture conditions to develop a protocol for the capture and proteomic identification of AlkFuc labeled glycoproteins. Initial efforts

were complicated by low capture efficiency. We briefly attempted other capture and elution methods such as avidin affinity chromatography, or utilizing a cleavable disulfide biotin tag for more efficient elution (data not shown), but we determined that streptavidin resin yielded the most efficient capture. Metabolically labeled neurons were biotinylated via CuAAC and enriched over streptavidin resin. Based on previous reports, we initially limited our washes to 40 CV of PBS (3). However, these washes were insufficient to minimize non-specific background, as there was no significant enrichment apparent in eluates after PBS-only washes (Figure 2.7A). To minimize non-specific interactions, we developed a wash protocol that included (i) a low salt, high detergent wash, (ii) a high salt, low detergent wash (18), (iii) a 4 M Urea, 1% SDS wash, followed by (iv) a 50 mM Tris, pH 7.5 wash. All washes were carried out at 4 °C, except for the urea-SDS wash, which was preformed at rt. Following extensive washing, the proteins were eluted in boiling elution buffer consisting of 6 M urea, 2 M thiourea, 30 mM biotin, and 2% SDS at pH 12 (19). Any milder conditions, such as a standard sample buffer elution, resulted in sub-quantitative elution (Figure 2.8B).

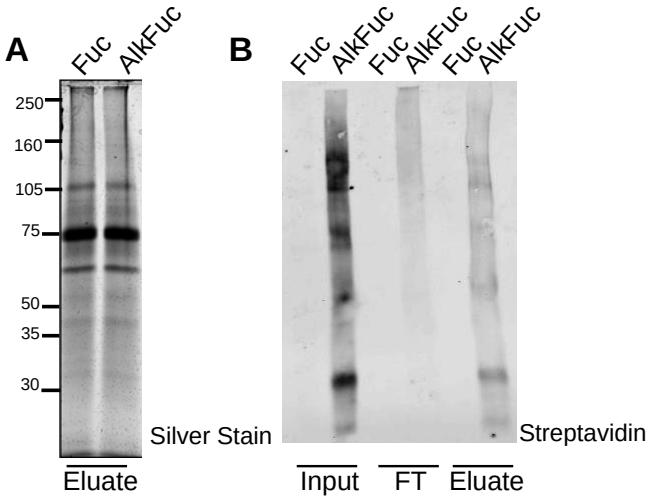

Figure 2.8 Optimization of Streptavidin Capture. (A) Silver stain of streptavidin-enriched proteins after of metabolic labeling and CuAAC. Elution after mild washes shows high non-specific binding. (B) Elution with 2X sample buffer does not yield quantitative elution. Elution shows no enrichment when the input (labeled lysate), flow through (FT), and elution are blotted with streptavidin to detect biotinylated proteins.

With an optimized capture strategy in hand, we proceeded to carry out the enrichment of neuronal fucosylated glycoproteins for LC-MS/MS analysis. Cortical neurons 8 DIV in culture were metabolically labeled and tagged with biotin as described above, and the biotinylated glycoproteins were isolated by streptavidin affinity chromatography. Eluates were concentrated and subsequently resolved by SDS-PAGE and silver stained to identify specific proteins present in the AlkFuc treated lysates, demonstrating a clean capture of neuronal fucosylated glycoproteins (Figure 2.8A). While some background was evident in the Fuc treated lysates, we observed significantly more proteins enriched from the AlkFuc treated lysates. Specifically, we observed fucosylated glycoproteins at 120, 110, 105, 90, 76, 75, 65, 60, 55, 45, 43, 40, 37, and 36 kDa. Seventeen bands from each lane (Figure 2.9B) were analyzed by LC-MS/MS in collaboration with Dr. Eric Peters at the Genomics Institute of the Novartis Research Foundation. The identified peptides were searched in Mascot against the SwissProt Database 57.15 and analyzed in Scaffold (Table 1). Proteins were considered putative fucosylated glycoproteins when at least three unique peptides were observed, resulting in a 99% probability that the protein is accurately identified (additional details in Experimental Methods).

We identified eleven proteins, 4 of which had not yet been previously identified (starred). The putative fucosylated glycoproteins could be broadly categorized into four classes, including cell adhesion molecules, selectin antigens, cell signaling proteins, and those proteins involved in neuronal growth and morphology (Table 1). We did observe significant protein degradation in the sample, as many of the proteins identified ran lower than their true molecular weights, possibly due to harsh processing conditions. However, we successfully identified several fucosylated glycoproteins, including NCAM and lysosomal-associated membrane glycoproteins 1 and 2, which have been previously reported to be fucosylated (20-22), validating this approach for the identification of fucosylated glycoproteins. Additionally, we identified proteins involved in neuronal growth and modulation, such as neuromodulin/growth-associated protein 43 (GAP-43) and the myristoylated alanine-rich protein kinase C susbtrate (MARCKS) (23-29). Notably, both MARCKS and GAP-43

are known to be membrane-associated, cytosolic proteins GAP-43 does have several potential N-glycosylation sites

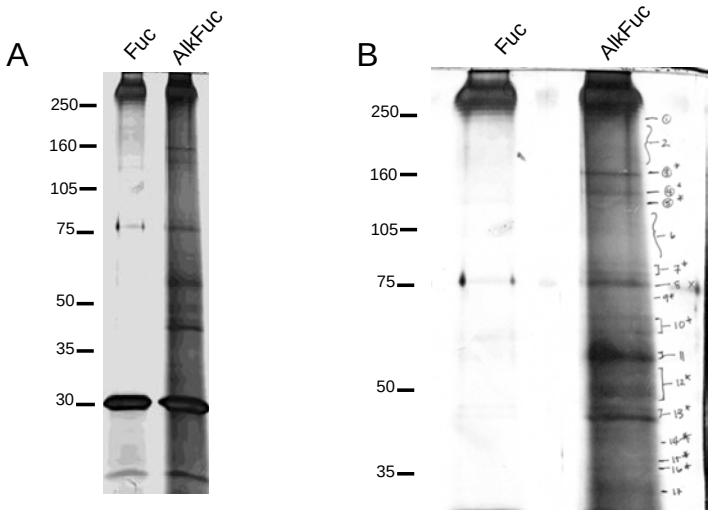

Figure 2.9 (A) Silver stain of proteins isolated from Fuc and AlkFuc labeled cortical neurons after CuAAC with azido-biotin and streptavidin affinity chromatography. (B) Bands excised for proteomic analysis.

Table 1 Fucosylated proteins identified from rat cortical neurons at 8 DIV

Identified Proteins	Function	Accession No.	MW (kDa)	Peptide No.	Seq. Coverage
	Cell Adhesion Molecules				
Neural Cell Adhesion Molecule	cell adhesion	P13596.1	95	12	22
Cell Adhesion molecule 2	cell adhesion	Q1WIM2.2	48	4	13
Phospholipase	Lipid metabolism	Q5FVH2.1	54	3	6
Prolow-density lipoprotein receptor-related protein	Regulates lipid metabolism and neural development	Q91ZX7.1	505	4	1
	Cell Growth/Morphology				
Myristoylated alanine-rich C-kinase substrate	Maintain Dendritic Spine Morphology	P30009.2	30	4	21
MARCKS-related protein	Maintain Dendritic Spine Morphology	Q3KRE8.1	20	3	31
Neuromodulin	Axonal Growth Development and Plasticity	P07936.1	24	4	22
	Cell Signaling				
14-3-3 protein gamma	Regulation of signaling cascades	P61983.2	28	3	20
14-3-3 protein theta	Regulation of signaling cascades	P63102.1	28	4	19
	Selectin Antigens				
Lysosome-associated membrane glycoprotein 1	Cellular Protein Degradation	P14562.1	44	4	11
Lysosome-associated membrane glycoprotein 2	Cellular Protein Degradation	P17046.2	45	3	9

.

based on consensus sequence, and has been suggested to be glycosylated (30). The MARCKS protein was recently suggested to bind the polysialic acid structures of NCAM (PSA-NCAM) (31), raising the possibility that MARCKS, also reported to be fucosylated by lectin affinity chromatography (32), was purified non-specifically along with NCAMWe also undertook the identification of the fucose proteome in 14 DIV neurons with the goal of identifying proteins that may be more highly expressed in mature neurons. We relied on the biotin-streptavidin enrichment strategy (Figure 2.9A and 2.9B); proteins identified are summarized in Table 2. We identified 51 putative fucosylated glycoproteins, of which 23 have not yet been reported (starred). Proteins identified have a wide range of biological roles and can be broadly categorized into four major functional classes: cell adhesion molecules, ion channels and solute carriers/transporters, selectin antigens, and synaptic proteins. Once again, several of the putative fucosylated glycoproteins identified, including NCAM, have been previously

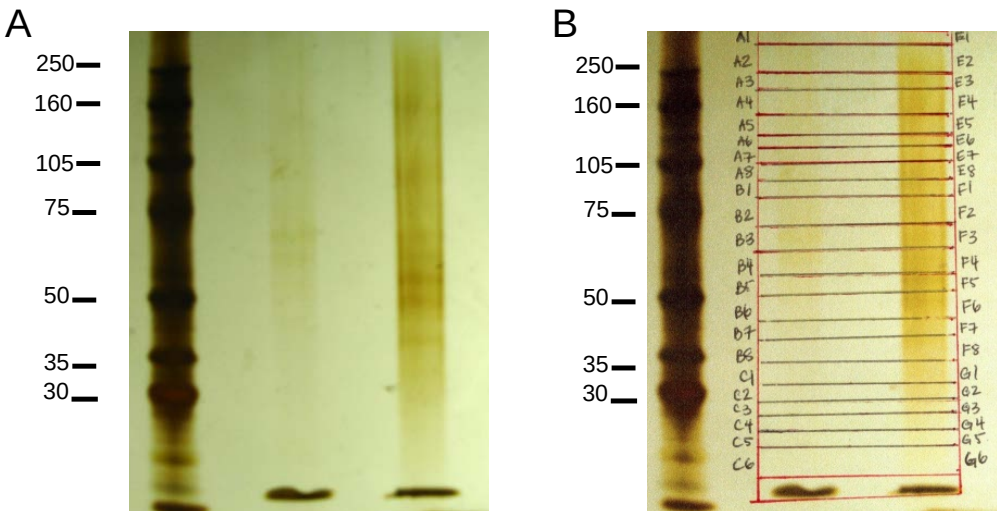

Figure 2.10 Streptavidin enrichment of metabolically labeled fucosylated glycoproteins in 14 DIV neurons. (A) Silver stain of captured fucosylated proteins (B) Bands excised for proteomic analysis.

characterized as fucosylated glycoproteins (21). In addition to NCAM1, we identify L1 CAM and NCAM2, cell adhesion molecules involved in cell adhesion, neuronal migration, axonal fasciculation, and synaptogenesis (33, 34). We also identified the ion channels, voltage-gated calcium channel alpha2/delta subunit and the sodium/potassium transporter ATPase subunits α3 and β1 as putative

Table 2. Fucosylated proteins identified from rat cortical neurons at 14 DIV

Proteins	Function	Accession No.	MW (kDa)	Peptide No.	Seq. Coverage
	Cell Adhesion Molecules				
Contactin-1	Axonal guidance	Q63198.2	113	23	30
Neural cell adhesion molecule 1	neurite outgrowth	P13596.1	95	16	29
Limbic system-associated membrane protein	neurite outgrowth	Q62813.1	38	8	29
Neural cell adhesion molecule L1	neuronal migration and differentiation	Q05695.3	141	4	5
*Neuronal growth regulator 1	axon sproutin	Q9Z0J8.1	38	10	34
Neural cell adhesion molecule 2	neurite outgrowth	O35136.1	93	5	7
*Cadherin-13	axon guidance	P55290.1	78	4	9
Intercellular adhesion molecule 5	leukocyte migration	Q60625.2	97	4	4
Neuronal cell adhesion molecule	neurite outgrowth	P97686.2	134	7	7
Neurofascin	axon targeting, synapse formation	P97685.2	138	4	3
Opioid-binding protein/cell adhesion molecule	synapse formation	P32736.2	38	6	21
*Tyrosine-protein phosphatase non-receptor type substrate 1	neurite outgrowth, synapse formation	P97710.1	56	4	12
Neurotrimin	neurite outgrowth	Q99PJ0.2	38	4	21
*Coxsackievirus and adenovirus receptor homolog	cell adhesion	Q9R066.2	40	6	16
*Protocadherin-10	synapse formation	Q9P2E7.2	113	6	8
Cell adhesion molecule 2	neurite outgrowth	Q00657.2	48	4	9
CD166 antigen	neurite outgrowth	O35112.1	65	5	10
*Neogenin (Fragment)	axon guidance	P61983.2	151	4	4
*Cell adhesion molecule 4	neurite outgrowth	Q1WIM1.1	43	3	12
*Contactin-5	neurite outgrowth, development	P97527.1	121	3	4
*Receptor-type tyrosine-protein phosphatase delta	dendrite morphology	P23468.2	215	3	2
*Protocadherin-9	cell adhesion	Q9HC56.2	136	3	3
*Receptor-type tyrosine-protein phosphatase S	cell adhesion	Q64605.2	212	3	2
IgLON family member 5	cell adhesion	Q8HW98.2	37	5	20
	Selectin Antigens				
Lysosome membrane protein 2	lysosomal transport	P27615.2	54	3	4
Lysosome-associated membrane glycoprotein 1	lysosomal transport	P14562.1	44	7	17
Lysosome-associated membrane glycoprotein 2	lysosomal transport	P17046.2	45	5	13
Golgi apparatus protein 1	binds to E - selectin	Q61543.1	132	7	7
	Ion Channels/Transporters				
4F2 cell-surface antigen heavy chain	solute carrier	Q794F9.1	58	9	24
Sodium/potassium-transporting ATPase subunit alpha-3	ion channel/atp hydrolysis	P06687.2	112	8	10
Sodium/potassium-transporting ATPase subunit beta-1	ion channel/atp hydrolysis	P07340.1	35	5	17
Voltage-dependent calcium channel subunit alpha-2/delta-1	ion channel	O08532.1	125	9	9
*V-type proton ATPase 116 subunit a isoform 1	proton pump	Q9Z1G4.3	96	3	4
*Voltage-dependent anion-selective channel protein 2	ion channel	P81155.2	32	5	21
*ADP/ATP translocase 1	transporter		33	3	
ATP synthase subunit beta, mitochondrial	ion transporter	P19023.1	59	4	11
Basigin	blood brain barrier	P26453.2	42	3	7
*Neuronal membrane glycoprotein M6-b	maintenance of actin cytoskeleton	P35803.2	36	3	6
	Neurotransmission and Synaptic Vesicle Proteins				
*Neuronal pentraxin receptor	Ca^{2+} binding glycoproteins	O35764.1	52	3	6
*Metabotropic glutamate receptor 7	neurotransmission	P35400.1	102	3	4
*Gamma-aminobutyric acid receptor subunit alpha-5	neurotransmitter receptor	P19969.1	52	3	8
Excitatory amino acid transporter 1	glutamate transporter	P24942.2	60	3	9
Large neutral amino acids transporter small subunit 1	glutamate transporter	Q63016.2	56	5	10
*Metabotropic glutamate receptor 5	glutamate receptor	P31424.2	132	4	4
*Glutamate receptor 1	neurotransmission	P23818.1	102	3	4
Prolow-density lipoprotein receptor-related protein 1	neurotransmission, endocytosis, intracellular signaling	Q91ZX7.1	505	15	4
*Synaptic vesicle glycoprotein 2A	maintains RRP of secretory vesicles	Q02563.2	83	3	5
Synaptotagmin-1	SV cycling	P21707.3	48	8	21
*Vesicle-associated membrane protein 2	Vesicle fusion	Q9N0Y0.3	13	3	34
ADP-ribosylation factor 1	vesicle regulation, recruit effectors to the GA, G protein	P84079.2	21	4	24
Major prion protein	membrane, GA, role in neuronal development and synaptic plasticity	P13852.2	28	3	13

fucosylated glycoproteins, which have functions in ion transport and neurotransmission (35), suggesting roles for fucosylation in ion transport, membrane excitability, ATP metabolism.

Notably, we identify several synaptic-vesicle associated proteins, such as synaptic vesicle glycoprotein 2A, synaptotagmin 1, and vesicle-associated membrane proteins 2 (Table 2), which have important roles in the docking and regulation of synaptic vesicle fusion (36). Synaptotagmin 1 has been shown to be an N- and O-linked glycoprotein, with glycosylation being critical to the targeting of synaptotagmin 1 to synaptic vesicles (37, 38). The detection of several synaptic proteins is consistent with a role for fucosylated glycans in synaptic signaling (32, 39). We also identify the glutamate receptor 1, metabotropic glutamate receptor 1, and GABA receptor subunit α5, with roles in neurotransmission and hippocampal-dependent learning (40). Taken together, the protein identifications suggest roles for fucose in cell adhesion and morphology, neuronal communication and synaptic signaling.

Cloning and Validation

In order to confirm the fucosylation of the putative fucosylated glycoproteins identified, we undertook a biochemical validation of selected proteins. To probe the fucosylation of endogenous neuronal proteins, neuronal cultures were metabolically labeled with the AlkFuc or Fuc molecules for 3 d, followed by CuAAC labeling with azido-biotin and enrichment of labeled proteins over streptavidin resin. The enriched fraction was probed for NCAM and L1 CAM. The presence of NCAM and L1 CAM in the lysates labeled with AlkFuc, but not in the lysates labeled with Fuc, confirmed the fucosylation of NCAM and L1CAM. As a negative control, we blotted for p44 MAPK, a kinase not known to be glycosylated. P44 MAPK was not enriched in the labeled lysates, indicating the specific labeling and enrichment of fucosylated glycoproteins (Figure 2.10A).

In addition to endogenous proteins, we biochemically validated the fucosylation of proteins over-expressed in HeLA cells. Specifically, the proteins MARCKS, voltage-gated calcium channel alpha2/delta subunit (Cacna3d1), and synaptotagmin 1 (Syt1) were cloned into a pCMV expression vector with a C-terminal 3X FLAG tag to construct FLAG fusion proteins. It should be noted that a

truncated SytI, with the known glycosylation sites intact, but with both lipid domains deleted, was ultimately used for the following validation assay (Syt1_1-140) (37); the presence of the lipid binding domains seemed to lead to non-specific interactions with the CuAAC reagents. The FLAG constructs were over expressed into HeLA cells that were metabolically labeled with AzFuc. The metabolically labeled lysates were then lysed and tagged with alkyne-biotin, followed by FLAG-affinity purification of the protein of interest. The eluates were analyzed by SDS-PAGE and Western blot to probe for the fucosylation of the protein of interest (Figure 2.10B). The detection of the fucosylated protein by streptavidin conjugated to Alexa Fluor 680 in the AzFuc treated lysates, but in the Fuc treated lysates, indicated the specific fucosylation of the protein. As a positive control, FLAG-Synapsin I was similarly expressed in metabolically labeled cells, and affinity purified subsequent to CuAAC labeling. Detection of the enrichment of glycosylated synapsin I in the AzFuc treated lysates is apparent, confirming the validation assay.

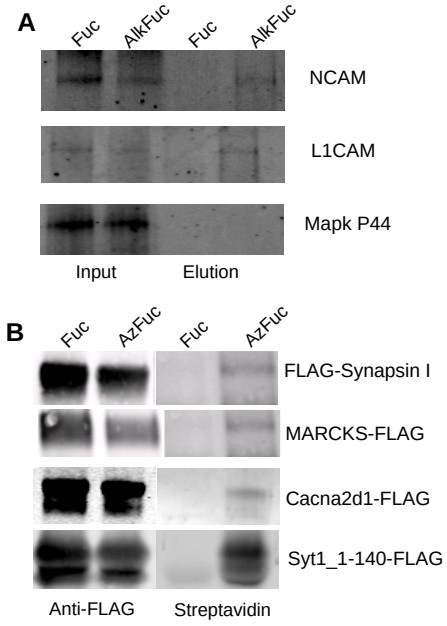

Figure 2.11 Biochemical validation of putative fucosylated glycoproteins. (A) NCAM and L1 CAM, but not the negative control p44 MAPK, are enriched from neurons metabolically labeled with AlkFuc and tagged with azido-biotin before streptavidin affinity purification. (B) FLAG-Synapsin I, MARCKS-FLAG, Cacna2d1-FLAG, and Syt1_1-140 FLAG are labeled with AzFuc when overexpressed in metabolically labeled HeLa cells.

Thus, the specific fucosylation of the proteins NCAM, L1 CAM, MARCKS, Cacna2d1, Syt1_1-140, and Syn I was confirmed using the non-natural fucose analogs, validating their use to probe specific neuronal proteins. Moreover, the fucosylation of two novel proteins, MARCKS and Cacna2d1, was validated, demonstrating the utility of the AlkFuc analog for the proteomic identification of fucosylated glycoproteins.

***In Vivo* Labeling of Fucosylated Glycoproteins.**

Having demonstrated the ability to chemoselectively label fucosylated proteins in dissociated neuronal cultures, we explored the potential to label fucosylated glycans *in vivo* in the brain. Based on previous reports that the expression of fucosylated glycans may be higher in postnatal pups (39), we elected to first attempt *in vivo* labeling in the brains of P1-8 mouse pups. Following protocols approved by the Institutional Animal Care and Use Committee (IACUC), C57/Bl6 pups were cryo-anesthetized and monitored until unresponsive by tail pinch. Using a stereotaxic device modified for mouse pups, 2 μL of 50 mM AlkFuc or Fuc was injected into the hippocampi utilizing a microinjector, using coordinates provided in the Allen mouse brain atlas. Subsequent to the injection, pups were placed on a heating pad and monitored until responsive. After 1 d of survival, pups were humanely euthanized and their brains dissected for analysis by CuAAC. The dissected brain tissue was homogenized and lysed in SDS, and tagged with azido-biotin as previously described. SDS-PAGE and Western blot detection with streptavidin conjugated to Alexa Fluor 680 indicated that some labeling was apparent, but it did not appear that a significant amount of AlkFuc was incorporated (Figure 2.12). To probe the subcellular localization of AlkFuc incorporation *in vivo* in more detail, the brains were removed, immersion fixed in paraformaldehyde solution, and sliced for immunohistochemistry. Briefly, slices

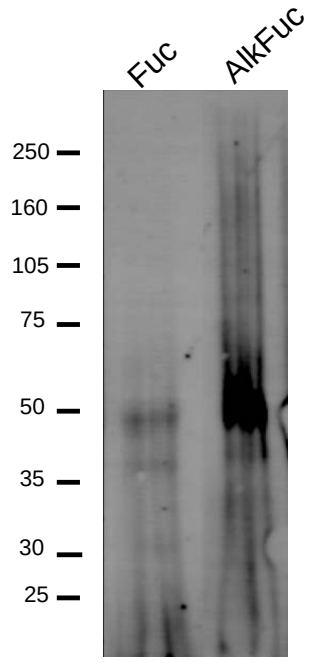

Figure 2.12 *In vivo* labeling of fucosylated glycoproteins in postnatal mice.

prepared on the Lyca Cryostat were blocked in goat serum and labeled via CuAAC overnight. To carry out CuAAC labeling, the CuAAC reaction mixture was prepared in PBS with 25 mM $CuSO_4$, 1 mM sodium ascorbate, .05 mM triazole ligand, and 0.05 mM azido-biotin, and incubated over the slices on the coverslip overnight at 4 °C. Subsequent to CuAAC labeling, the slices were washed in PBS and stained with DAPI or streptavidin conjugated to Alexa Fluor 546 to visualize AlkFuc labeling. When compared to the nuclear stain DAPI, it was not apparent that AlkFuc labeling was specifically localized to any subcellular structures (Figure 2.13). The staining also seemed localized in close proximity to the injection site, suggesting that the AlkFuc did not permeate the tissue.

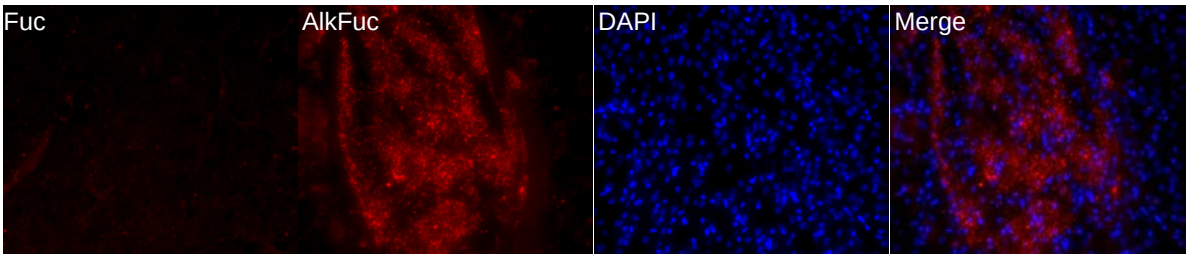

Figure 2.13 *In vivo* labeling of fucosylated glycoproteins in postnatal mice. Fuc or AlkFuc was injected into the hippocampi of WT postnatal mouse pups, after which the pups were humanely euthanized and the brains were dissected and lysed, labeled via CuAAC, and analyzed by histology.

In order to increase AlkFuc incorporation, we reasoned that it might be necessary to administer multiple doses of AlkFuc. As attempting survival surgery in P3 pups to such an extent was impractical, we decided to attempt injections into adult mice, in which we could readily insert cannulas for multiple injections. Importantly, we were able to utilize $Fx^{-/-}$ mice, which are deficient in the FX enzyme, a necessary enzyme for the biosynthesis of fucose (41). Consequently, the transgenic mice must be supplemented with exogenous fucose for survival. The deficiency in the fucose biosynthetic pathways implied to us that incorporation of the non-natural fucose analog could potentially be greater than in mice with intact biosynthetic machinery.

Using stereotaxic device, adult transgenic $Fx^{-/-}$ mice that had been fucose-starved (i.e. fed with normal rodent chow, rather than fucose-supplemented chow) for one week and then implanted

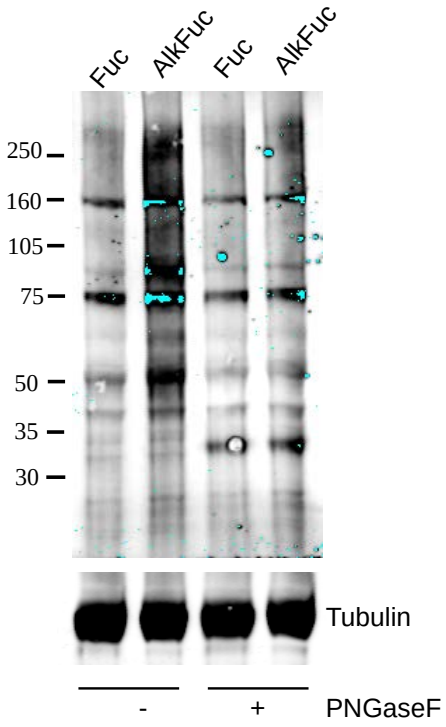

Figure 2.14 *In vivo* labeling of fucosylated glycoproteins in adult mice. Fuc or AlkFuc was injected via microcannula into the hippocampi of $Fx^{-/-}$ mice, after which the mice were humanely euthanized and the tissue was dissected, labeled via CuAAC, and analyzed by Western blot. Treatment with PNGase F significantly abolished signal from the AlkFuc labeled tissue, suggesting that AlkFuc was specifically incorporated into N-linked glycoproteins.

with microcannulae with access to the hippocampus, following approved survival surgery protocols. AlkFuc and Fuc were injected into the hippocampus through the cannula every 48 h for one week, for a total of three injections. One day subsequent to the final injection, the mice were humanely euthanized, and the hippocampal tissue was removed, homogenized, and labeled via CuAAC with azido-biotin. Lysates were resolved by SDS-PAGE and visualized by blotting with IRDye 800 conjugated to streptavidin (Figure 2.14). We observed a number of fucosylated glycoproteins between 50 and 250 kDa in the lysate from the AlkFuc treated animals, whereas there was very little labeling in control fucose injected animals. Notably, AlkFuc labeling was significantly decreased when the lysate was treated with PNGase F, a glycosidase that cleaves N-linked glycans, suggesting that the AlkFuc analog was specifically incorporated into N-linked glycans *in vivo*.

In order to probe the subcellular localization of AlkFuc incorporation *in vivo* in more detail, euthanized mice were perfusion fixed in paraformaldehyde solution. Following dissection, cryopreservation and slicing, brain slices were subjected to immunohistochemistry. However, though signal was apparent by Western blot, no specific signal was apparent in brain slices and the subcellular localization of AlkFuc could not be clarified. Whether incorporation of AlkFuc was too low or whether CuAAC conditions tested were not amenable to histological detection has not yet been determined.

However, the ability to label fucose *in vivo* does open new avenues where we might monitor fucosylation in living animals, particularly to elucidate the proteins involved in learning and memory consolidation. While CuAAC chemsitry is not always conducive to *in vivo* labeling (42), there have been recent developments in reagents that are capable of labeling azide and alkynye reporters *in vivo*, including strained promoted azide alkyne cycloaddition and chelating ligands that reduce the toxicity of copper (10, 43). Notably, these reagents have been used to label glycoconjugates in mice and zebrafish *in vivo*, suggesting their potential use in monitoring fucosylation dynamics in living mice (44, 45). Such studies will reveal molecular insights into learning and memory that have been unattainable by conventional biochemical approaches.

In summary, we exploited the non-natural fucose analog AlkFuc to probe the fucose proteome in cultured neurons and the brain *in vivo.* We show that AlkFuc is incorporated into N-linked glycoproteins in rat cortical neurons and identify the fucose proteome. We identified cell adhesion molecules, selectin antigens, ion channels and ATPases, and synaptic proteins, suggesting roles for fucose in cell adhesion and morphology, neuronal signaling, and synaptic vesicle cycling and neurotransmission.

Experimental Procedures

Copper-catalyzed azide-alkyne cycloaddition (CuAAC) reagents. Peracetylated natural Fucose (Fuc), peracetylated alkynyl-fucose (AlkFuc), peracetylated azido-fucose (AzFuc), azido-biotin, and triazole ligand were synthesized by Sarah Hanson in the laboratory of Dr. Chi-Huey Wong as previously described (17). All molecules were stored at -20 °C in DSMO at the following concentrations: 400 mM Fuc, 400 mM AlkFuc, 400 mM AzFuc, 50 mM azido-biotin, and 50 mM triazole ligand.

Rat Embryonic Cortical and Hippocampal Neuronal Culture. Timed-pregnant Sprague-Dawley rats at embryonic day 18 (E18) were purchased from Charles River Laboratories (Kingston, Mass)

and euthanized in accordance with IACUC protocols. Hippocampal neurons were cultured using a procedure modified from Goslin and Banker (46). Briefly, the hippocampi and cortices of E18 rat embryos were dissected and transferred to 4.5 mL of ice-cold Calcium and Magnesium Free-Hank's Balanced Salt Solution (CMF-HBSS). Trypsin (2.5%, EDTA free) was added to 5 mL, and the tissue was incubated for 15 min at 37 °C. The trypsin solution was then removed and the tissue sample washed three times with 5 mL of CMF-HBSS. Cells were then dissociated from the tissue in 1 mL of CMF-HBSS by passing through a P1000 pipet tip 10-20 times. The cells were counted, diluted into Minimal Eagle's Medium (MEM) supplemented with 10% fetal bovine serum (FBS; Life Technologies) and penicillin/streptomycin (10,000 U/mL; Life Technologies). Cortical neurons were plated on 10-cm tissue culture plates (BD Falcon) at a density of 20 million cells per plate. Hippocampal neurons were seeded on poly-DL-ornithine-coated glass coverslips (Carolina Biological) at a density of 75 cells/mm^2 (100 µL/coverslip) in a 12-well plate (BD Falcon). After 30 min, 500 µL of supplemented Neurobasal medium (47.5 mL Neurobasal medium (Life Technologies); 0.5 mL L-glutaMAX (200 mM; Life Technologies); 0.5 mL penicillin/streptomycin (10,000 U/mL; Life Technologies); 1.0 mL B-27 serum-free supplement (50X stock; Life Technologies); 50 µL of 0.5 M kynurenic acid in 1 N NaOH) was added to each well. The cultures were maintained in 5% CO_2 at 37 °C, and half the media was changed once a week.

Mouse Embryonic Fibroblast Isolation and Culture. Timed pregnant $Fx^{-/-}$ mice at E15 were euthanized and the embryos removed in accordance with IACUC protocols. Mouse embryonic fibroblasts were isolated by separating each embryo from the placenta and cutting away the brain and any dark red organs. The tissue was washed with ice cold CMF-HBSS, minced with sterile razor blades, and digested with trypsin as described above. Cells were dissociated from the tissue in 1 mL of CMF-HBSS by passing the tissue suspension through a P1000 pipet tip 20 times. The cells were diluted into DMEM supplemented with 10% FBS and penicillin/streptomycin (10,000 U/mL) and plated at the equivalent of one embryo per 10 cm plate in 10 mL media. Media was replaced the

following day, and cells were split 1:5 after confluent (3 to 5 days in culture). Cells were either maintained in culture for experiments or frozen in DMEM supplemented with 10% DMSO (Fisher) and 30% FBS and stored in liquid nitrogen until needed for culture.

HeLa Cell Culture. HeLa were cells grown in DMEM medium, supplemented with 10% fetal bovine serum (FBS), 100 units/mL penicillin, and 0.1 mg/mL streptomycin (Gibco). All transfections were carried out in antibiotic-free media. In all cases, cells were incubated in a 5% CO_2 humidified chamber at 37 °C.

Metabolic Incorporation of AzFuc and AlkFuc into Neuronal Proteins and CuAAC with alknyne-biotin. Neurons in culture were supplemented with 100 μM AlkFuc, AzFuc, or Fuc, by adding the appropriate volume of 400 mM stock solution into the culture media, for 3 d. For the specificity studies, tunicamycin (Sigma-Aldrich) in ethanol was added at a concentration of 25 μM to the indicated samples during the last 24 h of the metabolic labeling period, and was allowed to remain in the media through the metabolic labeling treatment. Cells were subsequently washed with PBS, pH 7.5, scraped off the plates, and lysed in boiling 1% SDS with sonication. Protein concentration was determined by BCA assay (Pierce), and lysate was subjected to CuAAC to tag metabolically labeled glycoproteins. Lysates in 1% SDS (2 μg/μL) were added into an equivalent volume of buffer containing 6% NP-40, 150 mM NaCl, 100 mM Na_2PO_4 and 2X Protease Inhibitor Cocktail (Roche, EDTA-free). Triazole ligand (0.1 mM), alkyne- or azido biotin (0.1 mM), $CuSO_4$ (50 mM), sodium ascorbate (20 mM) were added and the reaction buffer was incubated, rotating end over end, at 4 °C for 3 h. Labeled lysates were diluted with 4X sample buffer (200 mM Tris pH 6.8, 8% SDS, 400 mM DTT, 40% glycerol, 0.2% bromophenol blue), resolved on a NuPAGE 4-12% Bis-Tris gel (Life Technologies) and transferred to a polyvinylidene difluoride (PVDF) membrane (Milipore). The membrane was blocked in 3% BSA (Fisher) in TBST (50 mM Tris•HCl, 150 mM NaCl, 0.05% Tween

20, pH 7.4) for 1 h at rt, and blotted with streptavidin-Alexa Fluor 680 (0.01 μg/mL in TBST containing 3% BSA; Life Technologies) for 1 h at rt to visualize biotinylated proteins.

Purification of Biotin-Labeled Fucosylated Proteins. Biotinylated samples were prepared as described above, were precipitated using methanol/chloroform/water, and re-dissolved in boiling 1% SDS plus Complete™ protease inhibitors at a concentration of 2 mg/mL. The SDS was quenched with 1 volume of NETFD buffer (100 mM NaCl, 50 mM Tris•HCl pH 7.4, 5 mM EDTA, 6% NP-40) plus protease inhibitors. The samples were incubated with pre-washed streptavidin resin (Pierce; 100 μL/1 mg protein) for 2 h at 4 °C. The resin was washed thrice with 10 column volumes each of low salt buffer (0.1 M Na2HPO4 pH 7.5, 0.15 M NaCl, 1% Triton X-100, 0.1% SDS), thrice with 10 column volumes each of high salt buffer (0.1 M Na_2HPO_4 pH 7.5, 0.5 M NaCl, 0.2% Triton X-100), once with 10 column volumes of 4 M urea, 1% SDS in PBS, and twice with 10 column volumes of 50 mM Tris•HCl pH 7.4. Captured protein was eluted in boiling elution buffer (6 M urea, 2 M thiourea, 30 mM biotin, 2% SDS, pH 12) for 15 min. The eluate was diluted 10 times with PBS and concentrated to 50 μL in Amicon-4mL Ultra concentrators (Millipore).

TAMRA Labeling of Neuronal cultures and Purification of TAMRA-Labeled Fucosylated Proteins. Neurons in culture were supplemented with 100 μM AzFuc or Fuc, by adding the appropriate volume of 400 mM stock solution into neuronal growth meida, for 3 d. Cells were subsequently washed with PBS, pH 7.5, scraped off the plates, and lysed in 1% SDS with limited sonication. The samples were not boiled to avoid decomposition of the azide tag. Protein concentration was determined by BCA assay (Pierce) and lysates in 1% SDS (4 μg/μL) were subjected to copper catalyzed alkyne-azido cycloaddition utilizing reagents available from the ClickIT kit (Life Technologies). Subsequent to labeling, labeled samples were precipitated and resolubilized as described above at a concentration of 2 mg/mL. The SDS was quenched with 1 volume of NETFD buffer plus protease inhibitors. The samples were incubated with anti-TAMRA

antibody (Life Technologies) at 1 mg/mL(check) for 5 h at 4 °C, rotating end over end. The samples were subsequently incubated with pre-equilibrated Protein A/G beads (Pierce) for 1 h at 4 °C, rotating end over end, after which the beads were washed thrice with 1 mL binding buffer, and once with 1 mL of ice-cold 50 mM Tris, pH 7.5. Captured protein was eluted in 2X boiling sample buffer for 5 min.

LC-MS/MS Analysis. The eluate was resolved on a 10% acrylamide-SDS gel and visualized by silver stain. The bands were cut and destained and subsequently subjected to reduction with DTT, alkylation with iodoacetamide, and overnight tryptic disgestion. The resulting extracted enzymatic digest solutions were taken to dryness, and the samples were reconstituted with 20 μL 0.1 M HoAC, and their analyses were started immediately on an Orbitrap Velos, using a true nanoLC system. A "top 20 data dependent" experiment was performed on each reconstituted sample, meaning a full MS scan with high mass accuracy was taken followed by tandem MS of the top twenty m/z values. The samples were run with single peptide standards injected between each sample run to minimize carry over between samples, and two standards were injected after ever 10 samples. Samples were run such that a control band was always run before its sample counterpart, and pairs of bands of widely varying MW were run in varying order to help further distinguish hits specific to the AlkFuc lane. Upon manual inspection of the data, the system appeared to perform fine, as verified by the consistent retention time and signal of the standard run after reach gel band sample. All samples were searched by Mascot against the SwissProt database (version 57.15) with full tryptic specificity, allowing for +57 Da static modification of cysteine (iodoacetamide labeling) and +16 Da variable modification of methionine (oxidation that occurs as an artifact of processing). Precursor mass accuracies of +/- 25 ppm were used a second minimal criterion for peptide identification acceptance. Protein identification were accepted if three peptides each having a 95% certainty level together combined to give a protein identification with a 99.9% certainty, as defined by Peptide/Protein Prophet in Scaffold 2.0.

Western Blotting for Parallel Identification of AlkFuc Labeled Proteins. The purified, labeled lysates, as described in the main text Material and Methods, was resolved on a NuPAGE 4-12% Bis-Tris gel (Invitrogen) and transferred to a polyvinylidene difluoride (PVDF) membrane (Millipore). The membrane was blocked in 5% milk (BioRad) in TBST (50 mM Tris•HCl, 150 mM NaCl, 0.05% Tween 20, pH 7.4) for 1 h at rt. Primary antibodies in 5% milk in TBST were added overnight at 4 °C at the following concentrations: mouse anti-NCAM monoclonal antibody (Abcam) at 1 μg/mL, mouse anti-synapsin I ascites (Synaptic Systems) at 0.1 μg/ml, mouse anti-munc18-1 (Synaptic Systems) at 0.1 μg/mL, or mouse p44 MAPK monoclonal antibody (Cell Signaling) at 1:2000 dilution. Membranes were washed with TBST, incubated with the appropriate Alexa Fluor 680-conjugated (Invitrogen) or IR800-conjugated (Rockland) secondary antibody, and visualized using a LiCOR Odyssey Imaging System.

Biochemical Validation of the Proteins MARCKS, cacna2d21, and synaptotagmin 1: MARCKS, cacna2d1, and synaptotagmin 1 (syt1) cDNA was purchased from Openbiosystems and cloned into a pCMV mammalian vector with a C-terminal 3X FLAG peptide. Syt1 was truncated to the first 140 amino acids (37) to limit hydrophobic interactions between the syt1 lipid binding domains and reagents or resin. Proteins were expressed in primary P3 Fx-/- mouse embryonic fibroblasts or HeLA cells with Lipofectamine 2000 (Life Technologies) and concurrently treated with either 100 μM AlkFuc or Fuc. 24 h subsequent to transfection and treatment, cells were lysed in 1% SDS and labeled with azido-biotin via CuAAC as described in the main text Material and Methods. Labeled material was precipitated with MeOH/$CHCl_3$, resolubilized in 1 % SDS, and affinity purified over FLAG M2 resin (Sigma Aldrich). The purified, labeled material was resolved on a NuPAGE 4-12% Bis-Tris gel (Invitrogen) and transferred to a polyvinylidene difluoride (PVDF) membrane (Millipore). The membrane was blocked in 5% milk (BioRad) in TBST (50 mM Tris•HCl, 150 mM NaCl, 0.05% Tween 20, pH 7.4) for 1 h at rt. Mouse anti-FLAG antibody (Sigma Aldrich) was added at 0.5 μg/mL in 5% milk in TBST for 1 h at rt. Membranes were washed with TBST, incubated with

IR800 conjugated goat anti-mouse secondary antibody, or Alexa Fluor 680 conjugated streptavidin, and visualized using a LiCOR Odyssey Imaging System.

***In Vivo* Labeling by AlkFuc in Post-Natal Mice Pups.** All procedures were approved by IACUC and animals were handled according to the IACUC guidelines. For injection into neonatal rat pups, individual animals P1-P8 were removed from the dam and cryogenically anesthetized by placing them in a latex sleeve and gently submerging them in an ice bath until they appeared anesthetized. A tail pinch was used to determine if the anesthesia was sufficient. The skin on the head at the site of injection was cleaned with chlorhexidine. The skull of the rat pup is cartilaginous at this age, and thus injections can proceed without the need of a surgical incision. The pup was injected with a Hamilton syringe using a 33-gauge needle attached to a microinjector. The compounds were injected based on stereotaxic coordinates previously published, and were injected at 0.1 μl/min for a total volume of 1-2.5 μL unilaterally into the cortex. As a control, Fuc was injected into the hippocampus. After insertion of the needle, a 1 min resting period preceded the injection. The injection needle was withdrawn over a 2 min period. The puncture wounds were sealed with surgical glue. Pups were tattooed to identify AlkFuc and Fuc injected animals by using a 29-gauge needle to inject a small quantity of tattoo ink into one of the digits or footpad. After injection the pups were warmed on a water circulating heating pad until responsive. They were returned to the dam and maintained on a heat pad until the pups begin nursing. The rump of each pup was exposed to a small amount of urine from the dam to mask any odors that may be associated with the handling and injection procedure. Pups were observed for 4-6 hours post-surgery, and any pups that did not appear to be nursing by lack of a milk spot, or appeared cold or dehydrated were euthanized immediately. The pups were euthanized 1-3 days post-injection by CO_2, and the cortex was isolated. For pain relief, the dam of the injected pups was given 2 mg/kg ketoprofen subcutaneously just prior to the surgery in order that the pup received the analgesic and anti-inflammatory effects of the drug through nursing. The pups

were not treated post-operatively for pain relief as there is no information on a safe dosage to be administered directly to neonates, and the use of such drugs may induce aberrant behavior in the pups and can increase the chance of cannibalization.

Immunohistochemistry of Metabolically Labeled Mouse Brains. The brains of mouse pups were removed and immersion-fixed overnight in 4% paraformaldehyde in PBS at 4 °C. The following day, the solution was replaced with an ice-cold solution of 15% sucrose in PBS at 4 °C until the brains sank, followed by 30% sucrose in PBS. The brain tissue was mounted in OCT medium (Tissue Tek) and frozen in a dry ice/MeOH bath. Adult mice were perfusion fixed and the brains dissected, followed by immersion in 15-30% sucrose, as described above. Frozen brains were stored at -80 °C until they were processed for sectioning. Fixed tissues were cryogenically sliced on a Leica CM1800 cryostat in coronal or sagittal sections (20 μm sections for P3 pups and 50 μm sections for adult brain). Sections were dried at 37 °C for 20 min and then blocked in 10% donkey serum and 0.3% Triton X-100 in PBS for 1 h at rt. Sections were then subjected to CuAAC, and were incubated in 25 mM $CuSO_4$, 10 mM sodium ascorbate, 0.05 mM triazole, and 0.05 azido-biotin in PBS overnight at 4 °C. Subsequent to CuAAC labeling, sections were incubated with Alexa Fluor 488 conjugated streptavidin (1:1000 in 2% donkey serum and 0.1% Triton-X-100 in PBS, Sigma) for 1 h at rt. After staining, slices were mounted in Vectashield containing 40,6-diamidino-2-phenylindole (DAPI, Vector Laboratories) and fluorescence imaged on a Nikon T2000 with a 5X or 10x objective.

***In Vivo* Labeling by AlkFuc in Adult Mice.** All procedures were approved by IACUC and animals were handled according to the IACUC guidelines. Adult $Fx^{-/-}$ mice were maintained on normal rodent chow supplemented with 0.5 to 1% Fucose (Sigma). One week prior to surgery, animals were placed on a normal rodent diet to minimize levels of endogenous fucose. The animals were weighed, anesthetized under isoflurane, given and the appropriate amount of an analgesic (Ibuprofen, 2 mg/kg) via subcutaneous injection, and immobilized on a stereotaxic device. The crown of the head was

shaved and sterilized, and a fine dentist drill was used to drill through the skull. Microcannulas were implanted on one hemisphere at the coordinates (2 mm, 2 mm, 2 mm) to access the hippocampus, and 2 uL of 1 mM alkynyl fucose was injected via a Hamilton syringe with a 33 G needle. The wound was sealed using the surgical adhesive VetBond and the microcannula was capped using a removable cap. The animal was taken off the isoflurane, and placed on a covered heating pad in a new cage, with food and water easily accessible. The animals were typically mobile and responsive within 5 min. After recuperating for 2 d, the animals were once again anesthetized with isofluorane and immobilized on the stereotaxic device to deliver a second dose of alkynyl fucose. Subsequent to the injection, the microcannula was capped and the animal was allowed to recover as mentioned above. A third and final dose was administered in the same way 2 d later. One day following to the final dose of AlkFuc, and seven days subsequent to the surgery, the animals were humanely euthanized and the brain dissected. The hippocampus was removed and lysed in 1% boiling SDS with sonication, and the protein quantitated with the Pierce BCA assay. Lysates treated with both Fuc and AlkFuc were biotinylated via CuAAC as described in the main text Materials and Methods. Half the labeled sample was subjected to PNGaseF digest (NEB) according to reagent protocols subsequent to CuAAC labeling, and labeled lysates were analyzed by Western as described above.

References

1. Rabuka D, Hubbard SC, Laughlin ST, Argade SP, & Bertozzi CR (2006) A Chemical Reporter Strategy to Probe Glycoprotein Fucosylation. *Journal of the American Chemical Society* 128(37):12078-12079.

2. Hsu TL, *et al.* (2007) Alkynyl sugar analogs for the labeling and visualization of glycoconjugates in cells. *Proceedings of the National Academy of Sciences of the United States of America* 104(8):2614-2619.

3. Hanson SR, *et al.* (2007) Tailored Glycoproteomics and Glycan Site Mapping Using Saccharide-Selective Bioorthogonal Probes. *Journal of the American Chemical Society* 129(23):7266-7267.

4. Laughlin ST & Bertozzi CR (2007) Metabolic labeling of glycans with azido sugars and subsequent glycan-profiling and visualization via Staudinger ligation. *Nature protocols* 2(11):2930-2944.

5. Khidekel N, *et al.* (2003) A Chemoenzymatic Approach toward the Rapid and Sensitive Detection of O-GlcNAc Posttranslational Modifications. *Journal of the American Chemical Society* 125(52):16162-16163.

6. Shao J & Tam JP (1995) Unprotected Peptides as Building Blocks for the Synthesis of Peptide Dendrimers with Oxime, Hydrazone, and Thiazolidine Linkages. *Journal of the American Chemical Society* 117(14):3893-3899.

7. Agard NJ, Baskin JM, Prescher JA, Lo A, & Bertozzi CR (2006) A Comparitive Study of Bioorthogonal Reactions with Azides. *ACS chemical biology* 1(10):644-648.

8. Kohn M & Breinbaur R (2004) The Staudinger ligation - A gift to chemical biology. *Angewandte Chemie* 43(24):3106-3116.

9. Rostovtsev VV, Green LG, Fokin VV, & Sharpless KB (2002) A Stepwise Huisgen Cycloaddition Process: Copper(I)-Catalyzed Regioselective "Ligation" of Azides and Terminal Alkynes. *Angewandte Chemie* 41(14):2596-2599.

10. Agard NJ, Prescher JA, & Bertozzi CR (2004) A Strain-Promoted [3 + 2] Azide−Alkyne Cycloaddition for Covalent Modification of Biomolecules in Living Systems. *Journal of the American Chemical Society* 126(46):15046-15047.

11. Hubbard SC, Boyce M, McVaugh CT, Peehl DM, & Bertozzi CR (2011) Cell surface glycoproteomic analysis of prostate cancer-derived PC-3 cells. *Bioorganic & medicinal chemistry letters* 21(17):4945-4950.

12. Zaro BW, Hang HC, & Pratt MR (2013) Incorporation of unnatural sugars for the identification of glycoproteins. *Methods in molecular biology* 951:57-67.

13. Al-Shareffi E, *et al.* (2013) 6-Alkynyl fucose is a bioorthogonal analog for O-fucosylation of epidermal growth factor-like repeats and thrombospondin Type-1 repeats by protein O-fucosyltransferases 1 and 2. *Glycobiology* 23(2):188-198.

14. Krusius T & Finne J (1977) Structural Features of Tissue Glycoproteins: Fractionation and Methylation Analysis of Glycopeptides Derived from Rat Brain, Kidney, and Liver. *European Journal of Biochemistry* 78:369-379.

15. Laughlin ST & Bertozzi CR (2009) Imaging the glycome. *Proc. Natl Acad. Sci. USA* 106(1):12-17.

16. Kleene R & Schachner M (2004) Glycans and neural cell interactions. *Nature reviews. Neuroscience* 5(3):195-208.

17. Hsu T-L & Wong CH (2007) Personal Communication.

18. Khidekel N, *et al.* (2007) Probing the dynamics of O-GlcNAc glycosylation in the brain using quantitative proteomics. *Nat Chem Biol* 3(6):339-348.

19. Rybak JN, Scheurer SB, Neri D, & Elia G (2004) Purification of biotinylated proteins on streptavidin resin: a protocol for quantitative elution. *Proteomics* 4(8):2296-2299.

20. Wuhrer M, *et al.* (2003) Localization of defined carbohydrate epitopes in bovine polysialylated NCAM. *Biochimie* 85(1-2):207-218.

21. Liedtke S, *et al.* (2001) Characterization of N-glycans from mouse brain neural cell adhesion molecule. *Glycobiology* 11(5):373-384.

22. Pestean A, *et al.* (1995) Identification of the *Ulex europeaeus* agglutinin-I-binding protein as a unique glycoform of the neural cell adhesion molecule in the olfactory sensory axons of adult rats. *Neuroscience Letters* 195(2):117-120.

23. Laux T, *et al.* (2000) GAP43, MARCKS, and CAP23 Modulate PI(4,5)P2 at Plasmalemmal Rafts, and Regulate Cell Cortex Actin Dynamics through a Common Mechanism. *J. Cell Biol.* 149(7):1455-1472.

24. Meiri KF, Pfenninger KH, & Willard MB (1986) Growth-associated protein, GAP-43, a polypeptide that is induced when neurons extend axons, is a compoenent of growth cones and coresponds to pp46, a major polypeptide of subcellular fraction enriched in growth cones. *Proc. Natl. Acad. Sci. USA* 83:3537-3541.

25. Sheu FS, McCabe BJ, Horn G, & Routtenberg A (1993) Learning selectively increases protein kinase C substrate phosphorylation in specific regions of the chick brain. *Proc. Natl. Acad. Sci. USA* 90(7):2705-2709.

26. Strittmatter SM VT, Fishman MC (1992) GAP-43 as a plasticity protein in neuronal form and repair. *J. Neurobio.* 23(5):507-520.

27. Widmer F & Caroni P (1993) Phosphorylation-site mutagenesis of the growth-associated protein GAP- 43 modulates its effects on cell spreading and morphology. *J. Cell Biol.* 120(2):503-512.

28. Matus A (2005) MARCKS for Maintenance in Dendritic Spines. *Neuron* 48(1):4-5.

29. Robert KM, *et al.* (2005) Effect of myristoylated alanine-rich C kinase substrate (MARCKS) overexpression on hippocampus-dependent learning and hippocampal synaptic plasticity in *MARCKS* transgenic mice. *Hippocampus* 15(5):675-683.

30. Zwiers H, Verhaagen J, van Dongen CJ, de Graan PN, & Gispen WH (1985) Resolution of rat brain synaptic phosphoprotein B-50 into multiple forms by two-dimensional electrophoresis: evidence for multisite phosphorylation. *J. Neurochem.* 44(4):1083-1090.

31. Theis T, *et al.* (2013) Functional Role of the Interaction between Polysialic Acid and Myristoylated Alanine-rich C Kinase Substrate at the Plasma Membrane. *J. Biol. Chem.* 288(9):6726-6742.

32. Murrey HE, *et al.* (2009) Identification of the plasticity-relevant fucose-alpha(1-2)-galactose proteome from the mouse olfactory bulb. *Biochemistry* 48(30):7261-7270.

33. Walz A, Monbaerts P, Greer CA, & Treloar HB (2006) Disrupted compartmental organization of axons and dendrites within olfactory glomeruli of mice deficient in the olfactory cell adhesion molecule, OCAM. *Mol. Cell. Neurosci.* 32:1-14.

34. Godenschwege TA, Kristiansen LV, Uthaman SB, Hortsch M, & Murphey RK (2006) A conserved role for Drosophila Neuroglian and human L1-CAM in central-synapse formation. *Curr. Biol.* 16(1):12-23.

35. Palladino MJ, Bower JE, Kreber R, & Ganetzky B (2003) Neural Dysfunction and Neurodegeneration in *Drosophila* Na^+/K^+ ATPase Alpha Subunit Mutants. *J. Neurosci.* 23(4):1276-1286.

36. Rizo J & Sudhof TC (2002) Snares and munc18 in synaptic vesicle fusion. *Nat. Rev. Neurosci.* 3(8):641-653.

37. Han W, *et al.* (2004) N-Glycosylation Is Essential for Vesicular Targeting of Synaptotagmin 1. *Neuron* 41(1):85-99.

38. Fukuda M (2002) VAMP-2/synaptobrevin binding to synaptotagmin I promotes O-glycosylation of synaptotagmin I. *J. Biol. Chem.* 277(33):30351-30358

39. Murrey HE, *et al.* (2006) Protein fucosylation regulates synapsin Ia/Ib expression and neuronal morphology in primary hippocampal neurons. *Proc. Natl. Acad. Sci. U. S. A.* 103(1):21-26.

40. Mayer ML & Armstrong N (2004) Structure and function of glutamate receptor ion channels. *Ann. Rev. Phys.* 66:161-181.

41. Smith PL, *et al.* (2002) Conditional control of selectin ligand expression and global fucosylation events in mice with a targeted mutation at the FX locus. *J. Cell Biol.* 158(4):801-815.

42. Sletten EM & Bertozzi CR (2009) Bioorthogonal chemistry: fishing for selectivity in a sea of functionality. *Angew. Chem. Int. Ed. Engl.* 48(38):6974-6998.

43. Del Amo DS, *et al.* (2010) Biocompatible copper(I) catalysts for *in vivo* imaging of glycans. *J. Amer. Chem. Soc.* 132(47):16893-16899.

44. Chang PV, *et al.* (2010) Copper-free click chemistry in living animals. *Proc. Natl. Acad. Sci. U. S. A.* 107(5):1821-1826.

45. Laughlin ST, Baskin JM, Amacher SL, & Bertozzi CR (2008) In Vivo Imaging of Membrane-Associated Glycans in Developing Zebrafish. *Science* 320(5876):664-667.

46. Goslin K & Banker G (1991) *Culturing Nerve Cells*, eds Banker G & Goslin K (MIT Press, Cambridge, MA), pp 251-281.

CHAPTER 3

Fluorescence Detection of Fucosylated Glycans in Neurons

Introduction

Glycans are attractive targets for molecular imaging. As described in Chapter 1, these biopolymers have critical roles in many biological processes, and the cellular "glycome" can report on the physiological state of the cell. The ability to visualize these processes in cellular systems would increase our understanding of biology and accelerate the development of new clinical tools. However, the molecular imaging of glycan structures has been challenging due to their incompatibility with traditional imaging methods. Genetically encoded fluorescent proteins, such as GFP, cannot access specific glycan structures. Though fluorescent antibodies and lectins may have specificity for the glycan of interest, the large size of the protein conjugates can restrict their access into intracellular compartments, or perturb the localization and natural physiology of the glycan of interest. Lectin and antibody-based imaging methods can provide a snapshot of the glycome at a particular point in time, but are difficult to implement in the context of dynamic studies. Additionally, lectins typically have low affinity for the glycan epitope of interest, and require multi-valency for high-avidity binding (1).

Metabolic labeling with non-natural sugar analogs, followed by bioorthogonal detection techniques, fills the need for a chemoselective labeling technique that is compatible with complex cellular systems. Through the selective metabolic incorporation of a bioorthogonal handle, glycans can be tagged yet remain functional with the parameters of normal cell activity. At any point after labeling, these glycans can be selectively and sensitively detected using CuAAc or SPAAC, allowing spatial and temporal resolution of the metabolically tagged glycans. For example, sialic acid-containing glycans have been visualized using metabolic labeling with sialic acid precursors (e.g. ManNAz or alkynyl-ManNAc) (2, 3), or sialic acid derivatives (e.g. SiaNaz, or 9-azido Neu5Ac) (4, 5), in a variety of cellular systems (3, 6), as well as in mice and zebrafish *in vivo* (7, 8). Mucin-type O-linked glycans have been

detected with the metabolic labeling reporter Ac4GalNAz,(9) also in a variety of cellular systems, and mice and zebrafish *in vivo* (8, 10).

Non-natural fucose analogs have also been used in various cell lines to label and visualize fucosylated glycans. Chi-Huey Wong and coworkers utilized the AlkFuc analog to selectively label fucosylated glycoconjugates through the fucose salvage pathway in Hep3B cells and detect them by CuAAC labeling using a fluorescent or biotinylated azide (3). AlkFuc labeled glycoconjugates were visualized throughout the cells, with some colocalization with the Golgi marker WGA lectin. Additionally, the AlkFuc analog has been used to image fucosylated glycans in the *Arabidopsis thaliana* root cell wall (11), visualizing the localization and targeting of fucosylated glycans in growing cell walls and providing insight into the organization and dynamics of the pectin network. Bertozzi and coworkers were able to surmount low levels of metabolic incorporation of the non-natural fucose analogs by utilizing the GDP activated derivative of FucAz (GDP-FucAz) to bypass the biosynthetic machinery and to metabolically label developing zebrafish embryos in the first five days of development (12).

Given the biological relevance of fucosylated glycans in neuronal systems (described in Chapter 1), the fluorescence detection of fucosylated glycoproteins in neurons would have many exciting applications. Fucosylated glycans are reported to be enriched in synapses (13-15), and the cellular machinery responsible for protein glycosylation can be found within dendrites (16), raising the possibility that local protein synthesis and fucosylation may be occurring at synapses in response to neuronal stimulation. Hsieh-Wilson and co-workers have suggested the presence of Fucα(1-2)Gal glycoproteins in hippocampal neurons, using the lectin UEAI (17), although their specific subcellular localization remains to be determined.

In order to gain insight into the subcellular localization and dynamics of fucosylated glycans in neurons, we sought to develop a protocol using non-natural fucose analogs to image fucosylated glycans in neurons. As the ability to resolve the spatiotemporal dynamics of metabolically labeled fucosylated glycans could allow insights into their functional role at synapses, we also sought to develop an assay to

investigate the dynamics of glycoproteins within cells and to potentially measure changes in fucosylated glycoproteins in response to cellular stimuli or perturbations. In the following chapter, we describe efforts to track the subcellular localization of fucosylated glycoproteins in neurons, and to explore their trafficking within the cells.

Results and Discussion

We first determined whether the non-natural fucose analogs could be utilized for selectively imaging fucosylated proteins in neurons. Primary rat hippocampal neurons were cultured on coverslips and treated with 50 to 100 μM AlkFuc, AzFuc or Fuc in DMSO at 1 DIV. We observed that the hippocampal cultures tolerated 100 μM concentrations of AlkFuc and Fuc with only minimal cytotoxicity, whereas AzFuc caused significant cell death. As a result, the studies described only utilize the AlkFuc analog. After washing out excess molecule, neurons were fixed, permeabilized, and blocked with BSA. An additional blocking step with 1 μg/mL streptavidin in BSA was found to be necessary to limit background due to fluorescent streptavidin detection.

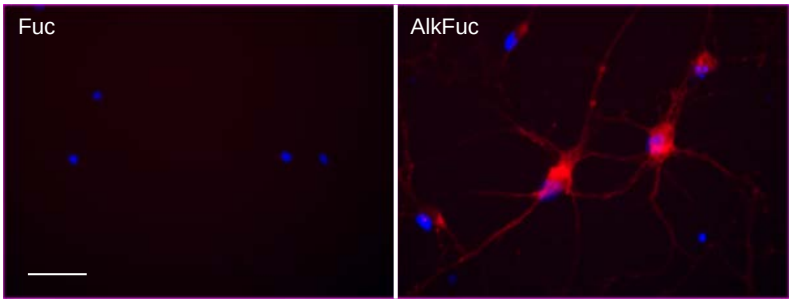

Figure 3.1 Fluorescence detection of AlkFuc labeling. Fuc and AlkFuc labeling (red) in 4 DIV hippocampal neurons after metabolic and CuAAC detection. Nuclei are stained with DAPI (blue). AlkFuc labeling is apparent throughout the soma and processes. Scale bar is 25 μM.

The fixed cells were then subjected to CuAAC labeling with azido-biotin. CuAAC reagents were added to a solution of PBS at 25 mM $CuSO_4$, 1 mM sodium ascorbate, 0.05 mM azido-biotin, and 0.05 mM triazole ligand, and the reaction mixture was added to each coverslip for an overnight incubation at 4 °C.

Subsequent staining with Alexa Fluor 488 conjugated streptavidin revealed extensive fluorescence in the cell body, as well as in the neuronal processes, in cells treated with AlkFuc, but not Fuc (Figure 3.1). In order to determine if AlkFuc labeling was specific to glycoproteins, cultures treated with AlkFuc were fixed and permeabilized utilizing MeOH to disrupt the lipid membrane, prior to detection with CuAAC and Alexa Fluor 488 conjugated streptavidin. Even after lipid disruption, AlkFuc labeling was still apparent throughout the soma and processes, indicating incorporation into glycoproteins (data not shown). Thus, we are capable of specifically labeling fucosylated glycoproteins in the cell body as well as along the neuronal processes of hippocampal cultures.

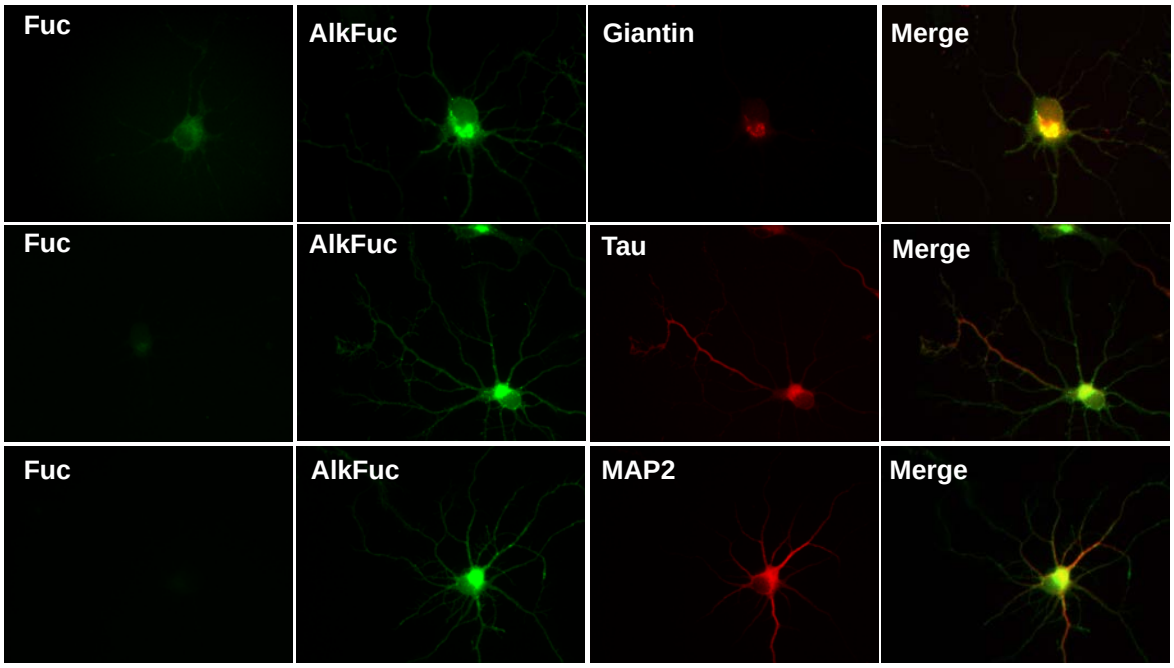

Figure 3.2 Subcellular localization of AlkFuc labeling in 4 DIV neurons. AlkFuc labeling (green) was compared to the Golgi marker Giantin, an axonal marker Tau, and the dendritic marker MAP2 (red). AlkFuc labeling overlayed strongly with the Golgi marker, and also localized to axons and dendrites. Scale bar is 25 µM.

Given that the AlkFuc analog was incorporated into neuronal glycoproteins, we sought to determine the subcellular localization of glycans labeled with AlkFuc. Neurons labeled with AlkFuc were

co-stained with the Golgi apparatus marker Giantin, the dendritic marker MAP2, or the axonal marker tau (Figure 3.2). Strong overlay of Alkfuc labeling with the Golgi marker (Figure 3.2, top) indicated the localization of AlkFuc labeled proteins to the Golgi apparatus, suggesting that fucosylated glycoproteins reside in the Golgi apparatus, consistent with previous results and the notion that fucosylated glycoproteins are synthesized in the GA (3, 18). In addition, we observed labeling of both axons and dendrites in 4 DIV neuronal cultures. Overlay of AlkFuc labeling with both MAP2 and Tau was observed, though AlkFuc labeling was stronger in the MAP2 stained dendrites, indicating that the AlkFuc-labeled glycoproteins were localized to axons and dendrites (Figure 3.2, middle and bottom).

For comparison, 14 DIV hippocampal neurons were also co-stained with the lectins *Ulex europaeus* agglutinin I (UEAI), which binds to Fucα(1,2)Gal glycans (19), *Lotus tetranoglobus* lectin (LTL), which binds to α-linked fucose and the Le^x and Le^y antigens (19), and *Anguilla anguilla* agglutinin (AAA), which binds to Fucα(1-2)Gal structures as well as H antigen types I and II (Figure 3.3) (20). UEAI, LTL, and AAA staining showed overlay with a portion of AlkFuc labeling, consistent with AlkFuc incorporation into fucosylated glycoproteins recognized by fucose specific lectins. However, a subset of AlkFuc labeling, particularly in the processes, was distinct from the staining of each particular lectin, suggesting that the AlkFuc analog labels a broader population of glycans not recognized by the lectins. The majority of fucosylated glycans are reported to exist in complex N-linked structures, which can be modified by fucose in a variety of linkages. The ability to label all fucosylated glycans, irrespective of linkage, would allow a broader investigation into the role of fucosylated glycans.

We also examined whether AlkFuc labeling in 14 DIV hippocampal neurons was enriched in synapses. Hippocampal neurons were labeled for 3 d with AlkFuc or Fuc, subsequently fixed, labeled via CuAAC, and immunostained with various markers. As in younger neurons, we observed the strongest AlkFuc labeling within the Golgi compartment of mature 14 DIV hippocampal neurons. In addition, we examined the colocalization of AlkFuc to synapses with the synaptic markers synapsin I (pre-synaptic

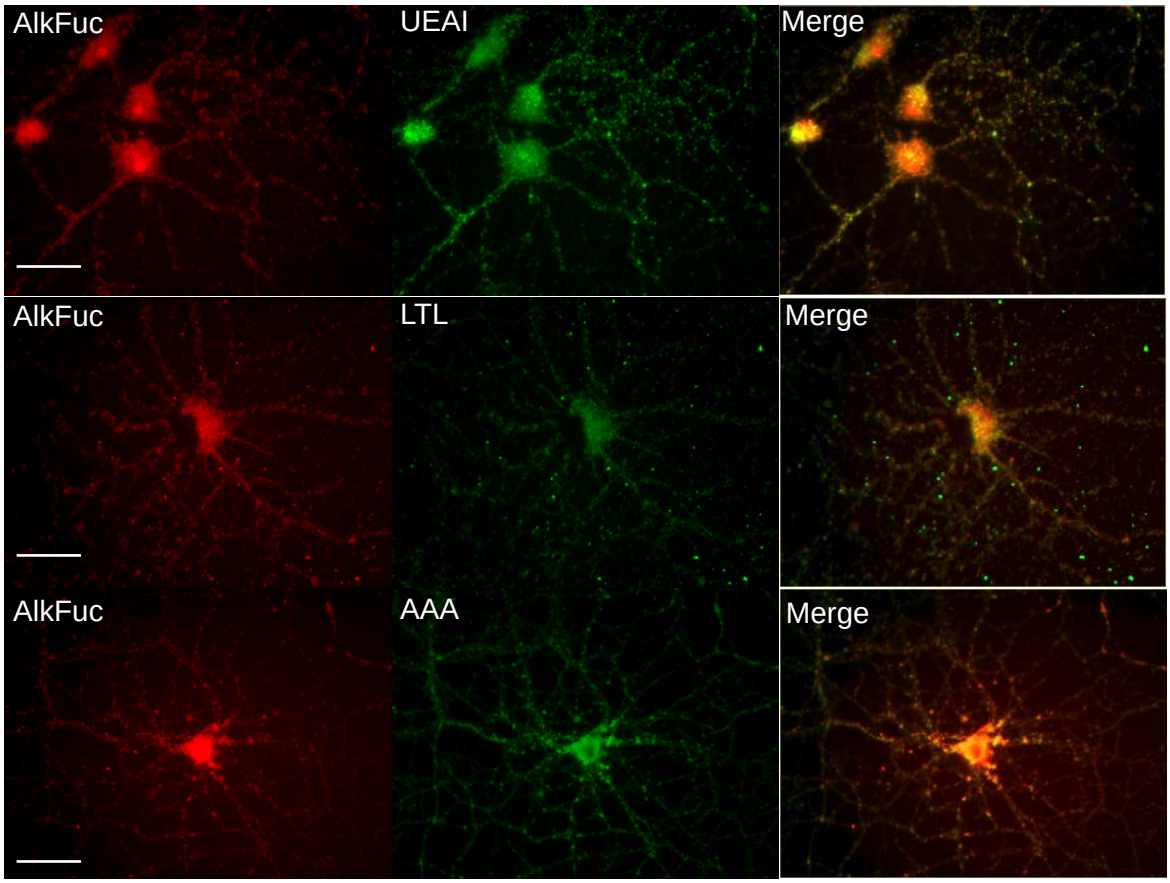

marker), PSD-95 (post-synaptic marker), and spinophilin (post-synaptic marker). Though there was some overlay to synapses indicated by yellow punctae, the majority of AlkFuc labeling was pervasive

Figure 3.3 AlkFuc labeling when compared to fucose-specific lectins. AlkFuc labeling (red) in 14 DIV neurons compared to the lectins UEAI, LTL, and AAA (green).

throughout the processes and did not appear to be highly localized to synapses (Figure 3.4), after 3 d of labeling.

In addition to taking a snapshot of fucosylated glycans in the cell at a particular moment, metabolic labeling provides the opportunity to track the dynamics of glycoproteins inside cells, affording greater insight into changes in subcellular localization in real-time that cannot be obtained using lectins or antibodies. To more closely investigate subcellular dynamics of AlkFuc labeled proteins, we treated hippocampal neurons at 4 DIV with a pulse of 200 μM AlkFuc for 1 h and chased with media lacking

AlkFuc for increasing periods of time before fixing. The resulting fluorescence after CuAAC labeling with azido-biotin and staining with streptavidin conjugated to Alexa Fluor 488 was observed by confocal microscopy. Until 16 h of incorporation, AlkFuc labeling was largely limited to the Golgi, co-localizing with the Golgi marker Giantin (Figure 3.5A), indicating fucosylated glycoproteins were located in the

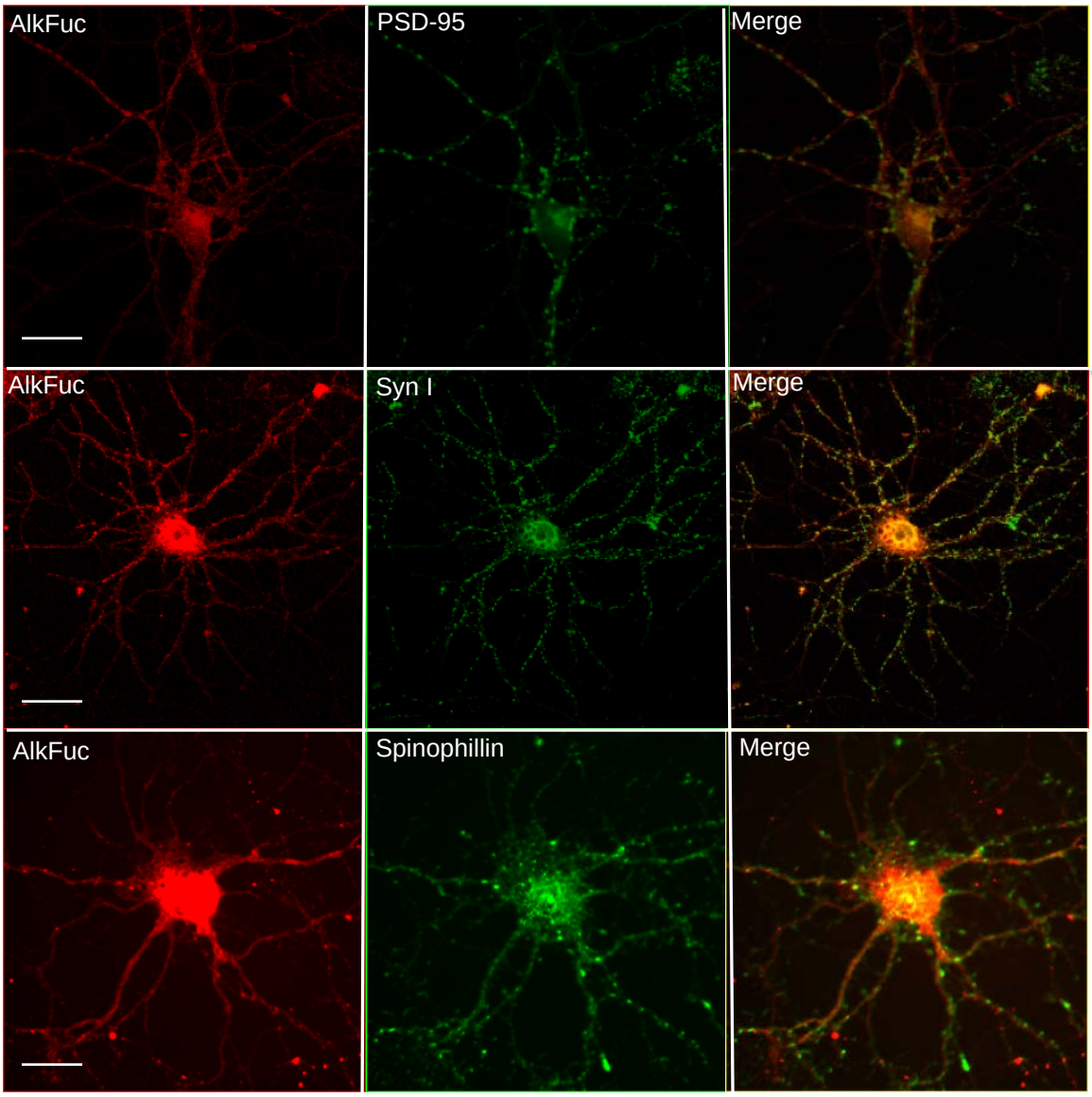

Figure 3.4 AlkFuc labeling in 14D IV neurons compared to the synaptic markers PSD-95, syn I, and spinophillin. AlkFuc overlay with synaptic markers was not apparent after metabolic labeling for 3 d with the AlkFuc analog. Scale bar is 25 μM.

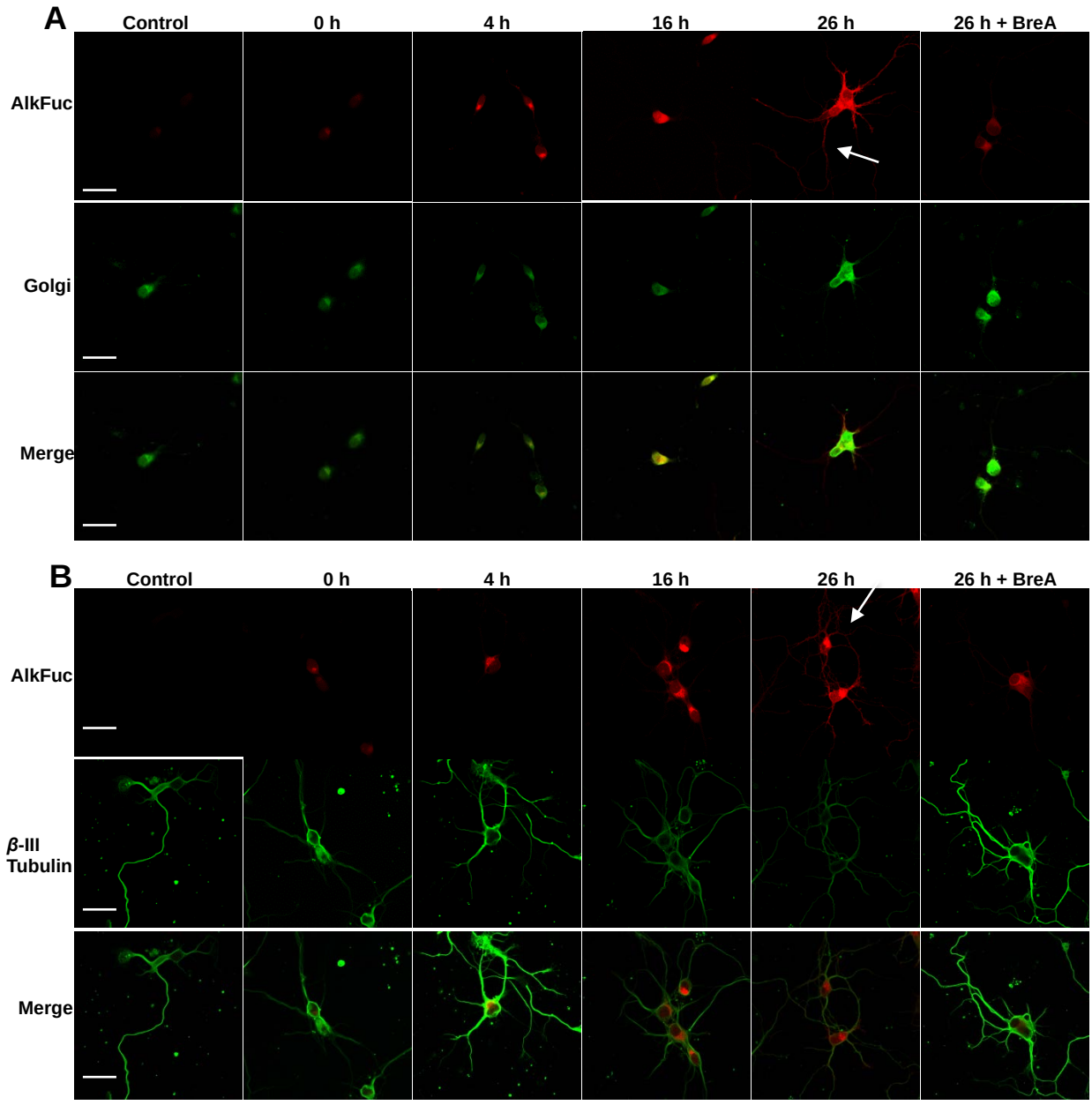

Figure 3.5 Pulse-chase analysis of AlkFuc incorporation in 5 DIV neurons. AlkFuc labeled proteins (red, top row) are detected in the Golgi after a 4 to 16 h chase with untreated media when compared to (A) the Golgi marker, Giantin, or (B) the neuronal marker *β*-III tubulin. Labeled proteins remain largely limited to the Golgi until 16 h after incorporation. Cells treated with a pulse of natural fucose (Fuc) show no labeling. By 26 h after incorporation, AlkFuc labeled glycoproteins are detected in neuronal processes, overlaying with *β*-III tubulin. Treatment with 2 µg/mL Brefeldin A (BreA), a protein secretion inhibitor, leads to diffuse AlkFuc labeling with limited labeling in neuronal processes. Scale bar is 50 µM.

Golgi apparatus (GA). After a 16 to 26 h chase, AlkFuc labeling was evident throughout the processes, overlaying with the cell marker tubulin (Figure 3.5B, arrow), suggesting AlkFuc labeled glycoproteins are delivered to neuronal processes after synthesis in the GA. To validate the conclusion that fucosylated glycoproteins are trafficked from the GA to the processes, we added the secretion inhibitor Brefeldin A (BreA) was added at various time points after the initial pulse of AlkFuc. BreA, a lactone isolated from fungi, interferes with the transport of proteins from the ER to the Golgi by reversibly disassembling the Golgi apparatus (21), and has shown to reversibly inhibit secretory trafficking in neurons (22). In all cases, the addition of BreA disrupted the GA, and AlkFuc labeling was confined to diffuse labeling in the soma, with limited labeling in the processes. Notably, when BreA was added at 16 h after the initial pulse of AlkFuc, the majority of AlkFuc labeling in the processes was abolished (Figure 3.5, right panel), suggesting that trafficking of AlkFuc labeled glycoproteins occurs 16 h after metabolic incorporation.

Intrigued by the possibility that fucosylated glycoproteins are enriched in synapses (23), the pulse-chase study was repeated in 23 DIV hippocampal neurons with formed synapses. After 18 h of incorporation, labeling was pervasive throughout neuronal processes (Figure 3.6A and 3.6B). After a 24 h chase, AlkFuc labeling manifested as distinct punctae, consistent with synaptic localization of labeled fucosylated glycoproteins. When compared to the pre- and post-synaptic markers synapsin I and GluR1, AlkFuc labeling showed significant co-localization with the post-synaptic marker GluR1, suggesting that AlkFuc significantly labeled post-synaptic proteins that are delivered to synapses after 36 hours after synthesis (Figure 3.6A and 3.6B). Alternatively, the signal may be the result of a sufficient accumulation of synaptic proteins by 36 h; the half-life of synaptic proteins, such as GluR1, have been reported to be fairly lengthy, from 1-10 d, depending on the stage of culture and type of neuron (24). Additional examples include NCAM, which has a half-life of 14-20 h in PC12 cells (25), and PSD-95, which has a half-life of 24-36 h (26). The turnover of synaptic glycoproteins has also been reported to be very slow; the half-lives of fucose-labeled glycoproteins of synaptic vesicles and the synaptosomal plasma membrane were noted to be between 26 and 36 days (27). As such, the fluorescence may be due to the

accumulation of long-lived labeled proteins. Curiously, we did not detect any labeling in dendrites in the early time points, which we might have expected given the discovery of dendritic glycosylation machinery (16).

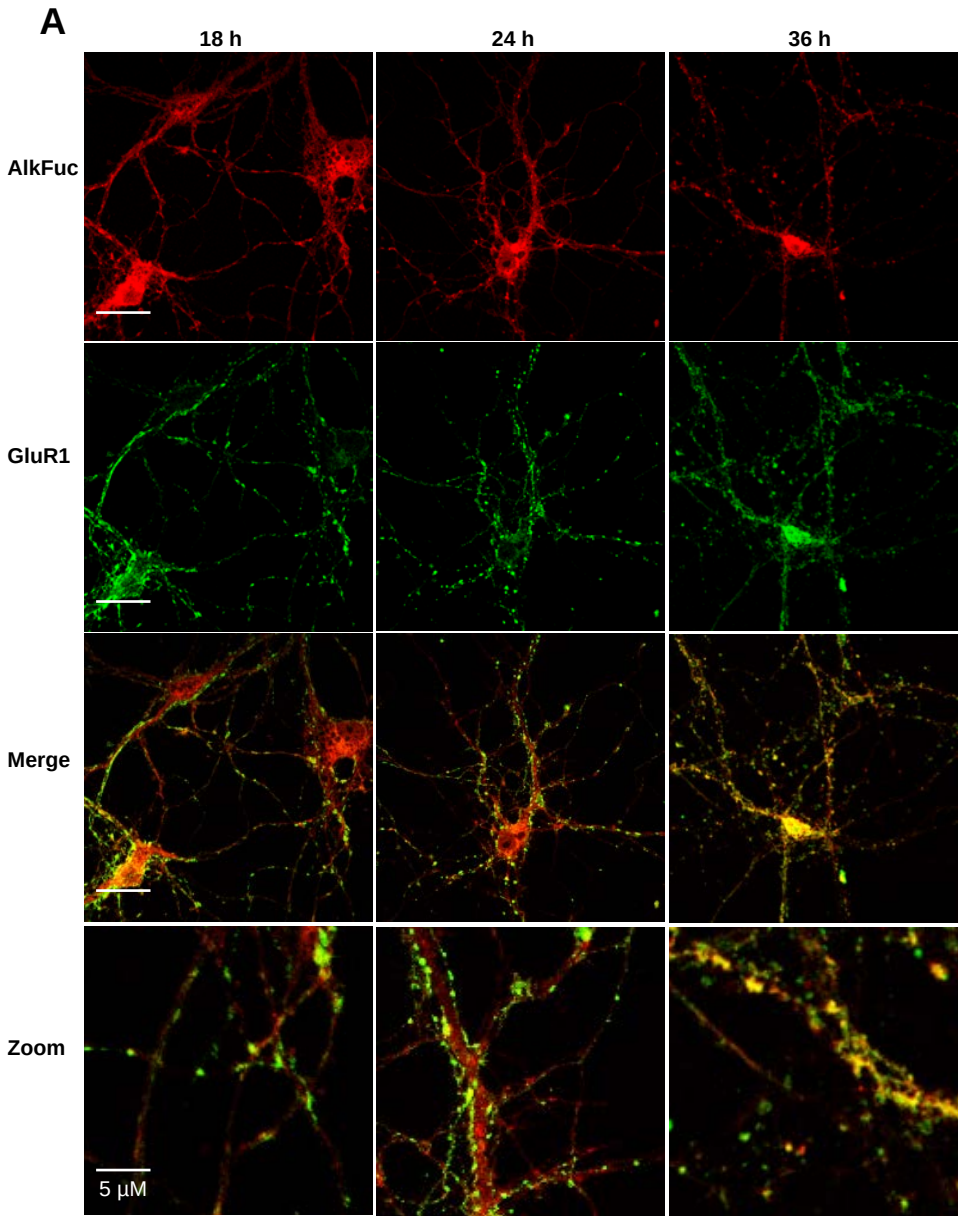

Figure 3.6. Pulse-chase analysis of alknyl-fucose incorporation in 23 DIV neurons. AlkFuc labeled proteins (red, top row) are pervasive through the cell body and processes after an 18 h chase. Between 24 h and 36 h after the chase, AlkFuc labeled glycoproteins manifest as distinct punctae, and co-localize with pre- and post-synaptic markers Syn I (A) and GluR1 (B), suggesting that alknyl-fucose labeled glycoproteins are delivered to the synapses. Scale bar is 25 µM except where indicated.

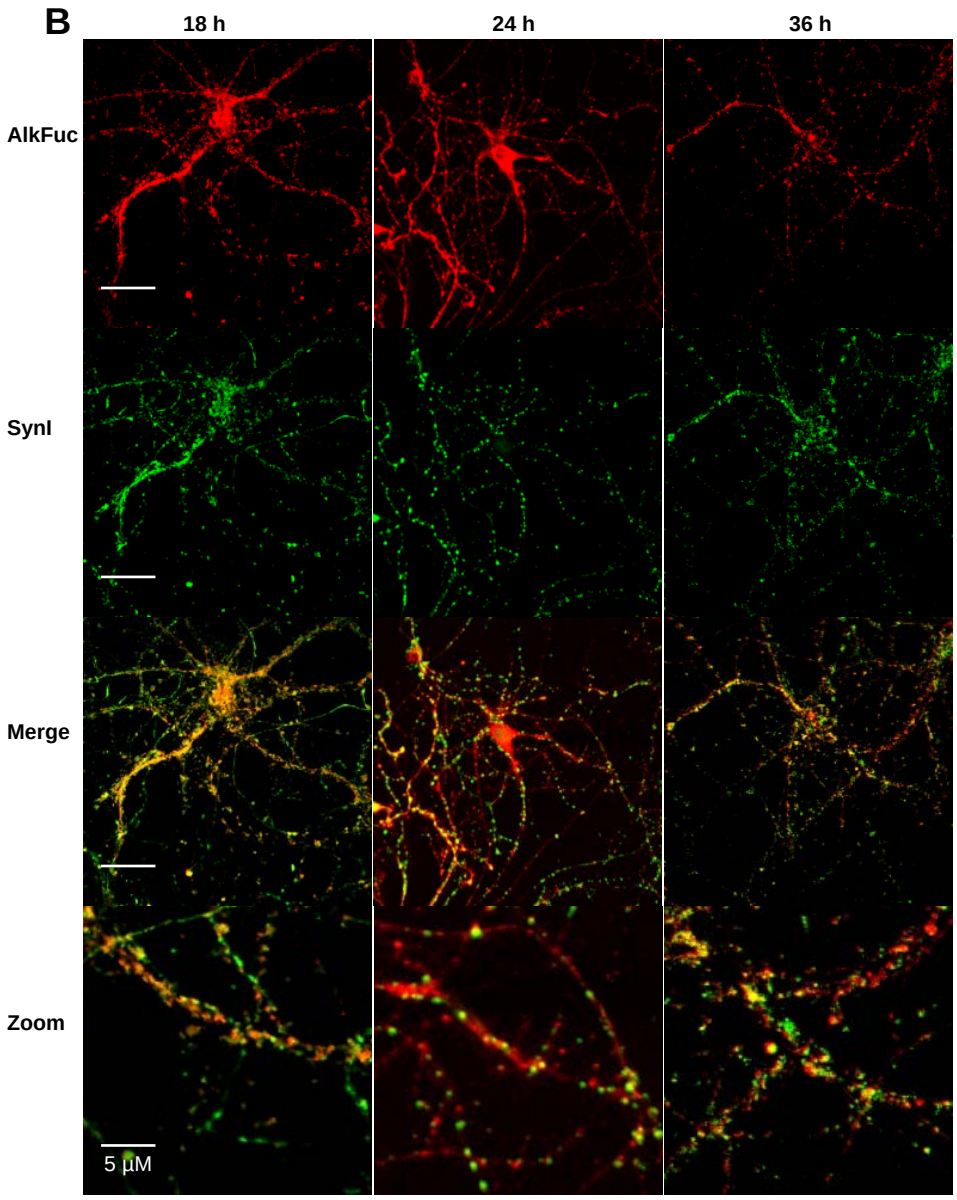

Figure 3.6. Pulse-chase analysis of alknyl-fucose incorporation in 23 DIV neurons. AlkFuc labeled proteins (red, top row) are pervasive through the cell body and processes after an 18 h chase. Between 24 h and 36 h after the chase, AlkFuc labeled glycoproteins manifest as distinct punctae, and co-localize with pre- and post-synaptic markers Syn I (A) and GluR1 (B), suggesting that alknyl-fucose labeled glycoproteins are delivered to the synapses. Scale bar is 25 µM except where indicated.

In addition to localization and pulse-chase studies, we were interested in investigating fucosylated glycoproteins in response to neuronal stimuli. In order to determine if AlkFuc labeling was perturbed in any way due to neuronal stimulation, hippocampal neurons at 14 DIV were metabolically labeled with AlkFuc and depolarized with KCl. Cultures were labeled with AlkFuc for 2 d prior to a 24 h co-treatment with tetrodotoxin (TTX) to ensure neurons were similarly silenced. AlkFuc labeling in TTX treated neurons was consistent with labeling observed thus far: strong labeling of the Golgi with some labeling apparent in neuronal processes (Figure 3.7). When treated with 50 mM KCl for 6 h, the Golgi was observed to fragment as determined by the Golgi marker Giantin, an interesting phenomenon recently reported to be caused by neuronal hyperexcitation (28), suggesting that neuronal activity serves as a signal to the Golgi. AlkFuc labeling was similarly diffuse and fragmented in the Golgi as a result of KCl depolarization, resulting in punctate labeling throughout the soma and early processes (Figure 3.7, arrow). Further studies are necessary to investigate whether neuronal stimulation leads to increased trafficking of fucosylated glycoproteins and what implications that may have on neuronal growth and morphology.

In summary, we are able to track the subcellular localization of AlkFuc glycoproteins in hippocampal neurons. Additionally, we are able to exploit the AlkFuc analog for pulse-chase investigations into the dynamic localization of AlkFuc labeled glycoproteins, showing that fucosylated glycoproteins are trafficked from the Golgi apparatus and localize to the synapses. The ability to label newly synthesized glycoproteins is a distinct advantage of the metabolic labeling technique over other methods, such as lectin staining or chemoenzymatic detection, and could be utilized to study the dynamics and trafficking of specific glycoproteins.

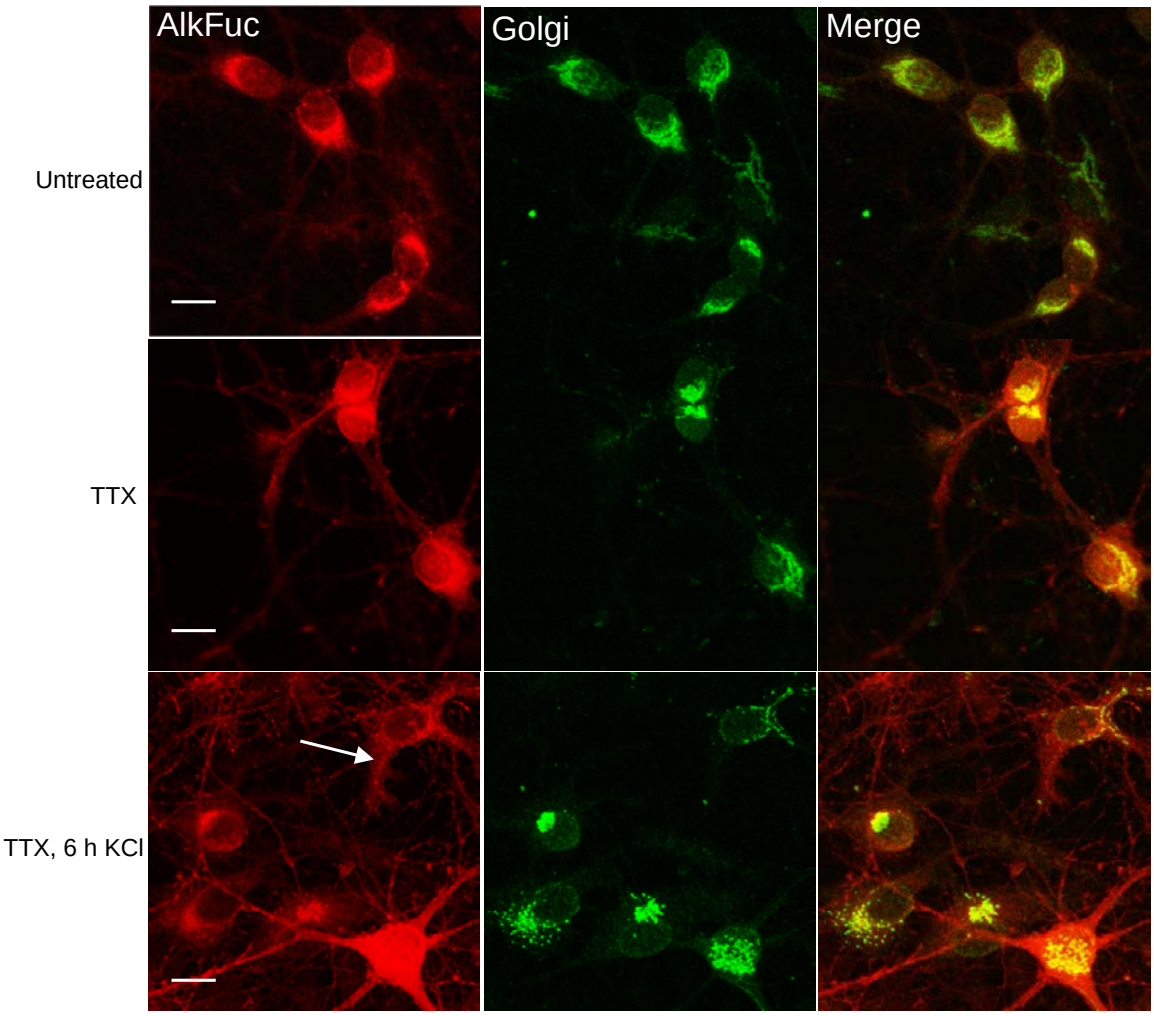

Figure 3.7 AlkFuc labeling after KCl depolarization**.** After KCl depolarization for 6 h, AlkFuc labeling in the Golgi appears diffuse and punctate. Scale bar is 25 µM.

Experimental Procedures

Fluorescent Imaging of Fucosylated Glycans in Hippocampal Neurons. After the indicated number of days in culture, hippocampal neurons on coverslips were treated with 50 µM Fuc or AlkFuc for 3 d. Subsequent to treatment in culture, the media was removed and cells were rinsed once with PBS, fixed and permeabilized in ice cold methanol, and washed twice with PBS. All coverslips were blocked in 3% BSA in PBS for 1 h at rt, followed by 1 µg/mL streptavidin in 3% BSA in PBS for 15 min at rt. Metabolically labeled proteins were tagged by treating the cells with 5 mM triazole ligand, 50 mM sodium ascorbate (Sigma Aldrich), 50 mM $CuSO_4$ (Sigma Aldrich), and 5 mM alkyne-biotin (CHW lab) in PBS (100 µL/coverslip) at 4 °C for 8 h, followed by detection with streptavidin Alexa Fluor 488 (Life

Technologies, 1:1000 in 3% BSA). The primary antibodies anti-synapsin (rabbit, 1:100; Sigma), anti-PSD-95 (mouse, 1:250; Affinity BioReagents), anti-giantin (Santa Cruz, 1:100), anti-NCAM (mouse, 1:100, Sigma) and UEAI conjugated to fluorescein (50μL/mL, Sigma) was added in 3% BSA in PBS, overnight at 4 °C. After the coverslips were washed three times with PBS, fluorophore conjugated secondary antibodies (goat anti-rabbit; 1:500 and goat anti-mouse; 1:500) were added in 3% BSA in PBS for one hour at rt. AlkFuc was detected with streptavidin-Alexa Fluor 488 (1:1000; Life Technologies) or Alexa Fluor 546 (1:1000, Life Technologies) added together with the secondary antibodies. The coverslips were washed three times with PBS and mounted onto slides with Vectashield with DAPI (Vector Labs) and sealed with clear nail polish. Cells were then subjected to fluorescence and confocal microscopy.

Pulse–Chase Analysis of AlkFuc Labeled Proteins. Hippocampal neurons at 23 DIV were treated with 200 μM AlkFuc in supplemented Neurobasal (Invitrogen) for 30 min, after which all the media was replaced with alknyl-fucose free media. Neurons were fixed and permeabilized as described above every two to four hours, and stored in PBS at 4 °C until the termination of the time-course. All coverslips were blocked first in 3% BSA in PBS for 1 h at rt, followed by 0.001 μg/μL streptavidin in 3% BSA in PBS for 15 min at rt. Metabolically labeled proteins were tagged by treating the cells 5 mM triazole ligand, 50 mM sodium ascorbate (Sigma Aldrich), 50 mM CuSO4 (Sigma Aldrich), and 5 mM alkyne-biotin in PBS (100 μL/coverslip)at 4 °C for 8 h, followed by detection with streptavidin Alexa Fluor 488 (Life Technologies, 1:1000 in 3% BSA). Synapsin I, GluR1, and Giantin were detected and the coverslips mounted as described above. Cells were imaged using a 40X or 63X Plan-Achromat objective on a Zeiss Meta510 or 700 inverted microscope.

Detection of AlkFuc labeled Proteins after Neuronal Stimulation. After the indicated number of days in culture, hippocampal neurons on coverslips were treated with 100 μM Fuc or AlkFuc for 3 d. 2

d into the treatment, neuronal cultures were treated with 1 μM tetrodotoxin (TTX; Sigma Aldrich). After 1 d of TTX treatment, neurons were stimulated with 50 mM KCl in PBS (Sigma Aldrich) for 5 min up to 25 h. Subsequent to treatment in culture, the media was removed and cells were rinsed once with PBS, fixed and permeabilized in ice cold methanol, and washed twice with PBS. All coverslips were blocked in 3% BSA in PBS for 1 h at rt, followed by 1 μg/mL streptavidin in 3% BSA in PBS for 15 min at rt. Metabolically labeled proteins were tagged by treating the cells 5 mM triazole ligand, 50 mM sodium ascorbate (Sigma Aldrich), 50 mM $CuSO_4$ (Sigma Aldrich), and 5 mM alkyne-biotin (CHW lab) in PBS (100 μL/coverslip) at 4 °C for 8 h, followed by detection with streptavidin Alexa Fluor 488 (Life Technologies, 1:1000 in 3% BSA). The primary antibodies anti-synapsin (rabbit, 1:100; Sigma), anti-PSD-95 (mouse, 1:250; Affinity BioReagents), anti-giantin (Santa Cruz, 1:100), anti-NCAM (mouse, 1:100, Sigma) and UEAI conjugated to fluorescein (50μL/mL, Sigma) was added in 3% BSA in PBS, overnight at 4 °C. After the coverslips were washed three times with PBS, fluorophore conjugated secondary antibodies (goat anti-rabbit; 1:500 and goat anti-mouse; 1:500) were added in 3% BSA in PBS for one hour at rt. AlkFuc was detected with streptavidin-Alexa Fluor 488 (1:1000; Life Technologies) or Alexa Fluor 546 (1:1000, Life Technologies) added together with the secondary antibodies. The coverslips were washed three times with PBS and mounted onto slides with Vectashield with DAPI (Vector Labs) and sealed with clear nail polish. Cells were then subjected to fluorescence and confocal microscopy.

References

1. Kiessling LL & Pohl NL (1996) Strenght in Numbers: Non-natural polyvalent carbohydrate derivatives. *Chemistry and Biology* 3:71-77.

2. Saxon E & Bertozzi CR (2000) Cell surface engineering by a modified Staudinger reaction. *Science* 287:2007-2010.

3. Hsu TL, *et al.* (2007) Alkynyl sugar analogs for the labeling and visualization of glycoconjugates in cells. *Proc. Natl. Acad. Sci. U.S.A* 104(8):2614-2619.

4. Luchansky SJ, Goon S, & Bertozzi CR (2004) Expanding the diversity of unnatural cell-surface sialic acids. *Chembiochem* 5:371-374.

5. Kosa RE, Brossmer R, & J. GH (1993) Modification of cell surfaces by enzymatic introduction of special sialic acid analogues. *Biochem. Biophys. Res. Commun.* 190:914-920.

6. Luchansky SJ, Argade S, Hayes BK, & Bertozzi CR (2004) Metabolic functionalization of recombinant glycoproteins. *Biochemistry* 43:12358-12366.

7. Prescher JA, Dube DH, & Bertozzi CR (2004) Chemical remodelling of cell surfaces in living animals. *Nature* 430:873-877.

8. Laughlin ST, Baskin JM, Amacher SL, & Bertozzi CR (2008) In Vivo Imaging of Membrane-Associated Glycans in Developing Zebrafish. *Science* 320(5876):664-667.

9. Hang HC, Yu C, Kato DL, & Bertozzi CR (2003) A metabolic labeling approach toward proteomic analysis of mucin-type O-linked glycosylation. *Proc. Natl. Acad. Sci. U.S.A* 100(25):14846-14851.

10. Dube DH, Prescher JA, Quang CN, & Bertozzi CR (2003) Probing mucin-type O-glycosylation in living animals. *Proc. Natl. Acad. Sci. U.S.A.* 103:14846-14851.

11. Anderson CT, Wallace IS, & Somerville CR (2012) Metabolic click-labeling with a fucose analog reveals pectin delivery, architecture, and dynamics in Arabidopsis cell walls. *Proc. Natl. Acad. Sci. U.S.A.* 109(4):1329-1334.

12. Dehnert KW, *et al.* (2011) Metabolic labeling of fucosylated glycans in developing zebrafish. *ACS Chem. Biol.* 6(6):547-552.

13. Murrey HE, *et al.* (2006) Protein fucosylation regulates synapsin Ia/Ib expression and neuronal morphology in primary hippocampal neurons. *Proc. Natl. Acad. Sci. U.S.A* 103(1):21-26.

14. Zanetta JP, Reeber A, Vincendon G, & Gombos G (1977) Synaptosomal Plasma Membrane Glycoproteins. II. Isolation of Fucosyl-Glycoproteins by Affinity Chromatography on the Ulex Europeus Lectin Specific for L-Fucose. *Brain Res.* 138:317-328.

15. Krusius T & Finne J (1977) Structural Features of Tissue Glycoproteins: Fractionation and Methylation Analysis of Glycopeptides Derived from Rat Brain, Kidney, and Liver. *FEBS J.* 78:369-379.

16. Gardiol A, Racca C, & Triller A (1999) Dendritic and postsynaptic protein synthestic machinery. *J. Neurosci.* 19(1):168-179.

17. Kalovidouris SA, Gama CI, Lee LW, & Hsieh-Wilson LC (2005) A role for fucose alpha(1-2) galactose carbohydrates in neuronal growth. *J. Am. Chem. Soc.* 127(5):1340-1341.

18. Becker DJ & Lowe JB (2003) Fucose: biosynthesis and biological function in mammals. *Glycobiology* 13(7):41R-53R.

19. Manimala JC, Roach TA, Li Z, & Gildersleeve JC (2006) High-Throughput Carbohydrate Microarray Analysis of 24 Lectins. *Angew. Chem. Int. Ed. Engl.* 45(22):3607-3610.

20. Baldus SE, *et al.* (1996) Characterization of the binding specificity of *Anguilla anguilla* agglutinin (AAA) in comparison to *Ulex europeaus* agglutinin I (UEA-I). *Glycoconjugate J.* 12(4):585-590.

21. Lippincott-Schwartz J, Yuan LC, Bonifacino JS, & Klausner RD (1989) Rapid redistribution of Golgi proteins into the ER in cells treated with brefeldin A: Evidence for membrane cycling from Golgi to ER. *Cell* 56(5):801-813.

22. Horton AC, *et al.* (2005) Polarized secretory trafficking directs cargo for asymmetric dendrite growth and morphogenesis. *Neuron* 48(5):757-771.

23. Kalovidouris SA, Gama CI, Lee LW, & Hsieh-Wilson LC (2005) A Role for Fucose α(1−2) Galactose Carbohydrates in Neuronal Growth. *J. Am. Chem. Soc.* 127(5):1340-1341.

24. Mammen AL, Hugnair RL, & O'Brien RJ (1997) Redistribution and Stabilization of Cell Surface Receptors during Synapse Formation. *J. Neurosci.* 17(19):7351-7358.

25. Park T-U, Lucka L, Reutter W, & Horstkorte (1997) Turnover Studies of the Neural Cell Adhesion Molecule NCAM: Degradation of NCAM in PC12 Cells Depends on the Presence of NGF. *Biochem. Biophys. Res. Commun.* 234:686-689.

26. Gray NW, Weimer RM, Bureau I, & Svoboda K (Rapid Redistribution of Synaptic PSD-95 in the Neocortex in vivo. *PLoS Biol.*

27. Marko P & Cuenod M (1973) Contribution of the nerve cell body to renewal of axonal and synaptic glycoproteins in the pigeon visual system. *Brain Res.* 62(2):419-423.

28. Thayer DA, Jan YN, & Jan LY (2013) Increased neuronal activity fragments the Golgi complex. *Proc. Natl. Acad. Sci. U.S.A.* 110(4):1482-1487.

CHAPTER 4

The Chemoenzymatic Detection of Fucose-α(1,2)-Galactose Glycans*

Introduction

As we have described in previous chapters, metabolic labeling is a powerful approach to detect glycans *in vivo* and to enrich glycoproteins for proteomic analysis (1, 2). However, one limitation of metabolic labeling is that it tracks only monosaccharides, each of which can be found on a large number of different cellular glycans. For example, although we are interested in Fucα(1-2)Gal structures, the metabolic labeling approach tracks fucosylated glycans of any linkage. Disaccharides or trisaccharides of specific sugar composition and glycosidic linkage are not uniquely accessible by hijacking the biosynthetic machinery with non-natural monosaccharide analogs. Moreover, the non-natural sugar is often incorporated sub-stoichiometrically into glycoconjugates, depending on its extent of cellular uptake and ability to compete with natural sugars.

The complementary approach of chemoenzymatic labeling exploits an exogenous glycosyltransferase to covalently tag specific glycans of interest with a non-natural sugar analog. Similar to metabolic labeling, the non-natural analog contains a bioorthogonal group that can be subsequently reacted with a variety of chemical reporters. Recently, this strategy has been used to detect and image *O*-linked β-*N*-acetylglucosamine (*O*-GlcNAc) glycosylated proteins (3, 4), to identify the *O*-GlcNAc proteome (5, 6), to quantify *O*-GlcNAc glycosylation stoichiometries (7), and to monitor the dynamics of *O*-GlcNAc glycosylation in response to cellular stimuli (3, 6-8). Because chemoenzymatic labeling is not limited by endogenous biosynthetic machinery and has the potential to proceed in quantitative yield, stoichiometric addition of the non-natural sugar can be achieved, resulting in high detection sensitivity relative to antibodies and lectins (3). Additionally, chemoenzymatic approaches have the ability to detect specific glycan motifs of a defined structure,

* Portions of this text are taken from: Chaubard, J.-L.; Krishnamurthy, C.; Yi, W.; Smith, D. F.; Hsieh-Wilson, L. C. *J. Am. Chem. Soc*. 2012, **134**, 4489−4492.

depending on the specificity of the exogenous tagging enzyme. For instance, Wu and coworkers recently demonstrated the detection of *N*-acetyllactosamine (LacNAc) on living cells and in developing zebrafish *in vivo* (9). However, the development of a successful chemoenzymatic strategy requires the identification and characterization of suitable enzymes for tagging specific glycans. For this reason, chemoenzymatic methods have only been developed in the few instances described above.

In the following chapter, we describe a new chemoenzymatic strategy for the detection of Fucα(1- 2)Gal glycans within the glycome. As described in Chapter 1, Fucα(1−2)Gal structures are found on *N*- and *O*-linked glycoproteins and glycolipids (10), and the Fucα(1-2)Gal epitope is an attractive biomarker and potential therapeutic target for cancer (11-13). However, the extent to which this sugar epitope serves as a marker of disease progression and its precise contributions to cancer pathogenesis are not well understood. The development of new methods to detect and study Fucα(1-2)Gal glycans would accelerate an understanding of their roles in vital biological processes and disease. We describe a chemoenzymatic approach that exploits the bacterial homologue to the blood group transferase A (BgtA), a recently reported bacterial glyscosyltransferases that synthesizes the blood group A antigen by transferring a GalNAc to the Fucα(1−2)Gal structure (Figure 4.1) (14).

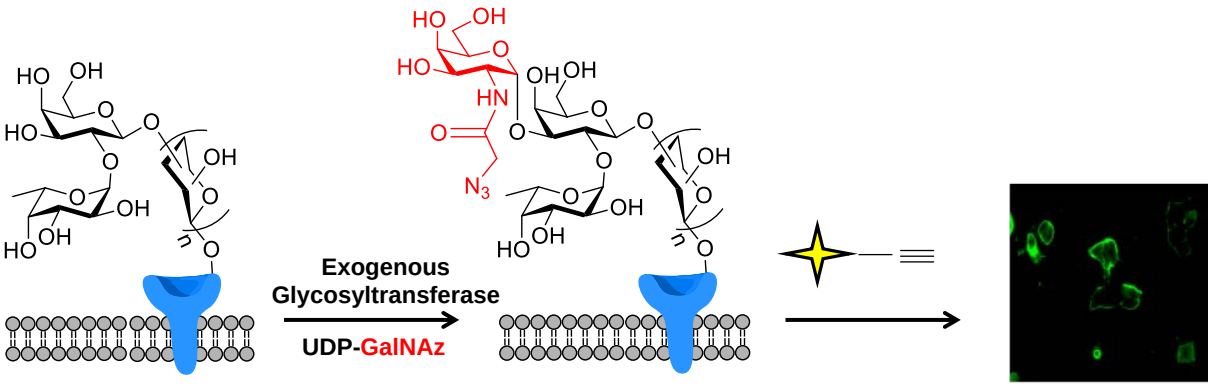

Figure 4.1 The chemoenzymatic strategy allows for the specific detection of Fucα(1-2)Gal glycans.

We take advantage of the specificity of BgtA for Fucα(1−2)Gal structures to develop a rapid, chemoselective, detection of the Fucα(1-2)Gal epitope on a wide range of oligosaccharide structures. We demonstrate that this approach can be used to selectively label glycoproteins in neuronal cell lysates and to track Fucα(1-2)Gal glycoconjugates on the surfaces of living cells. Moreover, we apply this approach to quantify the relative expression levels of Fucα(1−2)Gal glycans on normal and tumorigenic cells.

Results and Discussion

Expression and Purification of BgtA

The bacterial homologue of the human blood group A antigen glycosyltransferase (BgtA) was acquired as a His tagged construct in the pET28A vector from the laboratory of George Peng Wang (14). The enzyme was expressed and purified from Bl21 cells on a Ni-NTA column. Cells were cultured at 16 °C and protein expression was induced with 0.8 mM isopropyl β-D-1-thiogalactopyranoside (IPTG) when at an optical density (O.D) of 0.8 units. Protein was subsequently expressed at 16 °C for 16 h, after which the cells were pelleted and lysed for protein purification. Induction and expression of the enzyme was confirmed via SDS-PAGE prior to purification. The enzyme was purified on Ni-NTA resin over the period of two days, and eluted in increasing concentrations of imidazole. Fractions were analyzed via SDS-PAGE (Figure 4.2); the purified enzyme appears at a molecular weight of 37 kDa. Fractions containing pure enzyme were concentrated to 1 mg/mL and stored at 4 °C. Typically, 10 L of bacterial culture yielded 2-4 mg of purified enzyme.

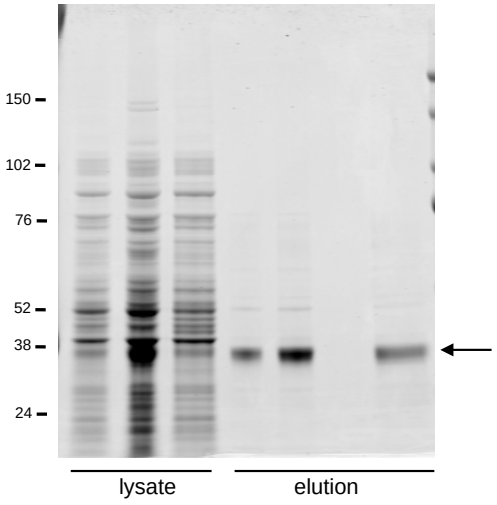

Figure 4.2 The expression and purification of BgtA

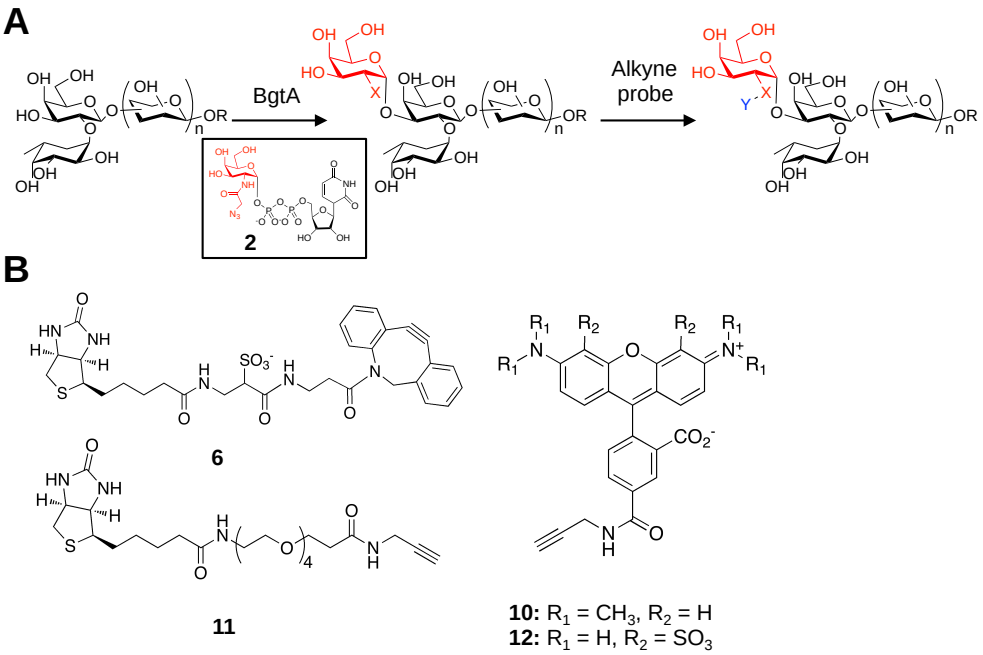

Figure 4.3 Chemoenzymatic strategy to detect Fucα(1-2)Gal glycans. (A) The chemoenzymatic detection strategy with the non-natural nucleotide sugar analog **2**, UDP-GalNAz (B) Alkyne probes for the detection of chemoenzymatically tagged glycans.

BgtA Accepts Non-Natural Substrates with Azido- Functionalities.

In order to design a method for the detection of Fucα(1-2)Gal glycans, we first investigated whether BgtA could be exploited to transfer a non-natural sugar analog to the Fucα(1-2)Gal structure. BgtA has been shown to transfer *N*-acetylgalactosamine (GalNAc) from UDP-GalNAc onto the C-3 position of Gal in Fucα(1-2)Gal structures (14). As other *N*-acetylgalactosaminyltransferases have been shown to tolerate substitutions at the C-2 position of GalNAc (15), we hypothesized that BgtA might also tolerate a substitution in the donor nucleotide sugar, allowing for the incorporation of an azido tag onto Fucα(1-2)Gal (Figure 4.3A). The labeled glycoconjugates could subsequently be detected with alkyne-functionalized probes using CuAAC chemistry (Figure 4.3B) (16-18). To test this approach, we synthesized the Fucα(1-2)Gal substrate **1** via reductive amination of 2'-fucosyllactose with *p*-nitrobenzylamine and sodium cyanoborohydride (Figure 4.4).

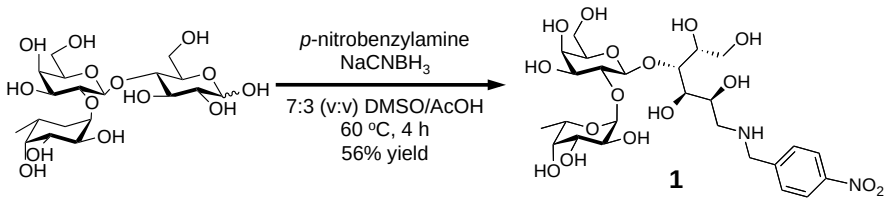

Figure 4.4 Synthesis of Fucα(1-2)Gal substrate **1**

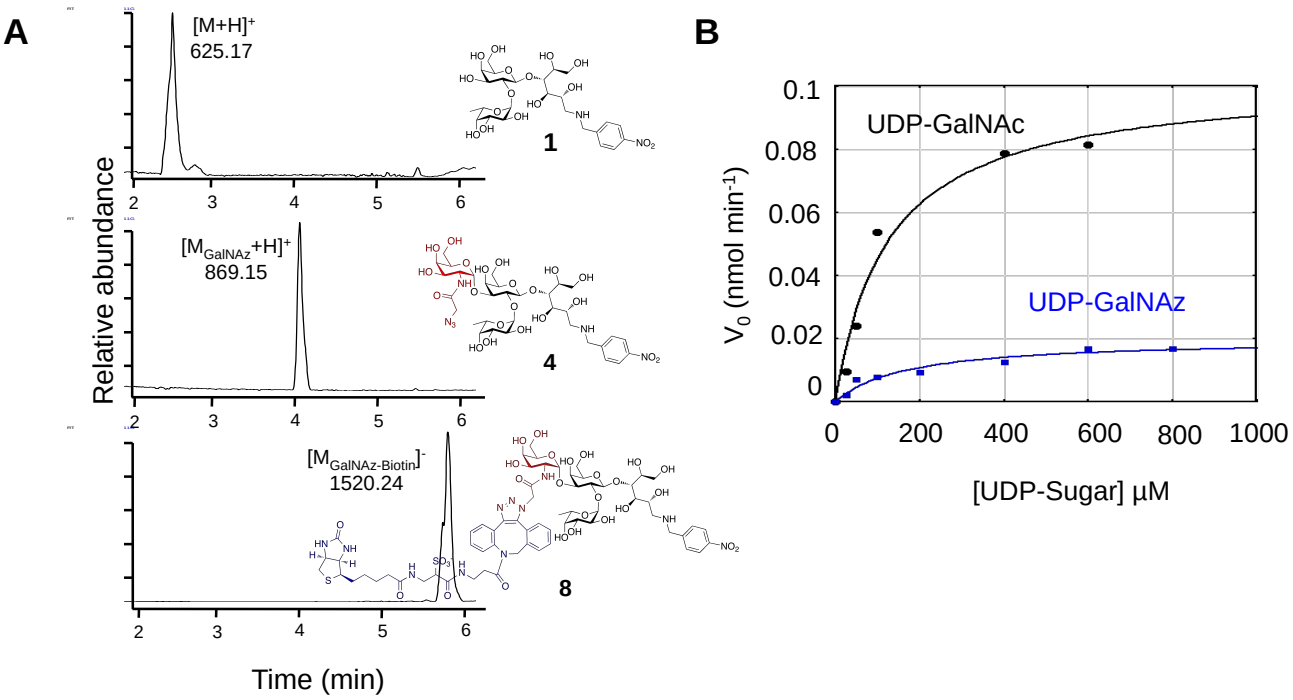

Figure 4.5 Labeling of substrate 1. (A) LC−MS traces monitoring the reaction progress at time 0 (top), 12 h after the addition of BgtA and 2 (middle), and 3 h after the addition of ADIBO-biotin 6 (bottom). (B) Kinetic comparison of the BgtA-catalyzed reaction of 1 with UDP-GalNAc (black) and UDP-GalNAz (blue). Reactions were performed in duplicate using 100 µM of acceptor 1 and varying concentrations of the donor. Initial rates as a function of substrate concentration were plotted and revealed apparent kcat/Km values of 5.7 nM-1min-1 and 40.4 nM-1min-1, respectively, and apparent Km values of 127 ± 36 µM and 168 ± 55 µM, respectively. The apparent Vmax value for UDP-GalNAc (0.100 ± 0.010 nmol•min-1) is approximately 5-fold higher than that of UDP-GalNAz (0.020 ± 0.002 nmol•min-1).

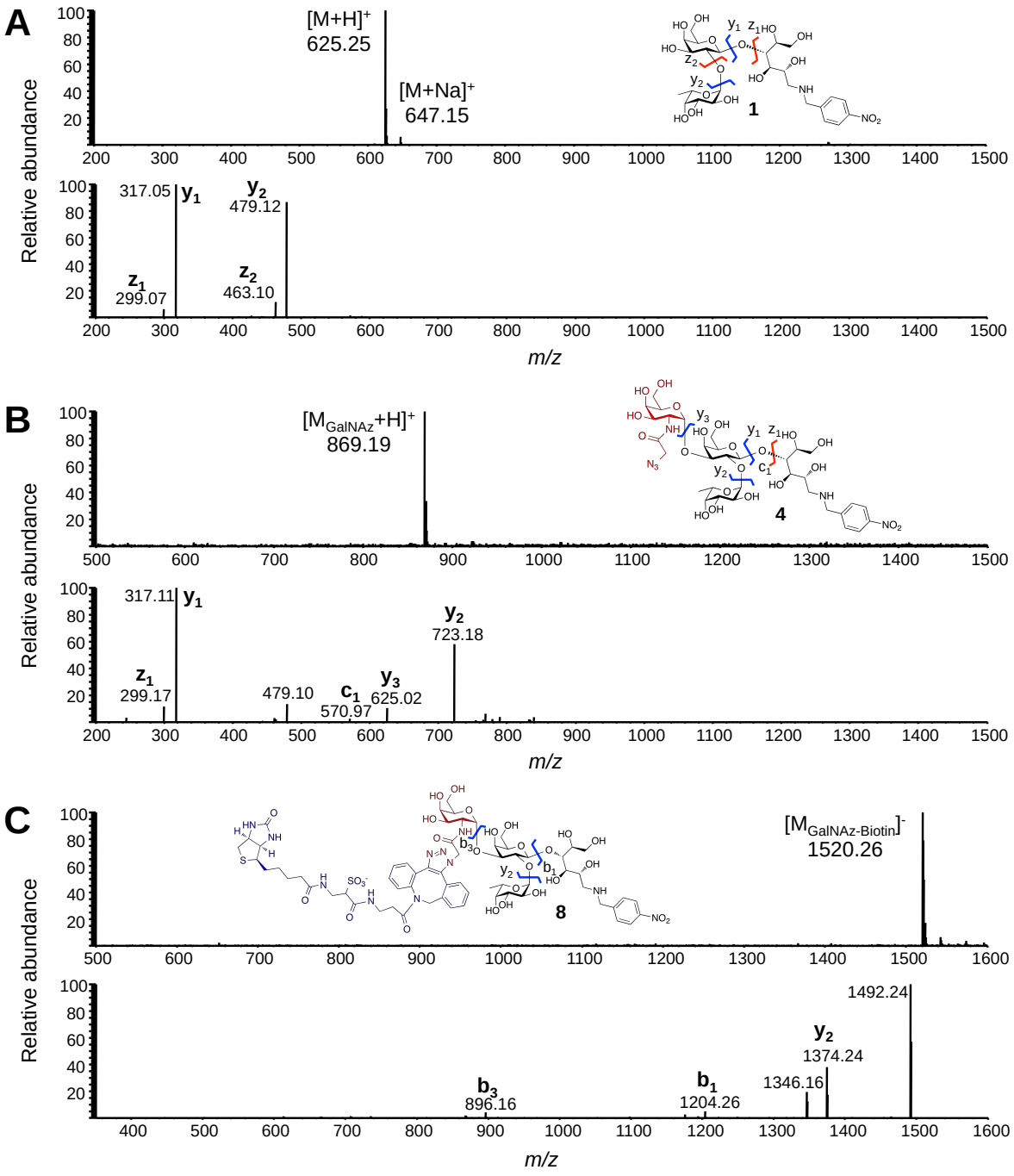

Figure 4.6 LC-MS/MS analysis of 1, 4 and 8 during the chemoenzymatic labeling reaction. (A) Compound **1** at time 0. (B) Compound **4**, generated 12 h after the addition of BgtA and UDP-GalNAz **2**. (C) Biotinylated glycan **8**, generated 3 h after reaction with ADIBO-biotin **6**.

BgtA was expressed in *E. coli* and purified to homogeneity as described above. Treatment of **1** with BgtA and UDP-*N*-azidoacetylgalactosamine (UDP-GalNAz, **2**; Figure 4.3A) led to complete conversion to the desired product **4**, after 12 h at 4 °C, as determined by liquid chromatography-mass spectrometry analysis (LC-MS; Figure 4.5A). Kinetic analysis revealed an apparent K_{cat}/K_m value of 5.7 nm^{-1} min^{-1} for UDP-GalNAz, approximately 7 fold lower than the value obtained for UDP-GalNAc, 40.4 nm^{-1} min^{-1} (Figure 4.5B). Subsequent reaction with an aza-dibenzocyclooctyne-biotin conjugate (ADIBO-biotin, **6**; Figure 4.3B) using copper-free click chemistry (3 h, rt) afforded the biotinylated product **8** (Figure 4.5). LC-MS/MS analysis of compounds **1**, **4**, and **8** identified masses and fragmentation patterns consistent with the expected structures (Figure 4.6). Thus, we determined that BgtA accepts the non-natural substrate UDP-GalNAz and can be exploited for efficient chemoenzymatic labeling of Fucα(1-2)Gal glycans.

BgtA Specifically Modifies Fucα(1-2)Gal Glycans on Carbohydrate Microarrays.[†]

A major advantage of chemoenzymatic tagging over metabolic labeling approaches is their ability tqo detect a specific subset of glycan structures, such as specific disaccharides. In order to profile the glycan specificity of BgtA, we utilized glycan microarrays provided by the Consortium for Functional Glycomics (19). The glycan microarrays are printed with 611 distinct glycan structures, and have been utilized to test the specificities of lectins and or antibodies, and profile the reactivity of glycosyltransferases (19-22). Glycosylation reactions were carried with BgtA and UDP-GalNAz on the microarray at 3 different time points (0.5, 2, and 12 h). A control reaction, with the UDP-GalNAz omitted, was carried out at 12 h. Subsequent to the chemoenzymatic labeling, the labeled glycans were reacted with ADIBO-Biotin and the biotinylated glycans were detected with Cy5-conjugated streptavidin. Strong fluorescence labeling of Fucα(1-2)Gal structures was observed within 0.5 h (Figure 4.7). The top 26 glycans labeled consisted of terminal Fucα(1-2)Gal structures, including the Globo H hexasaccharide (60; Figure 4.7), highlighting the specificity

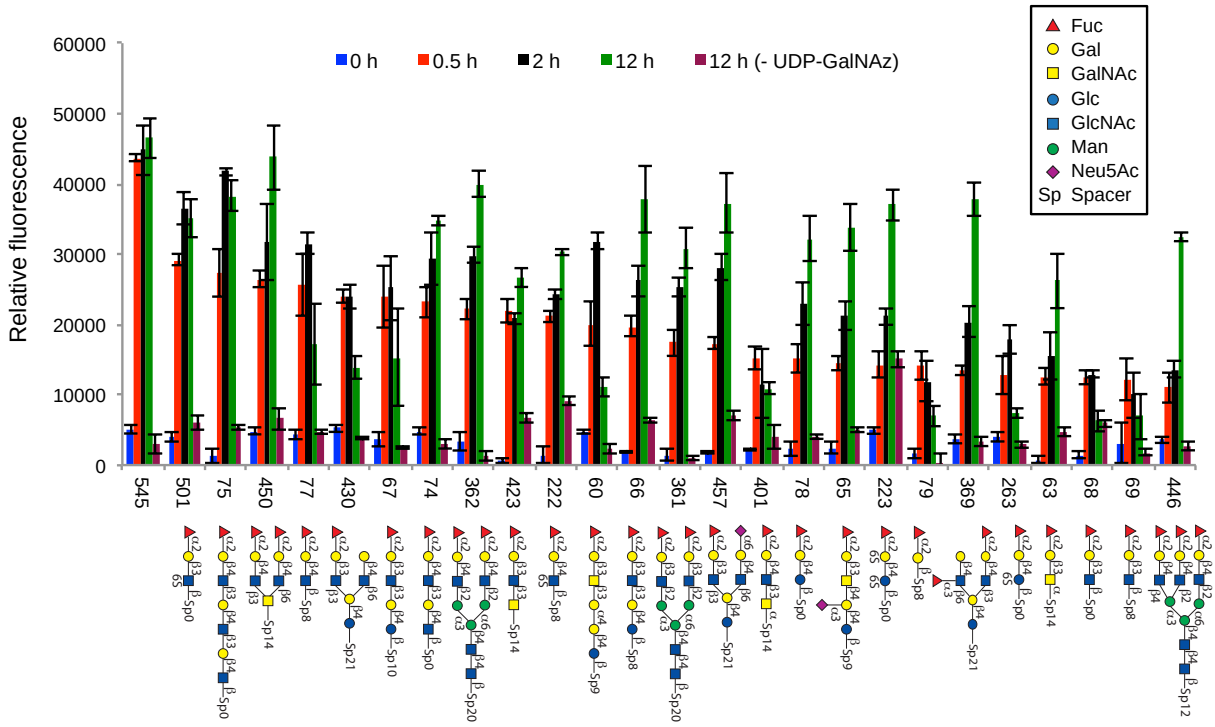

Figure 4.7 Time course analysis using glycan microarrays. Representative structures from the top 26 glycans with the highest relative fluorescence intensity after 0.5 h are plotted, all of which represent terminal Fucα(1-2)Gal structures. UDP-GalNAz was omitted as a control (12 h, -UDP-GalNAz).

of our chemoenzymatic approach. Notably, a wide variety of structures containing Fucα(1-2)Gal were efficiently labeled, including both linear (e.g., 501, 74, and 66; Figure 4.8A) as well as branched structures (e.g., 450, 362, and 457; Figure 4.8B). Moreover, ~91% of the Fucα(1-2)Gal glycans containing a free C-3 hydroxyl group on Gal were labeled on the array, demonstrating the sensitivity of the approach. In summary, our results demonstrate that chemoenzymatic labeling with BgtA is both sensitive and selective for glycans containing terminal Fucα(1-2)Gal structures, including the Lewis blood group antigens (type I and II) and the cancer-relevant Globo H antigen (23, 24)

Labeling of Fucα(1-2)Gal Proteins in Cell Lysates.

Having demonstrated the specificity of the approach, we next sought to determine whether the chemoenzymatic strategy could be used to detect Fucα(1-2)Gal glycoproteins in cell lysates. As it had been previously reported that Fucα(1-2)Gal glycoproteins are highly enriched in the olfactory

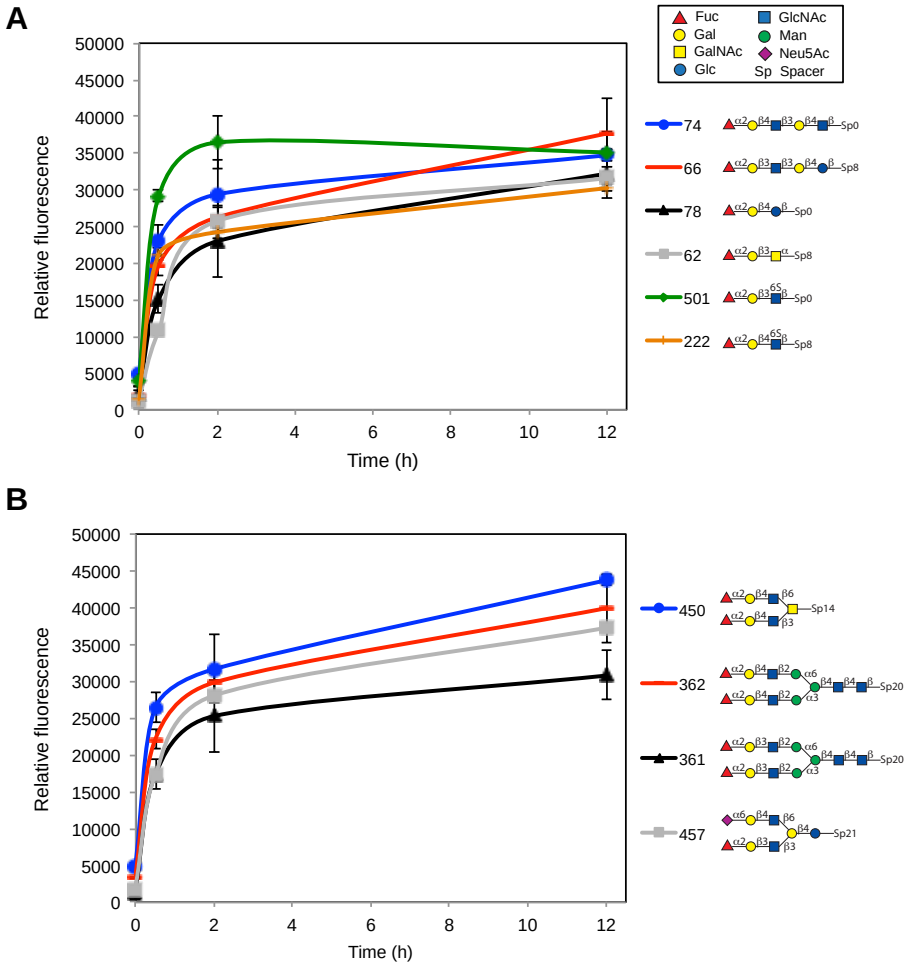

Figure 4.8: The chemoenzymatic approach labels a variety of linear (*A*) and branched (*B*) Fucα(1-2)Gal structures.

bulb of postnatal day 3 (P3) rat pups (25, 26), we elected to test the chemoenzymatic strategy in olfactory bulb lysates. Olfactory bulb lysates were chemoenzymatically labeled with BgtA and UDP-GalNAz, and then subjected to a CuAAC reaction with an alkyne-functionalized tetramethyl-6-carboxyrhodamine dye (alkyne-TAMRA, **10**; Figure 4.3B). Labeling with alkyne-TAMRA enabled direct visualization of the glycoproteins by in-gel fluorescence. As shown in Figure 4.9, we observed strong fluorescence labeling of Fucα(1-2)Gal glycoproteins (lane 1). Minimal non-specific labeling was detected in the absence of BgtA, UDP-GalNAz, or alkyne-TAMRA (lanes 2-4). Interestingly, BgtA itself was labeled, suggesting that it may bear a Fucα(1-2)Gal glycan and undergo autoglycosylation.

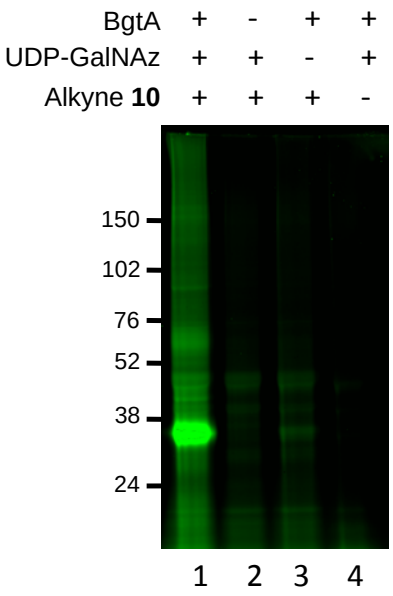

Figure 4.9 In-gel fluorescence detection of Fucα(1-2)Gal glycoproteins from olfactory bulb lysates. Low background fluorescence was observed in the absence of BgtA, UDP-GalNAz 2, or alkyne-TAMRA 10. The strong band at approximately 35 kDa is likely autoglycosylated BgtA.

Labeling and Enrichment of Specific Fucα(1-2)Gal Proteins

To confirm the specific labeling of Fucα(1-2)Gal glycoproteins, we biotinylated the chemoenzymatically labeled olfactory bulb lysates using the alkyne-biotin derivative **11** (Figure 4.4B), isolated the biotinylated proteins on streptavidin resin, and probed for the presence of known Fucα(1-2)Gal glycoproteins. Neural cell adhesion molecule (NCAM), synapsin I (syn I), and munc18-1 were all detected by immunoblotting, confirming the specific chemoenzymatic labeling of known Fucα(1-2)Gal glycoproteins (Figure 4.10A). None of the target proteins were detected in the streptavidin enriched fraction of control lysates labeled in the absence of BgtA. In addition to endogenous proteins, overexpressed synapsin I could also be labeled via the chemoenzymatic strategy. Glycosylated synapsin I could be readily detected following overexpression of Flag-tagged synapsin I in HeLa cells, chemoenzymatic labeling of the lysates with alkyne-TAMRA, synapsin immunoprecipitation, and visualization of the labeled sugar using an anti-TAMRA antibody (Figure 4.10B). Together, these results demonstrate that the chemoenzymatic tagging strategy can be utilized to label both endogenous and overexpressed Fucα(1-2)Gal glycoproteins from cells and tissues.

We also investigated whether the chemoenzymatic strategy was more sensitive than a lectin affinity chromatography method to detect Fucα(1-2)Gal glycoproteins. Olfactory bulb lysate was enriched over UEAI conjugated resin or control agarose resin, and probed for the enrichment of synapsin I. Importantly, UEAI lectin affinity chromatography failed to pull-down and detect glycosylated synapsin I, though the chemoenzymatic strategy detected a significant fraction of glycosylated synapsin I, when performed on the same scale (Figure 4.11). Moreover, previous studies have reported that the Fucα(1-2)Gal-specific antibody A46-B/B10 does not immunoprecipitate glycosylated synapsin I from the same neuronal lysates (25), indicating that the chemoenzymatic strategy is more sensitive than a fucose-specific lectin and antibody.

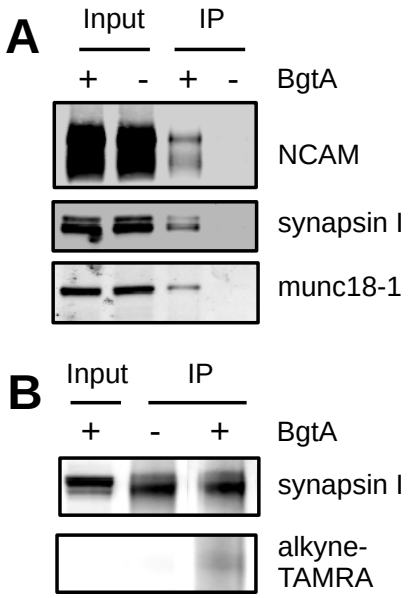

Figure 4.10 Chemoenzymatic Detection of Fucα(1-2)Gal Glycoproteins (A) Chemoenzymatic detection of endogenous Fucα(1-2)Gal glycoproteins from neuronal lysates. (B) Chemoenzymatic detection of FLAG-tagged synapsin I expressed in HeLa cells.

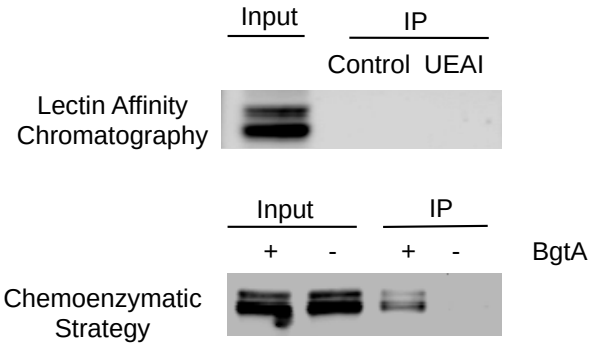

Figure 4.11 Lectin affinity chromatography with UEAI was performed on 500 μg of olfactory bulb lysate. No synapsin was detected in the enriched fraction, whereas synapsin was detected when the chemoenzymatic strategy was performed on 500 μg of olfactory bulb lysate, demonstrating that the chemoenzymatic strategy detects Fucα(1-2)Gal glycoproteins with greater sensitivity.

Imaging and Quantification of Fucα(1-2)Gal Glycans on Cells.

Finally, we investigated whether our chemoenzymatic labeling strategy could be used to image Fucα(1-2)Gal glycans in intact cells. We first sought to detect a known Fucα(1-2)Gal glycoprotein, and thus transfected HeLa cells with a Flag-tagged synapsin I construct. Expression of Flag-synapsin I was detected 24 h post-transfection using an anti-Flag antibody (Figure 4.12, red). To detect glycosylated synapsin, the cells were fixed, permeabilized, and chemoenzymatically labeled on coverslip with BgtA and UDPGalNAz. CuAAC chemistry was then performed using an alkyne-functionalized Alexa Fluor 488 dye (**12**; Figure 4.3B) to install a fluorescent reporter onto the Fucα(1-2)Gal glycans. Strong fluorescence labeling of cells transfected with synapsin I was observed (Figure 4.13, green), and the labeling showed excellent overlap with Flag-synapsin I expression (yellow). Cells expressing Flag-synapsin I that were not treated with BgtA did not exhibit strong labeling, suggesting the specific labeling of a Fucα(1-2)Gal structure on synapsin I (Figure 4.13, middle row). Chemoenzymatic labeling of cells not expressing Flag-synapsin I showed only weak labeling (Figure 4.13, bottom row), suggesting labeling of endogenous Fucα(1-2)Gal glycans.

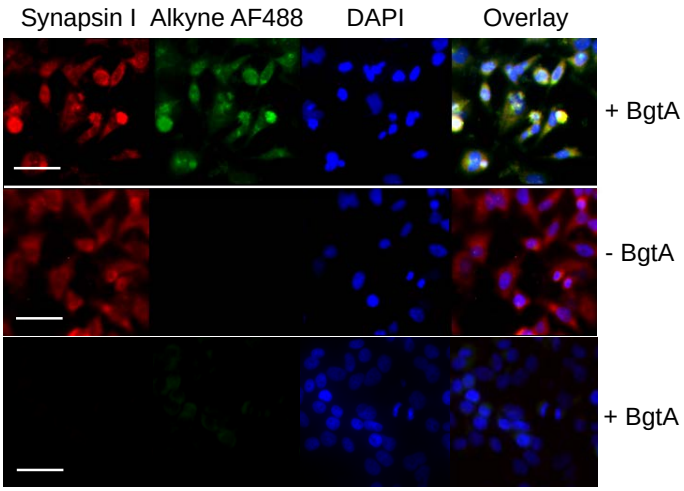

Figure 4.12 Fluorescence detection of Fucα(1-2)Gal glycans (green) shows significant overlay (yellow) with overexpressed FLAG-Synapsin I (red) in HeLa cells. Low levels of endogenous Fucα(1-2)Gal glycans are labeled in mock-transfected cells (bottom row.)

The Fucα(1-2)Gal epitope has been identified on the cell surface of breast, prostate, and ovarian cancer cells and may be a useful biomarker for carcinoma progression and prognosis.(23, 27) Therefore, we sought to apply our chemoenzymatic approach toward the detection of endogenous Fucα(1-2)Gal glycans on live cancer cells. Cells from the human breast adenocarcinoma cell line MCF-7, known to express high levels of the Globo H hexasaccharide (24), were first chemoenzymatically labeled with BgtA and the natural donor-sugar UDP-GalNAc, and detected with a anti-blood group A antibody conjugated to fluorescein to confirm the enzymatic labeling of surface Fucα(1-2)Gal glycans (Figure 4.13). Cell surface fluorescence was apparent, indicating that BgtA successfully labeled cell-surface glycans. MCF-7 cells were then labeled with BgtA and UDP-GalNAz for 1 h at 37 °C. We attempted to detect cell surface labeling with a variety of fluorescent strained-alkyne probes, including biarylazacycloocynone-fluorescein (BARAC-Fluor) and difluorinated cyclooctyne–Alexa Fluor 488 (DIFO-488) (28-30). However, low signal complicated our efforts and we were unable to successfully detect chemoenzymatically labeled Fucα(1-2)Gal glycans with the fluorescent strained alkyne probes. We resorted to a two-step detection strategy, consisting of tagging the chemoenzymatically labeled glycans with ADIBO-Biotin **6**, followed by

visualization with a fluorescent streptavidin conjugate. After reaction with ADIBO-biotin (1 h, rt), Fucα(1-2)Gal glycans were successfully detected using streptavidin conjugated to Alexa Fluor 488. Membrane-associated fluorescence was observed for cells treated with both BgtA and UDP-GalNAz, whereas no labeling was detected for control cells labeled in the absence of BgtA (Figure 4.14).

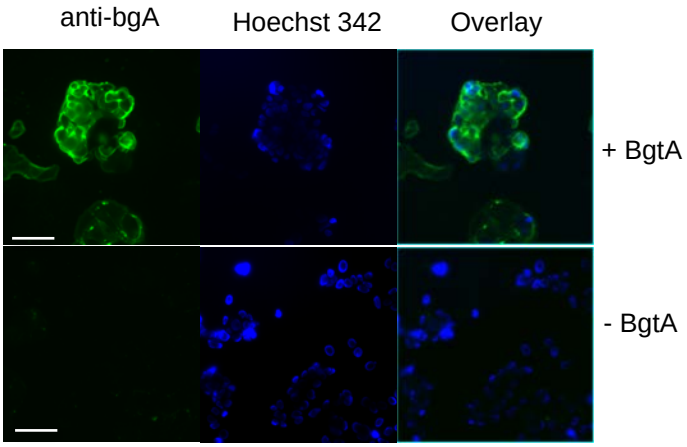

Figure 4.13 Chemoenzymatic Labeling with UDP-GalNAc. Fluorescence detection of Fucα(1-2)Gal glycans (green) on live MCF-7 cells with anti-BgA conjugated to flourescein. Cells were chemoenzymatically labeled, utilizing the natural donor UDP-GalNAc and detected with an antibody recognizing the blood group A antigen, anti-bgA. Nuclei were stained with Hoechst 342 (blue).

The ability to image Fucα(1-2)Gal glycans on living cells could facilitate comparisons of the expression levels of Fucα(1-2)Gal glycans across various cancers and the development of diagnostic tools to detect cancer progression. In order to assess the potential of the chemoenzymatic strategy for biomarker detection, several cancer cell lines were chemoenzymatically labeled to detect surface Fucα(1-2)Gal expression. MCF-7 (breast cancer), MDA-mb-231 (highly invasive breast cancer), H1299 (lung cancer), and LnCAP (prostate cancer) cell lines were chemoenzymatically labeled in suspension with BgtA and UDP-GalNAz (2 h, 37 °C), reacted with ADIBO-biotin (1 h, rt), and stained with streptavidin- Alexa Fluor 488 (20 min, 4 °C). Control reactions were undertaken with the UDP-GalNAz omitted, and cell surface fluorescence of viable cells was detected by flow cytometry. As shown by flow cytometry analysis, LnCaP cells displayed the highest levels of

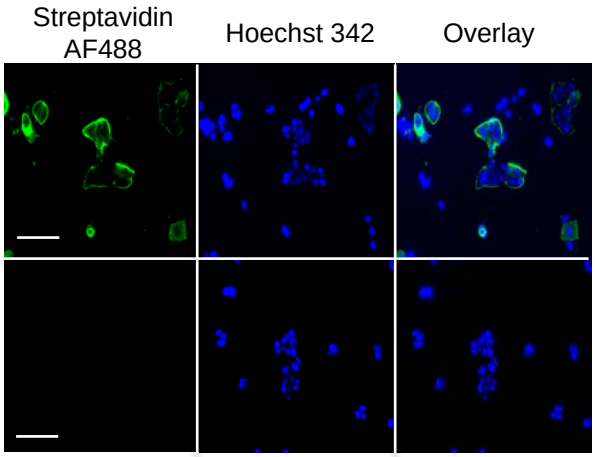

Figure 4.14 Fluorescence detection of Fucα(1-2)Gal glycans (green) on live MCF-7 cells. Nuclei were stained with Hoechst 342 (blue).

fluorescence, followed by the mammary cancer cells lines MCF-7 and MDA-mb-231, with H1299 cells showing lower fluorescence signal (Figure 4.14). MCF-7, MDA-mb-231 and LnCAP cells exhibited expression of Fucα(1-2)Gal, consistent with reports of high Globo H expression on mammary and prostate tumors (24, 31). H1299 cells, a model for non-small cell lung carcinoma and also reported to express Globo H (32), showed lower levels of Fucα(1-2)Gal expression as determined by chemoenzymatic labeling. As the Fucα(1-2)Gal antigen is a potential target for cancer therapeutics (11-13), the rapid profiling of Fucα(1-2)Gal expression levels on specific cancer cells or tissue may assist in determining whether the antigen is a useful therapeutic target for a particular cancer. Primary prostate epithelial cells (PrEC) were then labeled to determine whether our chemoenzymatic strategy could be used to detect changes in Fucα(1-2)Gal expression levels in normal versus cancerous cells. Flow cytometry analysis showed a strong difference in the fluorescence labeling of LnCAP cells compared to PrEC cells, with approximately a 50% increase in Fucα(1-2)Gal expression on the surface of LnCAP cells (Figure 4.15A and 4.15B). These results demonstrate that the chemoenzymatic approach can handily distinguish between cancerous cells and normal cells, providing a new potential strategy for biomarker detection. The method could be

particularly useful for the detection of prostate cancer from tissue biopsies, as the current standard of PSA detection to diagnose prostate cancer has a significant false-positive rate, leading to overtreatment (33). In addition to histological detection, our chemoenzymatic technique could provide a new potential strategy to distinguish normal PSA from tumorigenic PSA, which has higher levels of Fucα(1-2)Gal glycosylation (34). Future studies will optimize PSA detection strategies and explore the diagnostic applications of this approach to human disease.

In conclusion, we have developed a robust chemoenzymatic strategy for the rapid and sensitive detection of Fucα(1-2)Gal glycans, a disaccharide motif implicated in cognitive processes and a potential cancer biomarker. The approach enables the specific, covalent labeling of Fucα(1-2)Gal glycans in cell lysates and on the cell surface with a variety of chemical reporters. Given the versatility of the azide and ketone functionalities that can be installed onto the Fucα(1-2)Gal epitope, we envision a variety of diverse applications for this strategy, including biomarker detection, affinity enrichment, and isotopic labeling for comparative proteomics of Fucα(1-2)Gal glycoproteins. The ability to specifically detect Fucα(1-2)Gal glycans should facilitate investigations into the physiological importance of the Fucα(1-2)Gal epitope in both neurobiology and cancer. Such tools will expand the technologies available for glycomic studies and further our understanding of the roles of specific carbohydrate structures in physiology and disease

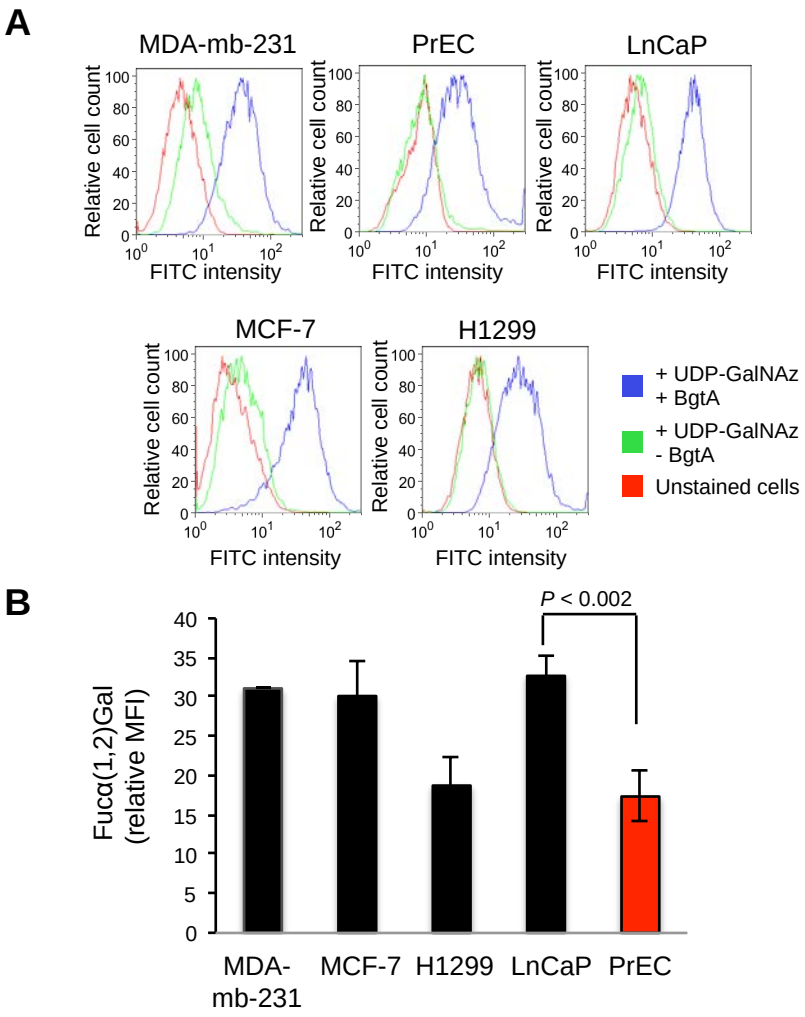

Figure 4.14 (A) Flow cytometry analysis of the relative expression levels of Fucα(1-2)Gal glycans across various cancer cell lines, with comparison to non-cancerous PrEC cells. Cells were untreated (red) or chemoenzymatically labeled in the presence (blue) or absence (green) of BgtA. (B) Quantification of the mean fluorescence intensity (MFI) relative to cells labeled in the absence of BgtA. Error bars represent data from duplicate (MCF-7, MDA-mb- 231, H1299) or triplicate (LnCAP, PrEC) experiments.

Experimental Methods

General Methods for Chemical Synthesis. Unless otherwise stated, all starting materials and reagents were purchased from Sigma-Aldrich and used without further purification. All ^{1}H and ^{13}C NMR spectra were recorded on a Varian Innova 600 spectrometer and referenced to solvent peaks. Data for ^{1}H NMR spectra are reported as follows: chemical shift (δ ppm), multiplicity (s = singlet, d = doublet, t = triplet, q = quartet, m = multiplet), coupling constant in Hz, and integration. Low-resolution mass spectra were recorded on an 1100 Agilent Liquid Chromatograph Mass Spectrometer with an Agilent SB-C18 reverse-phase column (3.5 μm, 4.6 x 250 mm) with monitoring at 280 and 310 nm. High-resolution mass spectra (HRMS) were obtained using an Agilent 6200 Series Time of Flight Mass Spectrometer with an Agilent G1978A Multimode source using mixed electrospray ionization/atmospheric pressure chemical ionization (MultiMode ESI/APCI).

Synthesis of 1-*p*-Nitrobenzyl-(2-fucosyl)-lactose (1). A 0.35 M solution of *p*-nitrobenzylamine in 7:3 (*v/v*) DMSO/AcOH (50 μL, 18 μmol) was added slowly to 2'-fucosyllactose (1.0 mg, 2.0 μmol) at rt. $NaCNBH_3$ (50 μL of a 1 M solution in 7:3 (*v/v*) DMSO/AcOH, 50 μmol) was then added slowly at rt, and the solution was stirred at 65 °C for 4 h. The reaction was quenched by adding 10 volumes of MeCN and incubated at -20 °C for 2 h. The precipitated mixture was then centrifuged at 10,000 x *g* for 5 min at 4 °C, and the supernatant was discarded. Ten additional volumes of MeCN were added to the pellet, and the vortexed mixture was incubated at -20 °C for 2 h and centrifuged as above. This step was repeated two more times to remove the excess *p*-nitrobenzylamine. The pellet was then resuspended in 5% MeCN and the product purified by semi-preparative HPLC (Agilent 1100) using two preparative reverse-phase columns (Agilent Eclipse XDB-C18; 5 μm, 9.4 x 250 mm) connected in series and a gradient of 5-20% B over 20 min at 4 mL/min (A, 0.5% aqueous AcOH; B, 100% MeCN). The product eluted at approximately 9.5 min. Lyophilization afforded a fluffy white solid (0.72 mg; 56% yield): ^{1}H NMR (600 MHz, D_2O) δ 8.33 (d, J = 8.6 Hz, 2H), 7.72 (d, J = 8.7 Hz, 2H),

5.31 (s, 1H), 4.60 (d, *J* = 7.8 Hz, 1H), 4.33 (q, *J* = 13.7 Hz, 2H), 4.23 (t, *J* = 6.3 Hz, 2H), 3.93 (d, *J* = 3.4 Hz, 1H), 3.91–3.86 (m, 4H), 3.83 (t, *J* = 4.4 Hz, 4H), 3.79–3.71 (m, 4H), 3.67 (dd, *J* = 9.5, 7.9 Hz, 1H), 3.32 (d, *J* = 11.7 Hz, 1H), 3.10 (t, *J* = 11.1 Hz, 1H), 1.23 (d, *J* = 6.6 Hz, 3H). ^{13}C NMR (151 MHz, D_2O) δ 147.86, 130.43, 124.09, 109.99, 107.14, 100.42, 99.65, 76.94, 76.65, 75.19, 73.42, 71.69, 70.48, 70.19, 69.45, 68.97, 68.51, 68.21, 67.18, 61.93, 60.90, 50.51, 49.52, 23.19, 15.29. HRMS: $[M+H]^+$ calculated for $C_{25}H_{40}N_2O_{16}$ 625.5996, found 625.2451.

Expression and Purification of BgtA. *E. coli* BL21 (DE3) harboring the recombinant plasmid vector pET28a-BtgA-His was kindly provided by Dr. Peng George Wang (Ohio State University). The protein was expressed and purified as described (14). Briefly, the cells were grown in LB medium (1L) at 37 °C. Isopropyl-1-thio-β-D-galactospyranoside (IPTG, 0.8 mM final concentration; Sigma) was added when the cells reached an OD_{600} of 0.8, and the cells were incubated for an additional 16 h at 16 °C. The pelleted cells were lysed in Cell Lytic B Lysis Reagent (Sigma-Aldrich) supplemented with EDTA-free Complete™ protease inhibitors (Roche), 0.5 M NaCl, and 20 mM imidazole (Sigma-Aldrich) by rotating end-over-end for 20 min at rt. After centrifugation, the clarified lysate was added to prewashed Ni-NTA beads and incubated at 4 °C for 1 h, washed in 20 mM Tris•HCl pH 7.5, 0.5 M NaCl and 50 mM imidazole, and eluted in a step gradient with the elution buffer (20 mM Tris•HCl pH 7.5, 0.5 M NaCl, and 100, 200 or 500 mM imidazole). After SDS–PAGE analysis, the purified protein was concentrated with 10,000 Da molecular weight cut-off (MWCO) spin filters (Millipore) and dialyzed into 20 mM Tris•HCl pH 7.5 containing 10% glycerol and stored at 4 °C.

BgtA Activity Assay and Monitoring of Chemoenzymatic Labeling Reactions by LC-MS/MS. The Fucα(1-2)Gal substrate **1** (10 μM) was dissolved in 20 mM Tris•HCl pH 7.5, 50 mM NaCl, and 5 mM $MnCl_2$. BgtA enzyme(14) and UDP-ketoGal **3(3)** or UDP-GalNAz **2** (Invitrogen) were added to final concentrations of 0.16 mg/mL and 50 μM, respectively, in a final volume of 100 μL. The

reaction was incubated at 4 °C in the dark for 12-16 h, and the reaction progress was monitored by LC-MS/MS. To label with aminooxy-biotin **7**, the reactions were diluted 5-fold with saturated urea, 2.7 M NaOAc pH 3.9 (50 mM final concentration and pH 4.8), and **7** (5 mM final concentration, Dojindo) and incubated for 20–24 h at rt. To label with ADIBO-biotin **6**, 250 μM of **6** (Click Chemistry Tools) was added, and the reaction was incubated for 3 h at rt. Following the labeling steps, the azido-labeled samples were filtered through a 3,000 Da MWCO Vivaspin 500 spin filter (GE Lifesciences) and injected on a reverse-phase HPLC column (Phenomenex Gemini; 5 m, 2.0 x 100 mm), fitted with a C8 guard column, using a ThermoScientific Accela 600 HPLC pump interfaced with a ThermoScientific LTQ mass spectrometer. A linear, 3-90% gradient of B (A: H_2O/0.1% aqueous formic acid B: MeCN/0.1% formic acid in MeCN) over 7 min was used to resolve peaks with a flow rate of 0.21 mL/min. Mass analysis was performed in positive ion mode except in the case of sulfated compound **8**, where the analysis was performed in negative ion mode.

Chemoenzymatic Labeling on the Glycan Array. Glycan Array version 5.0 was provided by the Consortium for Functional Glycomics. Pre-equilibrated arrays were treated with BgtA enzyme (0.16 mg/mL) and 500 μM UDP-GalNAz **2** in 20 mM Tris•HCl pH 7.4, 50 mM NaCl, 2 mM $MnCl_2$ containing 1% bovine serum albumin (BSA) for various times (0, 0.5, 2, and 12 h) at rt, washed 4 times with wash buffer (20 mM Tris•HCl pH 7.4, 50 mM NaCl, 0.1% Triton X-100) and then 4 times with rinse buffer (20 mM Tris•HCl pH 7.4, 50 mM NaCl). Arrays were then incubated with ADIBO-biotin (5 μM) in 20 mM Tris•HCl pH 7.4, 50 mM NaCl for 2 h at rt. After washing as described above, the arrays were washed further with 20% aqueous MeOH and then incubated with streptavidin Cy-5 (0.5 μg/mL; eBioSciences) in 20 mM Tris•HCl pH 7.4, 50 mM NaCl, 0.05% Tween-20, 1% BSA, for 1 h at rt. Arrays were then washed 4 times with wash buffer (containing 0.05% Tween-20 instead of 0.1% Triton X-100), 4 times with rinse buffer, and 4 times with water. Arrays were dried with a low stream of filtered air and analyzed using a PerkinElmer ScanArray Express.

Chemoenzymatic Labeling of Cell Lysates. The olfactory bulbs of postnatal day 3 rat pups were dissected on ice and lysed in boiling 1% SDS (5 volumes/weight) with sonication until the mixture was homogeneous. Protein was precipitated using methanol/chloroform/water. Briefly, protein was diluted to 200 μL and precipitated by sequential mixing with 600 μL of MeOH, 200 μL of $CHCl_3$ and 450 μL H_2O, after which the mixture was centrifuged at 23,000 x *g* for 15 min. Precipitated protein was washed with 450 μL of MeOH and centrifuged at 23,000 x *g* for 10 min. After the protein pellet was allowed to dry briefly, the pellet was re-dissolved at 5 mg/mL in 20 mM HEPES pH 7.9 containing 1% SDS, and diluted 5-fold into a buffer with the following final concentrations: 20 mM HEPES pH 7.9, 50 mM NaCl, 2% NP-40, 5 mM $MnCl_2$. UDP-GalNAz **2** (25 μM; Invitrogen) and BgtA (0.16 mg/mL) were added, and the samples were incubated at 4 °C for 16-20 h. The labeled proteins were precipitated as above and resuspended in 50 mM Tris pH 7.4 containing 1% SDS at 4 mg/mL. The resuspended proteins were subsequently reacted with alkyne-TAMRA **10** (Invitrogen) or alkyne-biotin **11** (Invitrogen) as per the Click-It™ TAMRA and Biotin Glycoprotein Detection Kit (Invitrogen) instructions, except that EDTA-free Complete™ protease inhibitors were added during the reaction. For TAMRA labeling, negative controls were performed under identical conditions except that BgtA, UDP-GalNAz **2**, or alkyne-TAMRA **10** was omitted from the labeling reaction. TAMRA-labeled proteins were resolved by SDS-PAGE and visualized in-gel using a Typhoon Scanner (GE Healthcare). For biotin labeling, negative controls were performed under identical conditions except that BgtA was omitted from the labeling reaction.

Purification of Biotin-Labeled Fuc α (1-2)Gal Proteins. Chemoenzymatically labeled samples were precipitated using methanol/chloroform/water as described above and re-dissolved in boiling 1% SDS plus Complete™ protease inhibitors at a concentration of 2 mg/mL. The SDS was quenched with 1 volume of NETFD buffer (100 mM NaCl, 50 mM Tris·HCl pH 7.4, 5 mM EDTA, 6% NP-40) plus protease inhibitors. The samples were incubated with pre-washed streptavidin resin (Pierce; 100

μL/1 mg protein) for 2 h at 4 °C. The resin was washed twice with 10 column volumes each of low salt buffer (0.1 M Na_2HPO_4 pH 7.5, 0.15 M NaCl, 1% Triton-X100, 0.1% SDS), twice with 10 column volumes each of high salt buffer (0.1 M Na_2HPO_4 pH 7.5, 0.5 M NaCl, 0.2% Triton-X100), and once with 10 column volumes of 50 mM Tris·HCl pH 7.4. Captured protein was eluted in boiling 2X sample buffer (100 mM Tris pH 6.8, 4% SDS, 200 mM DTT, 20% glycerol, 0.1% bromophenol blue; 50 μL /100 μL resin) for 5 min.

Western Blotting for Parallel Identification of Fuc α (1-2)Gal Glycoproteins. The purified, labeled material from above was resolved on a NuPAGE 4-12% Bis-Tris gel (Invitrogen) and transferred to a polyvinylidene difluoride (PVDF) membrane (Millipore). The membrane was blocked in 5% milk (BioRad) in TBST (50 mM Tris·HCl, 150 mM NaCl, 0.05% Tween 20, pH 7.4) for 1 h at rt. Primary antibodies in 5% milk in TBST were added overnight at 4 °C at the following concentrations: mouse anti-NCAM monoclonal antibody (Abcam) at 1 μg/mL, mouse anti-synapsin I ascites (Synaptic Systems) at 0.1 μg/ml, or mouse anti-munc18-1 (Synaptic Systems) at 0.1 μg/mL. Membranes were washed with TBST, and incubated with the appropriate Alexa Fluor 680-conjugated (Invitrogen) or IR800-conjugated (Rockland) secondary antibody, and visualized using a LiCOR Odyssey Imaging System.

Cell Culture. HeLa, MCF-7, and MDA-mb-231 cells were grown in DMEM medium supplemented with 10% fetal bovine serum (FBS), 100 units/mL penicillin, and 0.1 mg/mL streptomycin (Gibco). LNCaP and H1299 cells were grown in RPMI medium 1640 supplemented with 10% FBS, 100 units/mL penicillin, and 0.1 mg/mL streptomycin (Gibco). The PrEC line was maintained in PrEBM medium (Lonza). All transfections were carried out in antibiotic-free media. In all cases, cells were incubated in a 5% CO_2 humidified chamber at 37 °C. The PrEC line was obtained from Lonza; all other cell lines were obtained from ATCC.

Immunoprecipitation of TAMRA-Labeled Synapsin I from HeLa Cell Lysates. HeLa cells were transfected with pCMV-FLAG-synapsin Ia(25) using Lipofectamine LTX reagent (Invitrogen). The cells were lysed and chemoenzymatically labeled and protein was precipitated as described above. After the protein pellet was allowed to dry briefly, the pellet was re-dissolved in boiling 1% SDS plus Complete™ protease inhibitors at a concentration of 2 mg/mL. The SDS was quenched with 1 volume of NETFD buffer plus protease inhibitors, and the lysate was incubated with 40 μL of prewashed anti-Flag M2 Affinity Gel (Sigma-Aldrich) for 90 min at 4 °C. The resin was washed once with 4 column volumes of NETFD buffer and three times with 4 column volumes of NETF buffer (100 mM NaCl, 50 mM Tris·HCl pH 7.4, 5 mM EDTA). Captured protein was eluted in boiling 2X sample buffer (50 μL buffer/100 μL resin). Purified, labeled material was resolved by SDS-PAGE and transferred to a polyvinylidene fluoride (PVDF) membrane (Millipore). Western blotting was performed as above except the primary anti-TAMRA rabbit antibody (0.1 μg/μL; Invitrogen) was used.

Detection of Cell-Surface Fucα(1-2)Gal Glycans on Live MCF-7 Cells by Fluorescence Microscopy. MCF-7 cells (ATCC) were seeded at 2 x 10^5 cells/coverslip. Twelve hours after plating, the cells were washed twice with 1% FBS, 10 mM HEPES in calcium and magnesium free Hank's Balanced Salt Solution (CMF HBSS, Gibco) and incubated in the chemoenzymatic labeling buffer (2% FBS, 10 mM HEPES pH 7.9 in HBSS) with UDP-GalNAz **2** (500 μM) and BgtA (0.17 mg/mL) in a total volume of 100 μL for 2 h at 37 ºC. Mock reactions were performed without the addition of BgtA. After chemoenzymatic labeling, the cells were washed twice with 100% FBS and twice with the chemoenzymatic labeling buffer. Enzymatic addition of GalNAz onto Fucα(1-2)Gal glycans was detected by incubating the cells with ADIBO-biotin (20 μM in the chemoenzymatic labeling buffer; 500 μL) for 1 h at rt, washing the coverslips as described, and then incubation with

streptavidin-Alexa Fluor 488 (1 μg/mL in PBS containing 3% BSA; Invitrogen) for 30 min at rt. Cells were washed once with PBS, after which nuclei were stained with Hoechst-33342 (1 μg/μL; Invitrogen) in PBS for 15 min at rt. Coverslips were washed twice with 100% FBS and mounted in media (on ice), sealed with paraffin, and imaged immediately using a 40x Plan-Achromat objective on a Zeiss Meta510 inverted microscope.

Detection of Fucα(1-2)-Gal Glycans on Synapsin I in Fixed HeLa Cells by Fluorescence Microscopy. HeLa cells were plated onto 15 mm coverslips (Carolina Biologicals) at a density of 75 cells/mm^2. After 12 h, cells were transfected with pCMV-Flag-synapsin Ia (0.5 μg DNA/coverslip) using Lipofectamine LTX (4 μL in 200 μL Optimem; Invitrogen). After 24 h, the media was removed, and the cells were rinsed one time with PBS, fixed in 4% paraformaldehyde in PBS, pH 7.5 for 20 min at rt, washed twice with PBS, permeabilized in 0.3% Triton X-100 in PBS for 10 min at rt, and washed twice with the enzymatic labeling buffer (50 mM HEPES, 125 mM NaCl, pH 7.9). Reaction mixtures and negative controls (without BgtA) were prepared by adding 100 μL of 20 mM HEPES pH 7.9, 50 mM NaCl, 2% NP-40, 5 mM $MnCl_2$, UDP-GalNAz **1** (25 μM), and BgtA (0.17 mg/mL) at 4 °C for 24 h (100 μL/coverslip) in a humidified chamber. After chemoenzymatic labeling, the cells were washed twice with the chemoenzymatic labeling buffer. Enzymatic addition of GalNAz onto Fucα(1-2)Gal glycans was detected by treating the cells with 5 μM alkyne-functionalized Alexa Fluor 488 (Invitrogen), 0.1 mM triazoleamine ligand (Invitrogen), 2 mM sodium ascorbate (Sigma-Aldrich), and 1 mM $CuSO_4$ (Sigma-Aldrich) in 2% FBS (Gibco) in PBS at rt for 1 h. The coverslips were mounted onto glass slides using Vectashield mounting medium with DAPI (4 μL; Vector Labs) and sealed with clear nail polish. Cells were imaged using a Nikon Eclipse TE2000-S inverted microscope, and images were captured with Metamorph software using a 20x Plan Fluor objective.

Detection of Cell-Surface Fucα(1-2)Gal Glycans on Live Cancer Cells by Flow Cytometry. All cells were seeded at 4 x 10^6 cells per 10-cm plate in 10 mL of the appropriate media. On the day of analysis, cells were lifted off the plate with DNase (0.4 mg/mL; Worthington) and 1 mM EDTA and washed with 1% FBS, 10 mM HEPES in CMF HBSS. One million cells were chemoenzymatically labeled with UDP-GalNAz (500 μM) and BgtA (0.17 μg/μL) in 1% FBS, 10 mM HEPES in CMF HBSS (100 μL) for 2 h at 37 °C. Cells were spun twice through 100% FBS (1 mL) to remove excess reagent (500 x *g*, 5 min) and resupended in 1% FBS, 10 mM HEPES in CMF HBSS (100 μL) containing ADIBO-biotin (20 μM) and incubated for 1 h at rt. Cells were again spun twice through 100% FBS (1 mL), and washed with 3% BSA in PBS (1 mL). Cells were then resuspended in 3% BSA in PBS (100 μL) containing streptavidin-Alexa Fluor 488 (1 μg/mL) and incubated for 20 min at 4 °C. Cells were subsequently spun twice through 100% FBS (1 mL) and resuspended in 2% FBS, 10 mM HEPES in CMF HBSS (750 μL) for flow cytometry analysis. Immediately before analysis, 7-amino-actinomycin D (7-AAD, 5 μL; eBioscience) was added to measure cell viability. Cells were analyzed for FITC intensity on a Beckman Dickenson FACSCalibur flow cytometer equipped with a 488-nm argon laser. For each experiment, 10,000 live cells were analyzed, and data analysis was performed on FlowJo (Tristar Inc.). Data points for LnCAP and PrEC cells were collected in triplicate, and for all other cells, in duplicate.

References

1. Hanson SR, *et al.* (2007) Tailored Glycoproteomics and Glycan Site Mapping Using Saccharide-Selective Bioorthogonal Probes. *J. Am. Chem. Soc.* 129(23):7266-7267.

2. Laughlin ST, Baskin JM, Amacher SL, & Bertozzi CR (2008) In Vivo Imaging of Membrane-Associated Glycans in Developing Zebrafish. *Science* 320(5876):664-667.

3. Khidekel N, *et al.* (2003) A Chemoenzymatic Approach toward the Rapid and Sensitive Detection of O-GlcNAc Posttranslational Modifications. *J. Am. Chem. Soc.* 125(52):16162-16163.

4. Sakabe K, Wang Z, & Hart GW (2010) Beta-N-acetylglucosamine (O-GlcNAc) is part of the histone code. *Proc. Natl. Acad. Sci. U.S.A.* 107(46):19915-19920.

5. Khidekel N, Ficarro SB, Peters EC, & Hsieh-Wilson LC (2004) Exploring the O-GlcNAc proteome: Direct identification of O-GlcNAc-modified proteins from the brain. *Proc. Natl Acad. Sci. U.S.A.* 101(36):13132-13137.

6. Khidekel N, *et al.* (2007) Probing the dynamics of O-GlcNAc glycosylation in the brain using quantitative proteomics. *Nat. Chem. Biol.* 3(6):339-348.

7. Rexach JE, *et al.* (2010) Quantification of O-glycosylation stoichiometry and dynamics using resolvable mass tags. *Nat. Chem. Biol.* 6(9):645-651.

8. Wang Z, *et al.* (2009) Site-specific GlcNAcylation of human erythrocyte proteins: potential biomarker(s) for diabetes. *Diabetes* 58(2):309-317.

9. Zheng T, *et al.* (2011) Tracking N-acetyllactosamine on cell-surface glycans in vivo. *Angew. Chem. Int. Ed. Engl.* 50(18):4113-4118.

10. Becker DJ & Lowe JB (2003) Fucose: biosynthesis and biological function in mammals. *Glycobiology* 13(7):41R-53R.

11. Gilewski T, *et al.* (2001) Immunization of metastatic breast cancer patients with a fully synthetic globo H conjugate: a phase I trial. *Proc. Natl Acad. Sci. U.S.A.* 98(6):3270-3275.

12. Ragupathi G, *et al.* (1999) A Fully Synthetic Globo H Carbohydrate Vaccine Induces a Focused Humoral Response in Prostate Cancer Patients: A Proof of Principle. *Angew. Chem. Int. Ed. Engl.* 38(4):563-566.

13. Slovin SF, *et al.* (1999) Carbohydrate vaccines in cancer: Immunogenicity of a fully synthetic globo H hexasaccharide conjugate in man. *Proc. Natl Acad. Sci. U.S.A.* 96(10):5710-5715.

14. Yi W, Shen J, Zhou G, Li J, & Wang PG (2008) Bacterial Homologue of Human Blood Group A Transferase. *J. Am. Chem. Soc.* 130(44):14420-14421.

15. Hang HC, Yu C, Pratt MR, & Bertozzi CR (2003) Probing Glycosyltransferase Activities with the Staudinger Ligation. *J. Am. Chem. Soc.* 126(1):6-7.

16. Rostovtsev VV, Green LG, Fokin VV, & Sharpless KB (2002) A Stepwise Huisgen Cycloaddition Process: Copper(I)-Catalyzed Regioselective "Ligation" of Azides and Terminal Alkynes. *Angew. Chem. Int. Ed. Engl.* 41(14):2596-2599.

17. Agard NJ, Prescher JA, & Bertozzi CR (2004) A Strain-Promoted [3 + 2] Azide−Alkyne Cycloaddition for Covalent Modification of Biomolecules in Living Systems. *J. Am. Chem. Soc.* 126(46):15046-15047.

18. Shao J & Tam JP (1995) Unprotected Peptides as Building Blocks for the Synthesis of Peptide Dendrimers with Oxime, Hydrazone, and Thiazolidine Linkages. *J. Am. Chem. Soc.* 117(14):3893-3899.

19. Blixt O, *et al.* (2004) Printed covalent glycan array for ligand profiling of diverse glycan binding proteins. *Proc. Natl. Acad. Sci. U.S.A.* 101(49):17033-17038.

20. Manimala JC, Roach TA, Li Z, & Gildersleeve JC (2006) High-Throughput Carbohydrate Microarray Analysis of 24 Lectins. *Angew. Chem. Int. Ed. Engl.* 45(22):3607-3610.

21. Manimala JC, Roach TA, Li Z, & Gildersleeve JC (2007) High-throughput carbohydrate microarray profiling of 27 antibodies demonstrates widespread specificity problems. *Glycobiology* 17(8):17C-23C.

22. Blixt O, *et al.* (2008) Glycan microarrays for screening sialyltransferase specificities. *Glycoconjugate J.* 25(1):59-68.

23. Miyake M, Taki T, Hitomi S, & Hakomori S-i (1992) Correlation of Expression of H/LeY/LeB Antigens with Survival in Patients with Carcinoma of the Lung. *N. Engl. J. Med.* 327(1):14-18.

24. Mènard S, Tagliabue E, Canevari S, Fossati G, & Colnaghi MI (1983) Generation of Monoclonal Antibodies Reacting with Normal and Cancer Cells of Human Breast. *Cancer Res.* 43(3):1295-1300.

25. Murrey HE, *et al.* (2006) Protein fucosylation regulates synapsin Ia/Ib expression and neuronal morphology in primary hippocampal neurons. *Proc. Natl. Acad. Sci. U.S.A.* 103(1):21-26.

26. Murrey HE, *et al.* (2009) Identification of the plasticity-relevant fucose-alpha(1-2)-galactose proteome from the mouse olfactory bulb. *Biochemistry* 48(30):7261-7270.

27. Perrone F, Menard S., Canevari, S., Calabrese, M., Boracchi, P.,Bufalino, R., Testori, S.,Baldini, M., and Colnaghi, M.R. (1993) Prognostic Significance of the CaMBr1 Antigen on Breast Carcinoma: Relevance of the Type of Recognised Glycoconjugate. *Eur. J. Cancer* 29A(15):2113-2117.

28. Baskin JM, *et al.* (2007) Copper-free click chemistry for dynamic in vivo imaging. *Proc. Natl. Acad. Sci. U.S.A.* 104(43):16793-16797.

29. Agard NJ, Baskin JM, Prescher JA, Lo A, & Bertozzi CR (2006) A Comparitive Study of Bioorthogonal Reactions with Azides. *ACS Chem. Biol.* 1(10):644-648.

30. Jewett JC, Sletten EM, & Bertozzi CR (2010) Rapid Cu-Free Click Chemistry with Readily Synthesized Biarylazacyclooctynones. *J. Am. Chem. Soc.* 132:3688-3690.

31. Zhang S, Zhang HS, Cordon-Cardo C, Ragupathi G, & Livingston PO (1998) Selection of tumor antigens as targets for immune attack using immunohistochemistry: protein antigens. *Clin. Cancer Res.* 4(11):2669-2676.

32. Lee JS, *et al.* (1991) Expression of Blood-Group Antigen A — A Favorable Prognostic Factor in Non-Small-Cell Lung Cancer. *N. Engl. J. Med.* 324:1084-1090.

33. Schröder FH, *et al.* (2009) Screening and Prostate-Cancer Mortality in a Randomized European Study. *N. Engl. J. Med.* 360(13):1320-1328.

34. Peracaula R, *et al.* (2003) Altered glycosylation pattern allows the distinction between prostate-specific antigen (PSA) from normal and tumor origins. *Glycobiology* 13(6):457-470.